Transamazonian crustal growth and reworking as revealed by the 1:500,000-scale geological map of French Guiana (2nd edition)

Claude DELOR (1)*, Didier LAHONDÈRE (1)
Emmanuel EGAL (1)
Jean-Michel LAFON (2)
Alain COCHERIE (1)
Catherine GUERROT (1)
Philippe ROSSI (1), Catherine TRUFFERT (1)
Hervé THÉVENIAUT (3), David PHILLIPS (4)
Valter Gama de AVELAR (2)

Processus de croissance et de ré-activation crustale au Transamazonien, mis en évidence par la carte à 1/500 000 de Guyane (2ème édition)

Géologie de la France, 2003, n° 2-3-4, 5-57, 13 fig., 5 tabl.

Mots clés : Paléoprotérozoïque, Orogénie transamazonienne, Magmatisme, Migmatitisation, Datation Pb-Pb, U-Pb, U-Th-Pb, K-Ar, Sm-Nd, Ceinture de roches vertes, Géodynamique, Guyane, Bouclier guyanais.

Key words: Paleoproterozoic, Transamazonian orogeny, Magmatism, Migmatization, Dating, Pb/Pb, U/Pb, U/Th/Pb, K/Ar, Sm/Nd, Greenstone belts, Geodynamics, French Guiana, Guiana Shield.

Abstract

As a complement to the 1:500,000-scale Geological Map of French Guiana (2nd edition), we present a comprehensive and detailed overview of the wide spectrum of Paleoproterozoic terrains in the country on the basis of an airborne geophysical survey, geological field investigations, and about 100 new isotopic (Pb-Pb and Sm-Nd) data. We discuss French Guiana's complex Transamazonian orogenic evolution in terms of multi-stage crustal growth, with both Archean recycling and juvenile Paleoproterozoic accretion and reworking. This evolution began with the formation of juvenile oceanic crust at 2.26 - 2.20 Ga, as indicated by the Eorhyacian crystallization age of gabbroic rocks from "Île de Cayenne Complex" and by inherited zircon ages in reworked plutonic and metasedimentary rocks. Then, from 2.18 to 2.13 Ga, came a period of dominant tonalite-trondhjemite-granodiorite (TTG) type magmatism and regionally associated greenstone belts. This we interpret in terms of a Mesorhyacian multi-pulse island-arc plutono-volcanism in response to a main southward-directed subduction during a D1 event related to a N-S oriented convergence of the African and Amazonian Archean blocks. The age distribution of the TTG magmatism seems to be roughly dependent on the geographical location of the dated rocks within an intra-arc younging direction: the older (2.18 - 2.16 Ga) migmatitic TTG is found exposed in northern and southern French Guiana (Laussat and Tamouri complexes) while the youngest (2.15 - 2.13 Ga) generation occupies an inner position known as the Central TTG Complex. That the greenstone deposits were synchronous with the TTG magmatism is indicated by the emplacement of volcanics from 2.16 Ga to 2.14 Ga - for example, the basic to ultrabasic magmatism of the Tampok suite has been dated at 2.15 Ga and was therefore synchronous with the Mesorhyacian TTG magmatism. Low-pressure type metamorphism is also associated with D1, as revealed by an andalusite-type paragenesis in both the northern and southern branches of the greenstone belt.

Granitic magmatism and minor gabbroic intrusions then occurred at ca. *2.11 - 2.08 Ga in response to the closure of the island-arc basins, with an evolution from southward-directed subduction to sinistral wrenching (D2a). A first geochronological reference for this D2a event is registered in a syntectonic vein dated at 2098 ±*

(1) brgm, 3 avenue Claude-Guillemin, BP 6009, 45060 Orléans cedex 2, France
(2) Pará-Iso, Centro de Geociências, UFPA, Belém, Brasil.
(3) brgm Guyane, domaine de Suzini, route de Montabo, BP 552, 97333 Cayenne cedex 2, Guyane.
(4) School of Earth Sciences, The University of Melbourne, Australia.
(*) Corresponding author. E-mail:c.delor@brgm.fr

2 Ma. That migmatization accompanied this magmatic episode is indicated by the ca. *2.10 Ga age recorded in zircons and monazites in the migmatitic TTG domains of northern and southern French Guiana. In addition to field evidence of* in situ *melting of metatonalite, the existence of inherited zircons and monazites up to 2.19 - 2.17 Ga in age confirms that the migmatite originated from melting of a TTG-greenstone suite. In northern French Guiana, the D2a transcurrent sinistral event was marked by the opening of late detrital basins, along the northern limb of the central TTG complex (pull-apart basins).*

The age of a D2b event is inferred from the 2.07 - 2.06 Ga dating of late metaluminous monzogranite emplaced along a WNW-ESE dextral strike-slip corridor, and dissecting pull-apart basins. Further chrono-structural support is given by co-eval mesoscopic melt veins emplaced along N145 dextral shear planes dissecting the main D2 migmatitic foliation in the northern Laussat TTG complex. A low- to medium-pressure D2b counterclockwise metamorphism, recorded in the detrital basin units, reflects a lack of significant crustal thickening in the metasediments; it is best interpreted as an anomalously high geothermal gradient during burial followed by isobaric cooling. This metamorphic stage was contemporaneous with a similar counterclockwise Pressure-Temperature path exemplified farther west in Suriname, where it culminated in the formation of the Bakhuis ultrahigh-temperature (UHT) granulite belt dated at ca. *2.07 - 2.05 Ga. Such a metamorphic signature, together with the abundant granite magmatism produced by the melting of the TTG-greenstone belt at moderate pressures, are correlated with mantle upwelling during prolonged crustal stretching.*

The positive $\varepsilon_{(Nd)t}$ values both of the acid metavolcanic rocks and metagreywacke from the greenstone belts and of associated TTG granitoid, confirm the juvenile character of the TTG-greenstone complexes and preclude the involvement of significant pre-Transamazonian crust in their genesis. No preserved remnants of the Archean continents have been encountered in French Guiana. Archean fingerprinting is only displayed by negative $\varepsilon_{(Nd)t}$ values on metapelite, by 3.19 - 2.77 Ga detrital zircons in quartzite from the greenstone belt, and by negative $\varepsilon_{(Nd)t}$ values and inherited Archean zircon as old as 2.71 Ga in some granitoids from northern and southeastern French Guiana.

Dyke swarms, marking the precursor stages of the opening of the Atlantic Ocean, cut all the Paleoproterozoic lithologies. In addition to these well-known Mesozoic occurrences, NNE-SSW Paleoproterozoic (≥ 1.8 Ga) and NW-SE Neoproterozoic (809 Ma) generations of dykes have been identified by Ar-Ar and K-Ar dating, respectively, and by the paleomagnetic signature.

Résumé

Consécutivement à la réalisation de la carte géologique à 1/500 000 de Guyane (2ème édition), nous présentons une synthèse pluri-thématique et détaillée couvrant l'ensemble des formations paléoprotérozoïques de ce département. Ce travail de synthèse intègre l'apport d'une campagne géophysique aéroportée, de levés de terrain et la réalisation d'une centaine de nouvelles données isotopiques (Pb-Pb et Sm-Nd). Nous discutons l'évolution complexe de l'orogenèse transamazonienne en termes de croissance crustale multi-étapes, prenant en compte des processus de recyclage archéen ainsi que des processus d'accrétion juvénile et de réactivation thermotectonique au Paléoprotérozoïque. Cette évolution transamazonienne débute par la formation d'une croûte océanique juvénile à 2,26-2,20 Ga, comme en témoignent l'âge éorhyacien de cristallisation de gabbros du Complexe de l'Ile de Cayenne, et les âges de zircons hérités dans des termes plutoniques et sédimentaires déformés et métamorphisés. De 2,18 à 2,13 Ga, un magmatisme de type tonalite-trondhjemite-granodiorite (TTG) se développe de façon prédominante en association avec le dépôt de formations volcano-sédimentaires (ceintures vertes). Nous interprétons cet événement en termes de magmatisme plutono-volcanique d'arc multi-étapes d'âge mésorhyacien, à l'aplomb d'une zone de subduction à plongement sud, induite par la convergence des blocs archéens africain et amazonien pendant une phase D1. L'âge du magmatisme TTG reflète globalement sa géométrie : une première génération de TTG migmatitiques, datée à 2,18-2,16 Ga, affleure au Nord et au Sud de la Guyane (complexes Laussat et Tamouri) de part et d'autre d'une seconde génération de TTG, datée à 2,15-2,13 Ga, et à laquelle on se réfèrera comme le complexe TTG central de Guyane. Le caractère synchrone du dépôt des ceintures de roches vertes vis-à-vis de ce magmatisme TTG est démontré par l'âge de mise en place de termes volcaniques entre 2,16 et 2,14 Ga. Notamment, le magmatisme basique à ultrabasique de la suite Tampok est daté à 2,15 Ga et apparaît donc comme synchrone du magmatisme TTG mésorhyacien. Un métamorphisme de type basse pression est associé à la phase D1, comme en témoignent les paragenèses symptomatiques à andalousite du Nord et du Sud de la Guyane.

Un magmatisme granitique et en moindre proportion, des intrusions basiques, se mettent en place vers 2,11-2,08 Ga, et témoignent de la fermeture des bassins d'arc volcanique, avec une évolution du contexte de subduction initial vers un processus de coulissage sénestre (D2a) des blocs continentaux convergents. L'âge de cet événement D2a est calé par une veine syntectonique datée à 2098 ± 2 Ma. Le caractère synchrone d'un processus de migmatisation avec cet épisode magmatique est calé par l'âge à ca. *2,10 Ga de zircons et de monazites dans les TTG migmatitiques du Nord et du Sud de la Guyane.*

Parallèlement aux évidences de terrain témoignant d'une fusion in situ *de métatonalite, l'existence de zircons et de monazites d'âges aussi vieux que 2,19-2,17 Ga confirme que les produits de migmatitisation sont issus de la fusion des TTG et des ceintures vertes. Au Nord de la Guyane, l'épisode tectonique transcurrent sénestre D2a est marqué par l'ouverture de bassins tardifs de type détritique, le long de la bordure nord du complexe TTG central (bassins en "pull-apart").*

L'âge d'un épisode tectonique D2b est déterminé par la datation de monzogranites metalumineux à 2,08-2,06 Ga, mis en place le long de couloirs transcurrents dextres WNW-ESE, et qui recoupent les bassins en "pull-apart". Ce calage chronostructural est appuyé à l'echelle mésoscopique par l'observation de veines migmatitiques mises en place le long de plans de cisaillement N145° recoupant la foliation migmatitique D2 dans le complexe TTG septentrional (Laussat). Un métamorphisme « anti-horaire » de type basse-pression à moyenne-pression est enregistré dans les bassins détritiques et reflète l'absence d'épaississement crustal significatif dans les métasédiments. Il est interprétable en termes de gradient thermique anormalement élevé pendant une phase d'enfouissement, auquel succède un refroidissement isobare. Cet épisode métamorphique est contemporain d'un même type d'évolution Pression-Température anti-horaire démontré plus à l'Ouest au Suriname, où il culmine avec la formation du métamorphisme d'ultra-haute température des Monts Bakhuis, daté à ca. *2,07-2,05 Ga. Une telle signature métamorphique, ainsi que l'abondant magmatisme granitique produit par la fusion des TTG et ceintures de roches vertes à des pressions modérées, sont corrélés avec des processus de remontée mantellique en réponse à un étirement crustal prolongé.*

Les valeurs $\varepsilon_{(Nd)t}$ positives à la fois dans les métavolcaniques et métagreywackes des ceintures vertes et dans les termes plutoniques des TTG, confirment le caractère juvénile des complexes TTG-ceintures vertes et excluent pour leur genèse la participation significative d'une croûte pré-transamazonienne. Aucune relique de continent archéen n'a été reconnue en Guyane. Une empreinte archéenne est uniquement mise en évidence par les valeurs $\varepsilon_{(Nd)t}$ négatives de métapélites, par les âges à 3,19-2,77 Ga de zircons détritiques dans les ceintures vertes, et par les valeurs $\varepsilon_{(Nd)t}$ négatives et les zircons hérités aussi vieux que 2,71 Ga dans quelques granites du nord et du sud-est de la Guyane.

Les essaims de dykes, marquant les stades précurseurs de l'ouverture de l'Atlantique, recoupent toutes les lithologies paléoprotérozoïques. Parallèlement à ces occurrences mésozoïques, des générations de dykes NNE-SSW paléoprotérozoïques (≥ 1.8 Ga) et NW-SE néoprotérozoïques (809 Ma) ont été identifiées respectivement par datation Ar-Ar et K-Ar, ainsi que par leur signature paléomagnétique.

Resumo

Em complemento à realização da segunda edição do mapa geológico na escala 1:500000 da Guiana Francesa, apresentamos uma síntese pluri-temática detalhada sobre a geologia do referido território. Essa síntese integra resultados de campanha aerogeofísica, de levantamento de campo assim como uma centena de novos dados isotópicos (Pb-Pb e Sm-Nd, principalmente). A evolução complexa da orogênese Transamazônica é discutida em termos de crescimento multi-estágios levando em conta os processos de retrabalhamento de crosta arqueana e de acresção juvenil e de reativação termotectônica no Paleoproterozóico. Essa evolução transamazônica inicia-se com a formação de crosta oceânica juvenil a 2,26-2,20 Ga, evidenciada pelas idades eoriacianas de cristalização de gabros do Complexo "Île de Cayenne" e de zircões herdados em rochas plutônicas e sedimentares deformadas e metamorfisadas. Entre 2,18 Ga e 2,13 Ga, um magmatismo mesoriaciano de tipo tonalítico-trondjhemítico-granodiorítico (TTG) predomina, em associação com o depósito de formações vulcano-sedimentares do tipo greenstone belts. *Esse episódio magmático é interpretado em termo de magmatismo plutono-vulcânico multi-estágios em contexto de arco de ilhas relacionado a uma zona de subdução com vergência para sul, induzida pela convergência dos blocos arqueanos africano e amazônico durante uma fase D1. A idade do magmatismo TTG refleita globalmente a sua geometria: Uma primeira geração de TTG migmatíticos, datada em 2,18-2,16 Ga ocorre no norte e no sul da Guiana Francesa, em volta de uma segunda geração de TTG, datada em 2,15-2,13 Ga, denominada de complexo TTG central. O caráter síncrono da formação dos greenstone belts com o magmatismo TTG é demonstrado pela idade de formação dos termos vulcânicos entre 2,16 - 2,14 Ga. Em particular, o magmatismo básico-ultrabásico da suíte Tampok é datado em 2,15 Ga e é contemporâneo do magmatismo TTG mesoriaciano. Um episódio metamórfico de baixa pressão é associado a esta fase D1.*

Um episódio magmático essencialmente granítico, com intrusões básicas subordinadas, ocorre em torno de 2,11-2,09 Ga, testemunhando o fechamento das bacias de arcos vulcânicos, com uma evolução do contexto de subdução para um processo de transcorrência sinistral dos blocos continentais convergentes (D2a). A idade desse evento D2a é determinada por um veio sin-tectônico datada a 2098 ± 2 Ma. Um processo de migmatização, contemporânea deste episódio magmático, é identificada em torno de 2,10 Ga de acordo com as idades de zircões e monazitas dos granitóides TTG do norte e do sul da Guiana francesa. Em paralelo às evidencias no campo da fusão in situ *de metatonalitos, a existência de zircões e monazitas com idades em torno de 2,19-2,17 Ga confirma que os produtos da migmatização foram originados da fusão do magmatismo TTG e das seqüências de* greenstone. *No*

norte da Guiana Francesa, o episódio transcorrente sinistral D2a é marcado pela abertura de bacias detríticas tardias, ao longo da borda norte do complexo TTG central (bacias do tipo pull-apart*).*

A idade de um episódio tectônico D2b é definida pela datação de monzogranitos meta-aluminosos em torno de 2,08-2,06 Ga, que se formaram ao longo de corredores transcorrentes dextrais WNW-ESE, cortando as bacias do tipo pull-apart*. Essa configuração crono-estrutural é reforçada, em escala mesoscópica, pela observação, no campo, de veios migmatíticos ao longo de planos de cisalhamento N145 que cortam a foliação migmatítica D2 no complexo TTG setentrional (setor de Laussat). Um metamorfismo anti-horário de pressão baixa a intermediária é registrado nas bacias detríticas e reflete a ausência de espessamento crustal significativo nas rochas metassedimentares. É interpretado em termos de gradiente térmico anormalmente elevado durante uma fase de soterramento seguida de um resfriamento isobárico. Esse episódio metamórfico é contemporâneo de um tipo de evolução pressão - temperatura anti-horária encontrado mais a oeste, no Suriname, onde o mesmo culmina com a atuação de um metamorfismo de ultra-alta temperatura no setor dos Bakhuis Mountains, datados a 2,07-2,05 Ga. As características desse evento metamórfico, junto com a abundância de um magmatismo granítico produzido pela fusão dos granitóides TTG e das seqüências greenstones a pressão média são relacionadas a processos de subidas mantélicas em resposta a um estiramento prolongado em escala continental.*

Os valores positivos de $\varepsilon_{(Nd)t}$ encontrados tanto nas rochas metavulcânicas quanto nos metagrauvacas das seqüências greenstones, assim como nas granitóides TTG associados confirmam o caráter juvenil dos complexos granito-greenstones, excluindo uma participação significativa de crosta pré-transamazônica na sua gênese. Nenhuma relíquia preservada de continente arqueano foi encontrada na Guiana Francesa. Uma assinatura arqueana é evidenciada apenas pelos valores negativos de $\varepsilon_{(Nd)t}$ registrados em metapelitos e pelas idades entre 3,19-2,77 Ga de zircões detríticos de quartzito das seqüências greenstones, bem como pelos valores negativos de $\varepsilon_{(Nd)t}$ e zircões herdados com idades de até 2,71 Ga de alguns granitóides do norte e do sudeste da Guiana Francesa.

Exames de diques marcando estágios precursores da abertura do Oceano Atlântico cortam todas as litologias paleoproterozóicas. Junto com essa geração de diques mesozóicos, diques paleoproterozóicos (> 1,8 Ga), orientados NNE-SSW, e diques neoproterozóicos (809 Ma), orientados NW-SE foram identificados por datação Ar-Ar e K-Ar, respectivamente, e pela assinatura paleomagnética.

Introduction

French Guiana, situated between lat. 2° and 6° N, lies in the eastern part of the Precambrian Guiana Shield, north of the Amazon River. It has an equatorial type climate, which makes geological surveying difficult - the rain forest cover considerably slows geological field work (mapping, ground geophysics, geochemistry) and partially masks terrain observations. Despite these difficulties, our geological knowledge of French Guiana reached a first level of understanding due largely to the pioneering cartography of Choubert and co-workers, with the production of 1:100,000-scale geological maps in the 1960s and 1970s (see Choubert, 1974, for a synthesis), and later detailed mapping in the southern terrains by Marot (1988) and co-workers. The realization of successive mapping campaigns over a relatively long period of time has resulted in a "patchwork" of geological maps and associated data, with unavoidable heterogeneities and inconsistencies. Intercorrelations between these studies were, up until the last decade or so, hampered by the lack of sensitivity of isotopic methods and by the large errors (± 50-100 Ma) in age determinations; these precluded any attempt to establish a refined timing of lithostructural and metamorphic events.

Recent field and analytical studies by BRGM teams at the beginning of the 1990s built upon previous studies and brought our geological knowledge of the Precambrian terrains and associated mineralization processes in French Guiana to a second level of understanding in the light of modern geodynamic plate-tectonic processes (e.g. Ledru *et al.*, 1991; Egal *et al.*, 1992; Vernhet *et al.*, 1992; Milesi *et al.*, 1995; Vanderhaeghe *et al.*, 1998). Meanwhile, the merging of remote-sensing cartographic tools, such as satellite imagery and airborne geophysics, has led to a new cartographic campaign strategy that allows us to determine structures masked by the lateritic and/or forest cover. It was thus that, during the second half of 1996, BRGM organized a high-sensitivity airborne magnetometer-spectrometer survey aimed at providing French Guiana i) with a coherent, high-resolution, geophysical infrastructure to enhance detailed and comprehensive geological mapping, and ii) with a regional-planning tool to help in the sustainable management of the country's natural resources. The interpretation of radiometry for subsurface data, and of magnetism for deeper lithological signal integration, has enabled powerful discriminations (Delor *et al.*, 1997, 1998a). The precision of the survey points to within 10m, and the density of the flight lines, meant that the geological field checking carried out from 1996 to 1999 along major rivers and creeks could correlate the indirect physical parameter images in terms of geological map lithologies and structures, with more precise unit classifications through the help of mineral and bulk-rock analysis.

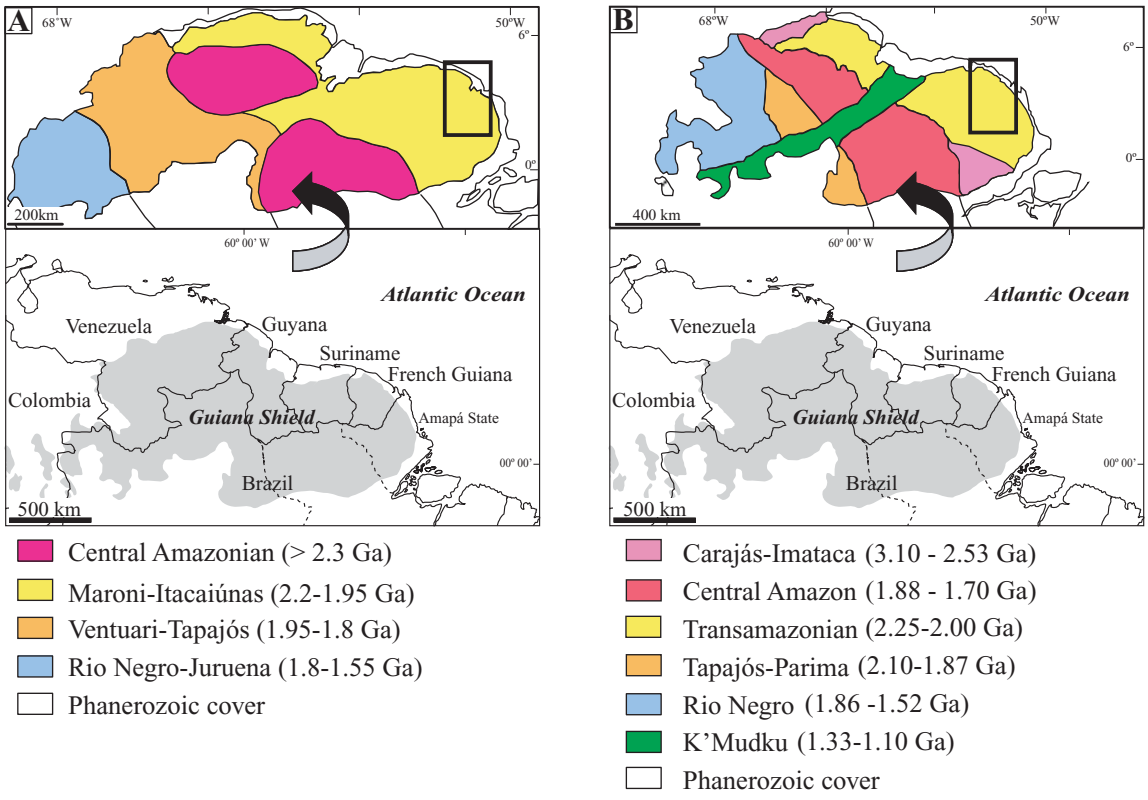

Fig. 1.- Simplified geological sketch maps of the Guiana Shield according to A: Tassinari *et al.* (2000) and B: Santos *et al*. (2000).

Fig. 1.- Schémas géologiques simplifiés du Bouclier guyanais selon A : Tassinari et al. *(2000) et B : Santos* et al. *(2000).*

In order to provide a unified legend for the revised mapping, absolute age bracketing of the updated lithological distribution has been constrained by more than 100 new isotopic investigations, mainly U-Pb and Pb-Pb zircon/monazite dating together with Sm-Nd model ages (Cocherie *et al*., 2000; Delor *et al*., 2001), in order to establish a refined chronology of the Transamazonian magmatic and metamorphic stages.

Here, with special reference to the second edition of the 1:500,000-scale geological map of French Guiana (Delor *et al*., 2001), we present a multi-thematic set of results obtained over the last decade from the use of these new tools, and its contribution to our understanding of Transamazonian crustal growth between *ca*. 2.26 and 2.06 Ga.

Geological setting

The Guiana Shield (Fig. 1), with an area of about 1.5 million km², is one of the major Precambrian terranes of western Gondwanaland. Located on the northern edge of the Amazonian Basin, it is almost entirely covered by tropical rainforest and, consequently, is poorly constrained from a geological standpoint. Archean protoliths have been reported at its edges both to the west (Imataca Complex in Venezuela: Montgomery and Hurley, 1978; Tassinari *et al*., 2001) and to the east (central and southwestern Amapá and northwestern Pará, Brazil: João and Marinho, 1982; Montalvão and Tassinari, 1984; Lafon *et al.*, 1998; Ricci *et al*., 2001; Rosa Costa *et al*., 2003). The Proterozoic crust between these protoliths shows evidence of southward-younging crustal growth and reworking (Fig. 1) from the northern Paleoproterozoic granite-greenstone complex (2.2 - 2.0 Ga), down the Atlantic coast to the southern volcanic sequences (Uatumã, 2.10 - 1.8 Ga), sedimentary deposits (Roraima, 1.89 - 1.78 Ga) and alkaline magmatic rocks (1.7 -1.3 Ga) near the Amazon Basin. Two models have been proposed to account for the classification of geological provinces - the one by Cordani *et al.* (1979) refined by Tassinari and Macambira (1999) and Tassinari *et al*. (2000) (Fig. 1A) and the other by Santos *et al.* (2000) (Fig. 1B).

Within this Paleoproterozoic framework, the Precambrian basement of French Guiana has been described in terms of volcano-sedimentary sequences (Paramaca) wrapped around igneous domains during the so-called Transamazonian event, for which the pioneering work of Choubert (1974) defined an early suite of meta-intrusives known as the "Guyanais" magmatic suite, and late granitic suites with "Caraibe" and "Galibi" sub-distinctions. This relative chronostratigraphic terminology has often been applied to the Guiana Shield, with unavoidable correlation difficulties due to the use of local names from one country to another (see review and compilation work in Gibbs and Barron, 1983, 1993).

Isotopic age determinations have been carried out progressively over the past two decades to provide absolute age bracketing. Most of the first available geochronological data from French Guiana were obtained by Rb-Sr and K-Ar methods with a few Sm-Nd and Pb-Pb results on whole rocks (Teixeira *et al*., 1984; 1985; Gruau *et al*., 1985). These studies confirmed that the main evolution of French Guiana occurred between 2.2 and 1.9 Ga, with only a single report of possible Archean ages for the Île de Cayenne migmatitic series (Choubert, 1964). The assumption of Archean rocks, however, has not been confirmed either by later Rb-Sr dating (Teixeira *et al*., 1984, 1985) or by later zircon dating on the northern Atlantic margin of the country (Milesi *et al.*, 1995; Vanderhaeghe *et al.*, 1998). Another set of radiometric ages, obtained mostly by the single-zircon evaporation technique (Milesi *et al*., 1995; Vanderhaeghe *et al*., 1998) and conventional U-Pb zircon systematics (Norcross, 1998; Lafrance *et al*., 1999; Norcross *et al*., 2000) with a precision of ± 1-10 Ma, significantly improved the determination of formation ages for the main geological units in eastern Guiana Shield. Along with the chronological re-appraisal of the lithological formations, a two-step tectonic evolution has been documented in the northern part of the country. The D1 and D2 events, although referring initially to structural stages, have been progressively documented as major regional tectonometamorphic events linked with contrasting magmatic suites (Ledru *et al.*, 1991; Milesi *et al.*, 1995; Vanderhaeghe *et al*., 1998). Thus, following the formation of oceanic crust (2.17 Ga), the D1 stage was marked by the emplacement, between 2.14 and 2.10 Ga, of juvenile calc-alkaline volcano-plutonic complexes such as the Île de Cayenne Complex and the Central Guiana Complex. D2, at about 2.11-2.08 Ga, was a stage of "tectonic accretion and crustal recycling" marked by i) the formation of the sedimentary basins separating the middle and the northern volcano-plutonic complexes, ii) convergence of the juvenile blocks during the Transamazonian orogeny, iii) an oblique convergence responsible for the formation of foreland basins in a pull-apart system (Ledru *et al.*, 1991; Egal *et al*., 1992; Milesi *et al.*, 1995), iv) the emplacement of high-K granite, indicative of a crustal thickening process, and v) a final stage of oblique convergence with the lateral extrusion of blocks responsible for burial of the foreland basins and the emplacement of leucogranite.

Airborne geophysics

During the 1996 airborne geophysical survey over French Guyana, the Earth's magnetic field and gamma-ray spectra were both recorded (see Appendix A for specifications), north of lat. 3° N. The resultant magnetic and radiometric maps that were compiled each shed a particular light on the various geological units and structures of French Guiana (Delor *et al*., 1997). The magnetic map covers the whole of French Guiana, as the results were merged with those of a previous geophysical campaign covering southern French Guiana, while the radiometry map concerns only the 1996 airborne campaign results.

Magnetism

The reduced-to-the-pole total field anomaly map (Fig. 2) reveals contrasting colour domains reflecting the differences of registered magnetic signal, expressed in nanoteslas (nT).

The overall Precambrian basement of French Guiana (granite massifs, volcano-sedimentary basins) is shown up by the longest wavelength anomalies. In the central part of the country we see a clear contrast between high (positive) and low (negative) nT values, which according to the available cartographic compilations (Choubert, 1974; Milesi *et al.*, 1995), can be correlated respectively with the central French Guiana granitoid and the surrounding volcano-sedimentary formations. In the west of the country, the total field anomaly map clearly shows, in terms of nT contrasts, linear structures with "curved" trajectories; this particular image fits globally with the Upper Detrital Unit defined by Milesi *et al*. (1995), and the observed trend variations seem to reflect lithological heterogeneities within the basin. Farther north, close the Atlantic margin, the aeromagnetic map highlights elliptical domains of positive magnetic values within a regional background characterized by negative magnetic values; the former anomalies are inferred to reflect granitoid while the background is known to reflect the dominant volcano-sedimentary formations (Choubert, 1974; Milesi *et al.*, 1995). In the southern part of French Guiana, the highest magnetic signals correspond to granitic domains.

A major network of NNW-SSE-trending anomalies to the southeast of Cayenne is clearly related to a Jurassic dolerite dyke swarm that reflects the precursor stages of the opening of the Atlantic Ocean. Also, a single alignment of 'en relais' linear structures, suspected as reflecting dykes, shows a striking NNW-SSE trend in the southwestern part of the magnetic map.

Radiometry

The results were surprisingly accurate despite the thick rain-forest cover over most of French Guiana. Fig. 3 displays radiometric ternary composition (U: blue; K: red; Th: green) draped upon the magnetic field reduced to pole. Variations in the potassium (K), uranium (U) and thorium (Th) contents of the geological formations are expected to be dominant in granite and sedimentary formations, either due to the presence of K-rich phases (mica, K-feldspar) or due to the higher amount of U-Th in the so-called 'secondary minerals' (mainly zircon and monazite).

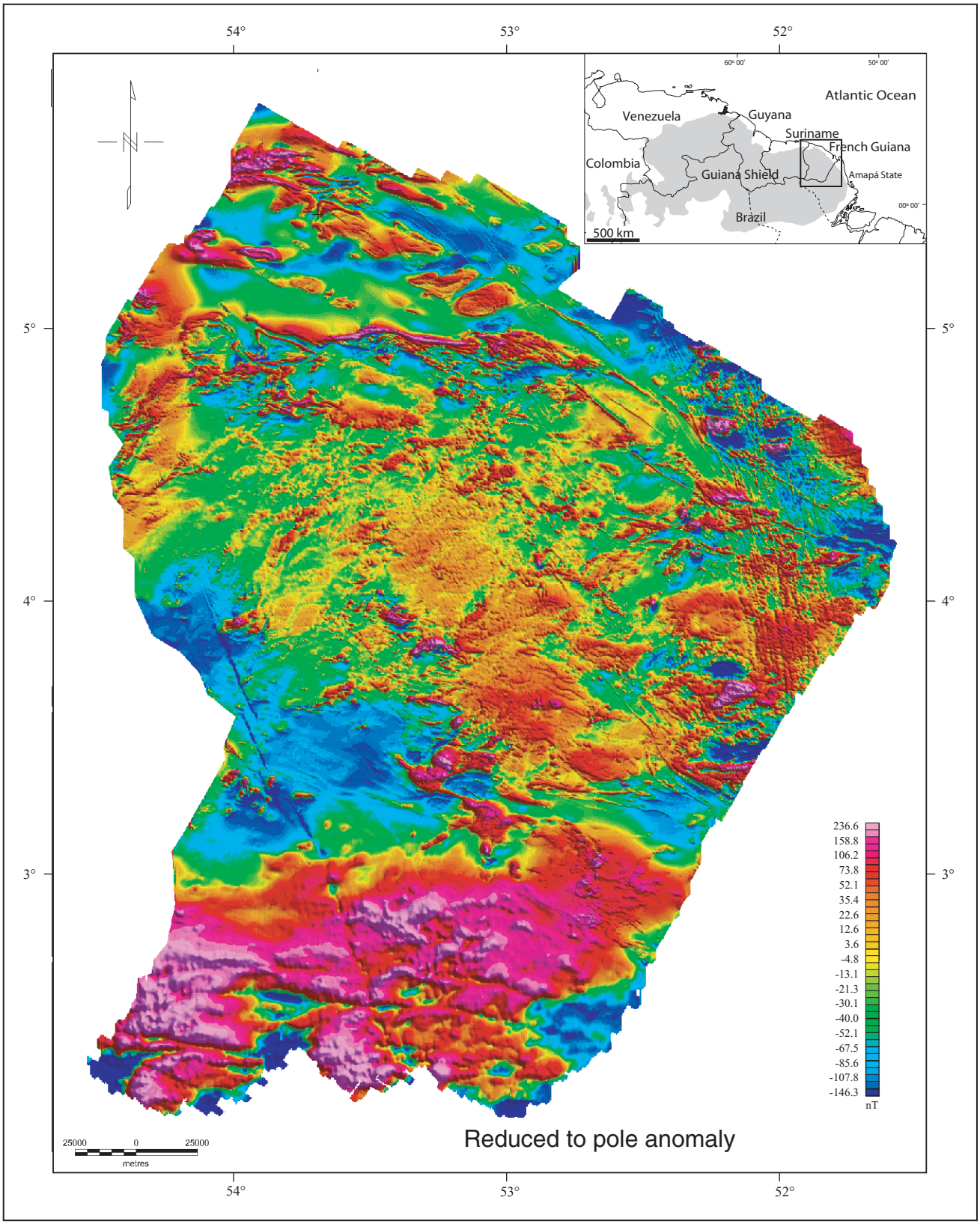

Fig. 2.- Magnetic (reduced to pole anomaly) map of French Guiana compiled from the 1974 airborne survey and 1996 airborne survey (Delor *et al*., 1997).

Fig. 2.- Carte magnétique (anomalie réduite au pôle) de Guyane intégrant les données de la campagne aéroportée de 1974 et de la campagne aéroportée de 1996 (Delor et al.*, 1997).*

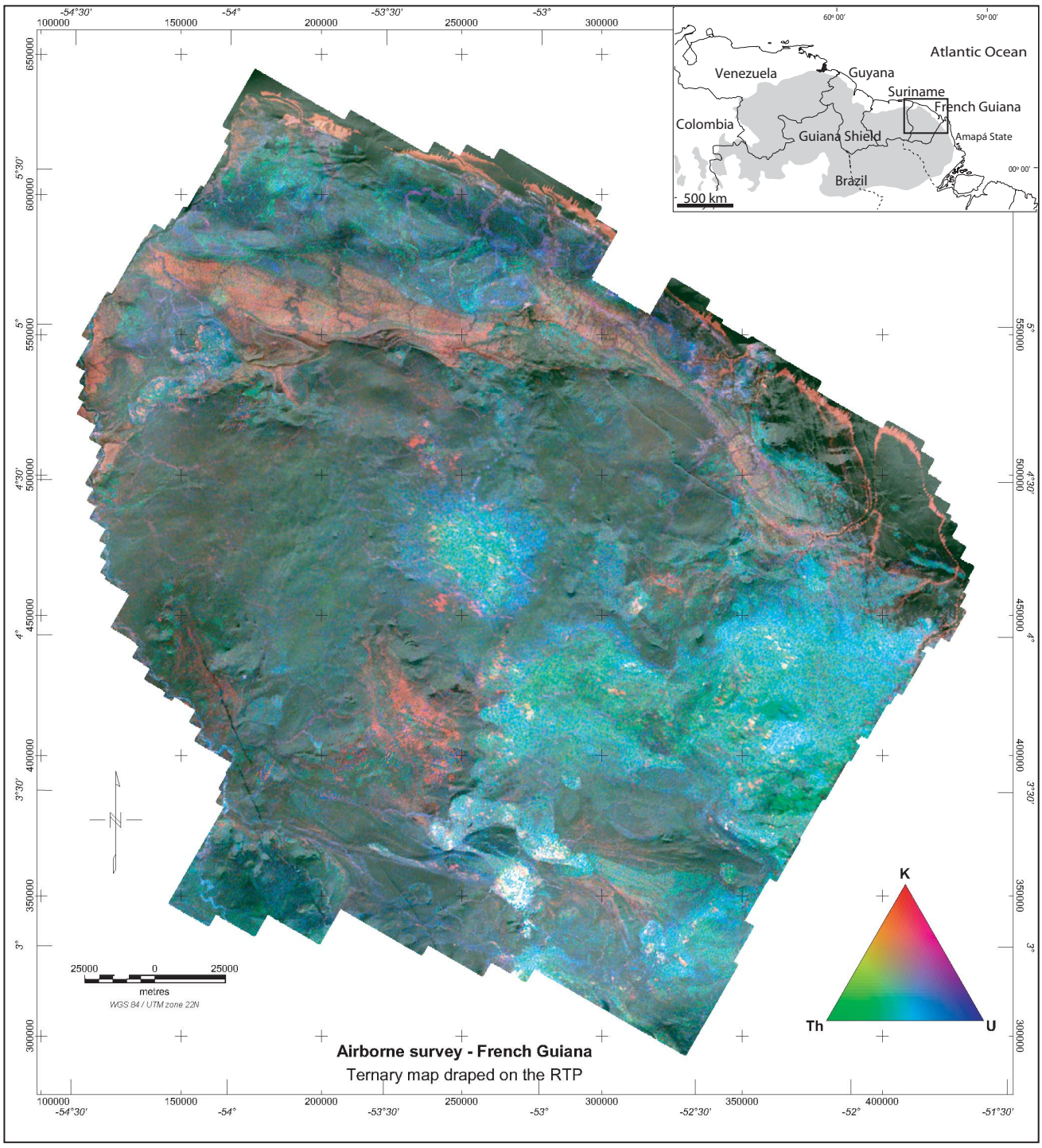

Fig. 3.- Radiometric ternary composition (U: blue; K: red; Th: green) draped over the magnetic field reduced to pole map. Data come from the 1996 airborne survey (Delor *et al*., 1997).

Fig. 3.- Carte radiométrique, avec composition ternaire (U : bleu, K : rouge, Th : vert) drapée sur la réduction au pôle du champ magnétique.

The most striking features of the radiometric map are:

- The high radiometric (light blue and light green colours) contrasts in the dominant plutonic domain of eastern and central French Guiana, against a background of low radiometric values. Such contrasts are best interpreted in terms of a dominant granitic composition where K-U-Th are maximum, as opposed to a tonalite and granodiorite composition where both K-feldspar and U-Th secondary phases are generally poorly expressed.

- A specific 10-km-wide contrasting feature (red colour), mainly K-rich, inside the well-known northern French Guiana sedimentary basin. This feature, which had never been mapped before, indicates a more pelitic deposition within the sedimentary succession. Moreover, the linear structures with 'curved' trajectories shown up by the magnetic relief can also be traced here. They are mainly outlined by Th content (thin green bands).

Geological map

The aim of the second edition (2001) of the Geological Map of French Guiana was to decipher the chronology of the different thermal and tectonic events in order to be able to correlate this information with the other Transamazonian formations of the Guiana Shield. Such long-distance correlations were not possible with the first edition of the map (Choubert, 1960), which was based only on lithologies and 'ageless' formations.

In the second edition, the lithology and age of the plutonic, volcanic, volcano-sedimentary, and sedimentary rocks are represented by different colour shades. Moreover, each formation is annotated by a specific number for a better understanding - this number is indicated both on the map (Fig. 4a) and in its legend (Fig. 4b). Tectonometamorphic events are indicated by the use of coloured dots superimposed on the formation colour, plus a specific code number. In order to rank the various azoic formations according to age, systematic geochronological dating, with more than 100 isotopic measurements, was carried out on samples mainly from the southern part of the country: the results, together with other relevant published data, are listed in Table 1 and the corresponding numbers are indicated on the map (Fig. 4a).

In the following sections we present a comprehensive overview of the lithological units of French Guiana in terms of rock type as determined both in the field and in the laboratory. The former regional subdivisions, although referred to in each section, are not taken into account as first-order discussion criteria; instead, in line with the 1:500,000-scale geological map, we use rock types established on the qualitative ratio of minerals such as quartz, K-feldspar, plagioclase and Fe-Mg phases (see Streckeisen, 1967, 1976). The lithological unit numbers shown on the map are also used in the text for a better understanding.

Discussion of the formations at regional scale is in chronological order on the basis of i) their cross-cutting and spatial relationships, and ii) available isotopic constraints, and is accompanied, where necessary, by reference to the magnetic and radiometric anomaly maps (Figs. 2 and 3). More detailed geochronological discussion is presented in a specific section.

Amphibolite and metagabbro (29) and trondhjemitic gneiss (30) - "Île de Cayenne" Complex

The "Île de Cayenne" trondhjemitic/gabbroic Complex, along the Atlantic coast, includes amphibolitic gneiss, metagabbro, amphibolite and leucocratic quartz-plagioclase gneiss (Fig. 5a). The complex is highly metamorphosed, with evidence of migmatization, and has been described as the metamorphic equivalent of the volcanic formations of the so-called Paramaca sequence (Egal *et al*., 1994). These lithologies are interpreted as an association of trondhjemite and volcanic to volcanoclastic end-members resulting from the "fractionated crystallization" of a tholeiitic magma similar to the present-day MORB type (Milesi *et al*., 1995). The amount of acid to intermediate rock types in this bimodal igneous suite is significantly higher than in present-day oceanic crust. On the basis of the above-mentioned approach by "rock type" based on mineralogical and geochemical factors, the new Geological Map of French Guiana has extended the inferred trondhjemitic formations (similar to those of Île de Cayenne case study) along the entire coast. This is nevertheless debatable in the light of the wider TTG-suite evidence in French Guiana, as discussed below and in the geochronology section.

Tonalitic, trondhjemitic and granodioritic migmatitic gneiss (27 and 28) - Northern "Laussat" and southern "Tamouri" migmatized TTG domains

These plutonic domains crop out along the Atlantic coast (Laussat Complex) and in the south of French Guiana (Tamouri Complex). The area along the Atlantic coast, previously considered as Île de Cayenne trondhjemite (Delor *et al*., 2001), presents clear similarities with the migmatized TTG of southern French Guiana and has therefore been represented as coeval with unit code 27 on Figure 4. Typical facies are exposed in a quarry in the vicinity of the Laussat River, from which the name "Laussat Complex" (Fig. 5b), is derived. The migmatitic TTG in the south of the country is associated with gneiss containing varied amounts of biotite, garnet and sillimanite; it has been named the "Tamouri Complex" in accordance with earlier proposed terminology (Marot, 1988). The TTG and gneissic formations are associated with well-characterized granitoid layers, which can be interpreted as the melting product of the former TTG-sedimentary protolith. Both the Laussat and the Tamouri tonalite and trondhjemite show a hypidiomorphic-granular texture. The tonalite is composed of oligoclase, amphibole, biotite, chlorite, quartz and oxides, while the trondhjemite paragenesis comprises sodic plagioclase (oligoclase), biotite, muscovite chlorite, K-feldspar (microcline), epidote, sphene and quartz. In both tonalite and trondhjemite, biotite occurs as tablets or euhedral to sub-euhedral hexagonal sections. Microcline in the trondhjemite is interstitial and in places forms poikiloblasts enclosing biotite and plagioclase.

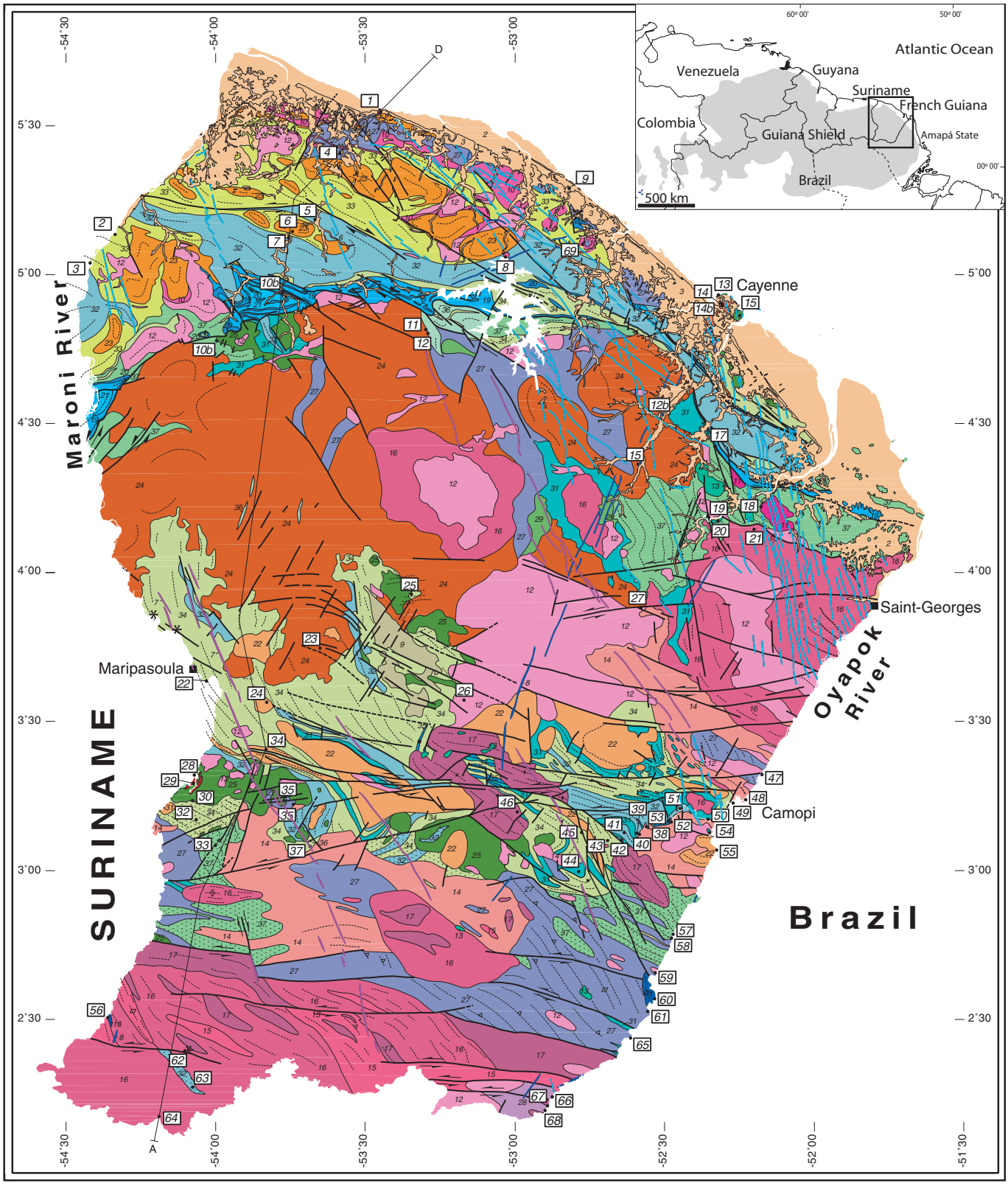

Fig. 4a.- Geological map of French Guiana (Delor *et al.*, 2001). Unboxed numbers in italic refer to the rock units as listed in Fig. 4b. Boxed numbers refer to isotopic data as listed in Table 1.

Fig. 4a.- Carte géologique de la Guyane (Delor et al.*, 2001). Les nombres non inclus dans des carrés se réfèrent aux formations géologiques listées en fig. 4b. Les nombres inclus dans des carrés se réfèrent aux données isotopiques listées en Table 1.*

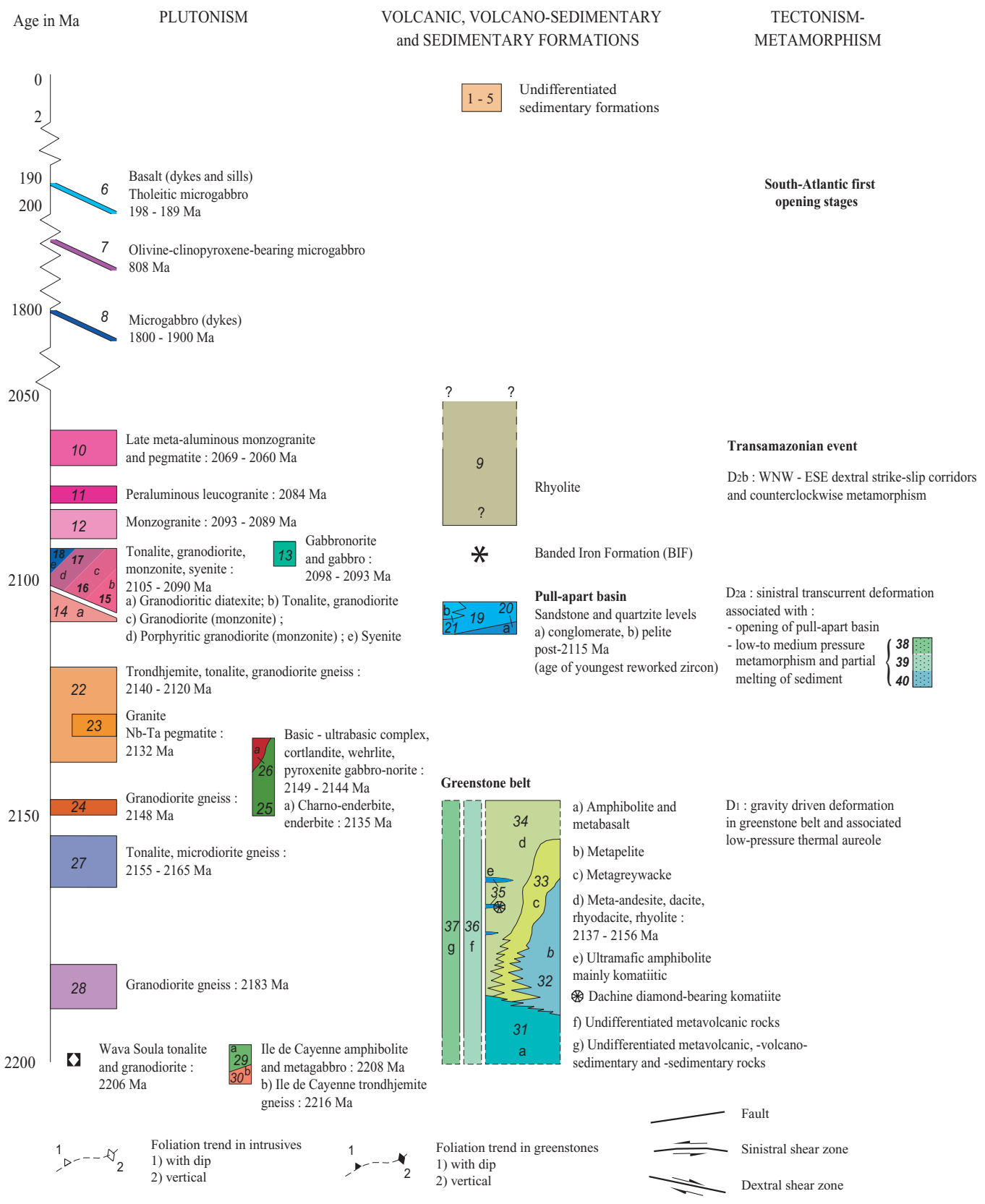

Fig. 4b.- Geological legend for Fig. 4a.

Fig. 4b.- Légende géologique de la Fig. 4a.

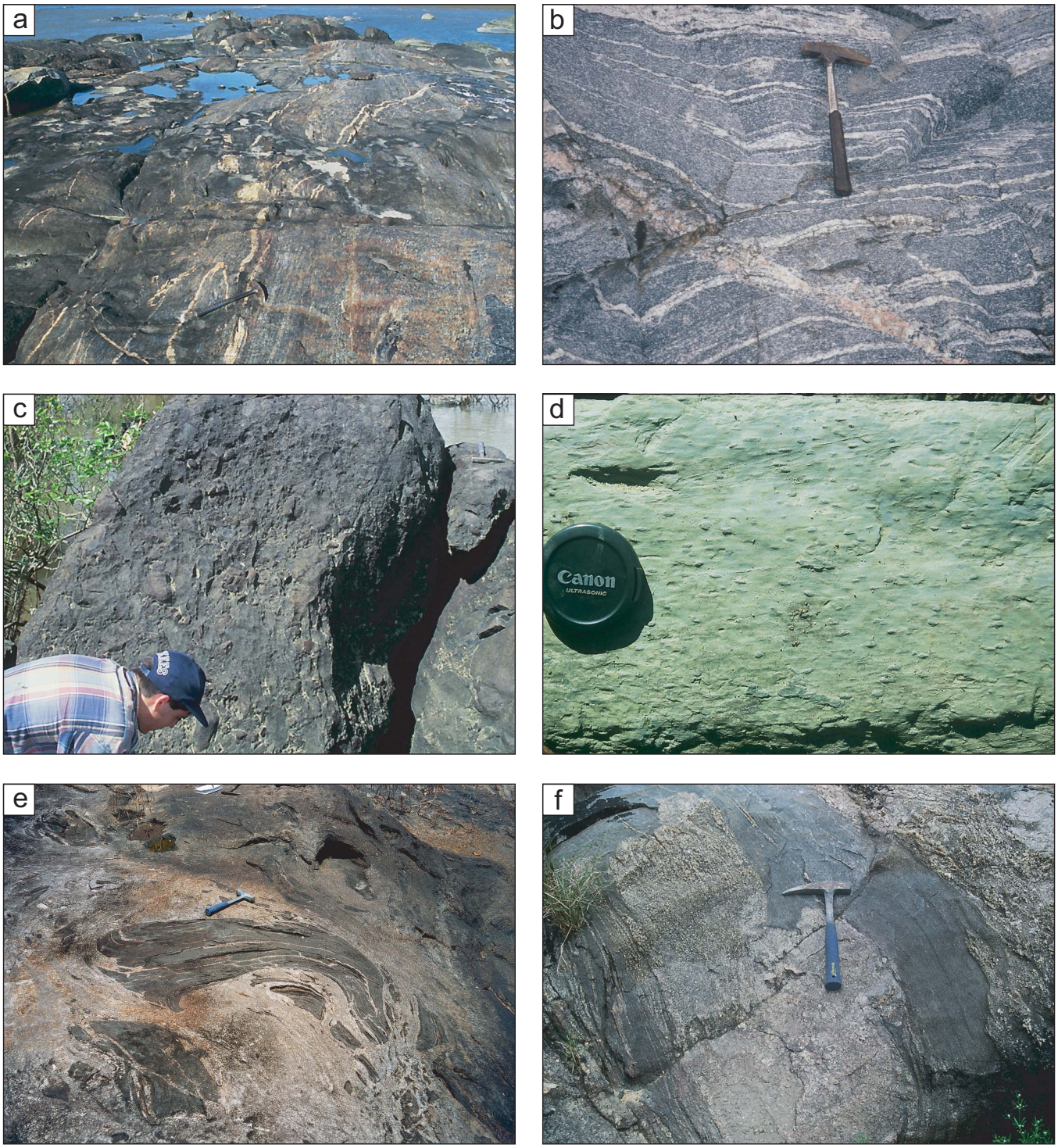

Fig. 5.- Field photographs – a) metagabbro from the Île de Cayenne area; b) tonalite from Carrière Laussat, with indications of *in situ* melting along D2a foliation, and melt collection inside late D2b N145 dextral-normal fault; c) typical volcanoclastics with clasts of the scale of several tens of cm (Tampok river); d) contact metamorphism in pelite at the contact with the Saut Tamanoir granite dated at 2132 ± 3 Ma (Mana river) - elongate spots, constituted of biotite-andalusite intergrowth are underlining a down-dip D1 mineral-stretching lineation at lower pressure conditions; e) granite with basic greenstone enclaves (Oyapok river); f) granite injection with possible inferred way-up melting criteria to the right (north) of the photograph (Oyapok river).

Fig. 5.- Photos de terrain - a) métagabbro de l'Île de Cayenne; b) tonalite de la Carrière Laussat, montrant la fusion in situ *le long des plans de foliation D2a, et la migration de ces jus de fusion le long des plans de cisaillements tardifs D2b orientés N145 et à jeu dextre-normal ; c) formations volcanoclastiques typiques avec présence de clastes de 10 cm de taille (Rivière Tampok); d) métamorphisme de contact dans les pélites au contact du massif granitique de Saut Tamanoir daté à 2132 ± 3 Ma (Rivière Mana) - les tâches allongées sont constituées d'intercroissance à biotite-andalousite soulignant une linéation minérale et d'étirement à fort plongement, pour des pressions de métamorphisme peu élevées ; e) granite à enclaves basiques provenant des ceintures de roches vertes (Rivière Oyapok) ; f) injection de granite avec critère de polarité magmatique éventuel vers la droite (nord) (Rivière Oyapok).*

Tonalitic, trondhjemitic and granodioritic gneiss (22, 23, 24) - Central TTG Complex

A second TTG generation occurs mainly in the central part of French Guiana, forming a batholith that has often been referred to as the "Complexe Guyanais" (Choubert, 1974; Milesi *et al*., 1995). Both the aeromagnetic and the radiometric maps (Figs. 2 and 3) emphasize its contrast with the surrounding greenstone belt. Of special interest is that the radiometric map exhibits peculiar elliptical structures, which can be interpreted as reflecting a stage of successive and interfering pluton emplacement within the main TTG batholith, hereafter defined as the Central TTG Complex. A striking, higher Th-enhanced radiometric response in the middle of this complex (Fig. 2), corresponds to later granitic suite - more details are given later. From a mineralogical standpoint, the rocks consist mainly of well-zoned plagioclase, quartz, biotite and amphibole; K-feldspar (microcline) is quite rare, to moderately developed, and thus the composition is granodioritic to tonalitic.

In the northern part of the Central TTG Complex, the rocks are variably deformed as orthogneiss and locally migmatized. Their compositions include tonalitic and granitic end-members, with aplite- and pegmatite-rich zones developed at their margins. According to Choubert (1974), the granite inside the complex is characterized by a lower amount of microcline and a low lithium content.

The rocks of the southern part of the Central TTG Complex were studied in the Inini River area. They generally show a weak foliation, apart from local zones where magmatic fabrics are concordant with the surrounding metavolcanites, which would suggest a syn- to late-tectonic emplacement. Upstream the Mana River, the granodiorite and tonalite have undergone heterogeneous deformation with a local shallow-dipping penetrative foliation. A major distinction between the Central TTG Complex and the northern and southern TTG domains, is that the Central Complex shows no significant sign of melting. Nevertheless, migmatized TTG remnants are observed within a granitic suite in the Tampok River area, at the eastern limit of the complex between lat. 3°30' and 4° N; further detailed studies are needed to determine whether these remnants are equivalent to the Central TTG formations and whether the southern/northern TTG are also represented.

Basic to ultrabasic suite (25) - "Mahury" and "Tampok" suite

The Mahury suite, in the northern part of French Guiana, concerns Mounts Lucifer, Bois Violet, Gabrielle and Mahury. The gabbro massifs, with a noritic end-member, commonly include pyroxenite and peridotite, and the diorite massifs include saturated diorite, quartz-diorite and granodiorite (Choubert, 1974; Milesi *et al*., 1995). Diorite and tonalite from Mount Mahury have similar geochemical characteristics to those of present-day subduction zones (Milesi *et al.*, 1995; Vanderhaeghe *et al*., 1998).

Massifs are recognized in each section of the Mana River along the southern limb of the Central TTG Complex (Barruol *et al*., 1978). They include gabbro and pyroxenite, and minor serpentinized peridotite; diorite and amphibolite are associated. The rocks are all metamorphosed, hydrothermally altered, and locally deformed.

In the southern part of French Guiana, between lat. 3° and 3°30' N, the Tampok gabbro includes a suite of basic to ultrabasic intrusions with a cumulate character. According to Marot *et al*. (1983), this suite comprises metadiorite, hornblende-bearing metagabbro, metagabbro-norite (clinopyroxene or olivine-rich) and hornblende ± olivine websterite where: i) the metagabbro is unfoliated with a granoporphyroblastic texture and consists of plagioclase, biotite, amphibole, chlorite and quartz; ii) the hornblende-bearing websterite shows a granoporphyroblastic texture with no preserved primary magmatic mineral – the metamorphic paragenesis consists of enstatite, diopside, Mg-hornblende and titanomagnetite; and iii) the metagabbronorite shows polygonal association of ferrosilite, diopside, quartz and Mg-hornblende. Relics of gneiss and charnockite (see later) are found within the Tampok gabbro.

Charnockite and enderbite (26) - "Antecume Pata" suite

In the Maripasoula area, along the Maroni River, the Antecume Pata charnockite-enderbite suite is closely associated with the Tampok gabbro suite. Texture is granoblastic with oligoclase, ferrosilite, biotite, quartz and titanomagnetite. Orthopyroxene shows local recrystallization as aggregates or layers, which can be interpreted as successive steps of protracted high-temperature conditions maintained during the formation of the Tampok gabbroic suite. Amphibole occurs only as a late mineral in the paragenesis.

Greenstone belt (31 to 37) - "Paramaca/Armina" volcano-sedimentary formations

Volcano-sedimentary basins of the Paramaca greenstone belt form two major E-W-trending branches, one to the north and one to the south of the Central TTG Complex, that merge at the western end of the complex to extend westward into Suriname as a single N100-120°-trending greenstone domain. The two branches narrow and also seem to converge on the eastern side of the Central TTG Complex, at the frontier with Amapá State (Brazil); their possible merging in Amapá, however, is hidden by strong granite overprinting (Fig. 4a - also see Fig. 12). The greenstone belt succession

comprises volcanic end-members known as the so-called "Paramaca" formations, and flyschoid-type sediments known as the "Armina" formation (Ledru *et al*., 1991).

The main lithological end-members of this succession are described in the following paragraphs.

Undifferentiated metavolcanites (36)

The volcanic formations within the greenstone facies consist mainly of lavas and pyroclastics (Fig. 5c) whose varied compositions reflect the varied nature of the dismembered source rock (Egal *et al.*, 1994; Milesi *et al.*, 1995). The volcanite compositions vary from basalt to rhyolite end-members, but where no further mineralogical distinction is available they are shown on the map as undifferentiated metavolcanites. For instance, along the Grand Inini and Mana rivers, in the southern part of Central TTG Complex, and at the periphery of Saül, lavas predominate over pyroclastics. Their compositions vary from acid to basic, with no possible subdivision at the 1:500,000 map scale.

Acid to intermediate metavolcanites (34)

North of the Ouaqui River, the metavolcanites are mainly metapyroclastic andesites showing well-preserved microlithic textures despite the low-grade metamorphism. Plagioclase phenocrysts (as laths or aggregates) and Fe-Mg mineral phases (probably pyroxene) in a fine-grained matrix of quartzofeldspathic aggregates, are remnants of the primary magmatic paragenesis. A secondary metamorphic assemblage consists of i) Na-K feldspar as a retrograde product of plagioclase, ii) chlorite, epidote and actinolite as retrograde products of primary Fe-Mg phases, and iii) Mg-hornblende as a partly armoured relict inside actinolite.

The synthesis presented by Marot (1988) gives a comprehensive overview of the acid to intermediate lavas from west to east, i.e. from the Araoua to the Camopi-Alicoto quadrangles. In the westernmost area, he concludes as to the presence of two major volcanic cycles: i) a first, lower, unit made up of coarse-grained pyroclastics reflecting a significant explosive volcanic context - proximal activity was specifically considered for the western Araoua quadrangle; and ii) a second, upper, unit consisting of fine-grained pyroclastics and interbedded tuffisites and sediments, reflecting a more distal explosive activity and/or reworking of the lower unit. Marot (1988) also concludes as to the presence of two formations in the easternmost areas, i.e. a lower dacitic unit and an upper unit characterized by coarse-grained pyroclastics of mainly rhyolitic composition.

It is worth noting that the above-mentioned mineralogical characteristics and preserved textural facies are best documented in the northern part of the southern greenstone branch. Increasingly higher metamorphic conditions southward lead to progressive structural and mineralogical overprinting; this is described in more detail later under *Metamorphism*.

From a geochemical standpoint, the geochemical variations of the basic to intermediate rock types fall within the field of present-day continental-type tholeiite (Milesi *et al*., 1995; Vanderhaeghe *et al*., 1998). The calc-alkaline lavas are described by the above authors mainly as arc-type dacite and soda-rhyolite, similar to ancient tonalite-trondhjemitic suites and to modern adakite from an arc context.

Amphibolite and metabasalt (31)

The amphibolite and metabasalt units are described mainly from the southern greenstone branch, between lat. 3° and 3°30 N (Marot, 1988), where they occur continuously from east to west. In the northern part of the branch, referred to as the Couata-Alikene area by Marot (1988), the metabasite includes both fine-grained facies with a granonematoblastic texture, and amphibolitic schist with relict porphyritic textures. The common paragenesis consists mainly of green-hornblende augite and plagioclase in a matrix of plagioclase, epidote, biotite, sphene, calcite and ore minerals (Marot, 1988). Metamorphic recrystallization under greenschist-facies conditions resulted in a new assemblage of actinolite, K-Na feldspar, epidote and quartz; this strong recrystallization was associated with ductile shearing along the Ouaqui River. Other minor associated facies include coarser grained amphibolite, cumulative-type facies, and vesicular facies with subophitic textures. According to Gruau *et al*. (1985), all these basic lavas correspond to oceanic tholeiite.

In the southernmost part of the southern greenstone branch, the metabasite includes banded amphibolite of inferred basaltic composition, and amphibolitic gneiss of dominant andesitic to basaltic composition. The mineralogy of the latter is dominated by labradorite-bytownite, green hornblende and clinopyroxene. The absence of a relict porphyritic texture contrasts with the northernmost metabasite mentioned above.

In general terms, as regards the basic occurrences of the entire greenstone belt, it is worthwhile noting that pyroxene-garnet assemblages have not been recorded in the highest grade metamorphic rocks.

Ultrabasic lava, mainly komatiite (35)

These rocks, whose origin is inferred to be flows or sills, crop out as variably foliated recrystallized greenschist in the eastern part of the southern greenstone branch. They are closely associated with amphibolitic schist and amphibolite. Tremolite and clinochlore form the dominant mineral

association and define a granonematoblastic texture (Marot *et al*., 1988). From a geochemical standpoint, they have a peridotitic komatiitic composition, although no spinifex texture has been observed. Following BRGM's discovery of diamonds above weathered ultrabasic rock (Marot *et al.*, 1979; Picot, 1982), further work by a Guyanor exploration team led to the rock source being identified as volcaniclastic komatiite (Capdevila *et al*., 1999). The occurrence is located precisely on the 1:500,000-scale map, on the basis of Guyanor field mapping.

Metasediments and metavolcano-sedimentary rocks (32, 33, 37)

Metasediments have been recognized in both the northern and southern branches of the French Guiana greenstone belt. In the southern branch, they alternate at kilometre scale with metavolcanites.

In the northern part of French Guiana, between the Central TTG Complex and the dominant plutonic rocks that can be traced up along the Atlantic coast, metasediments define an arcuate belt that broadens from east to west. The formations consist of alternating fine-grained sandstone, greywacke and pelite. The pelite corresponds to the Orapu Schist described by Choubert (1974), while the dominant sandstone compositions are the equivalent of the Bonidoro Formation of Choubert's classification (op. cit.). Tuffaceous intercalations within the pelite indicate discontinuous volcanic activity. Other compositional layer heterogeneities include lenses of metacarbonates, talc schist, and Fe-Mn-rich facies. At a mesoscopical scale, such an alternance highlight the stratification trends, rather well preserved in a global context marked by low metamorphic grade. Locally, recrystallization and associated foliation are developing close to kilometer-scale plutons, thus pointing to thermal aureoles and contact metamorphism (Fig. 5d).

At regional scale, the broad high-K area shown on the radiometric map (Fig. 3) was checked in the field; it clearly corresponds to dominant pelitic compositions overlying metagreywacke. Similar radiometric responses, i.e. high potassium and thorium content, were recorded in the southern greenstone branch where field checking showed them to represent metapelite.

In the southern greenstone branch, the exposed metasediments are a higher-grade metamorphic equivalent of above-mentioned pelite. Biotite-garnet gneiss and biotite-garnet ± sillimanite-bearing gneiss become dominant south of lat. 3°- 3°30 N. They exhibit a granonematoblastic texture of plagioclase, biotite, garnet and quartz, with the biotite marking a rough foliation, in places with sillimanite. More basic compositions are represented by foliated two-mica - amphibole gneiss, as well as by banded rocks with a rather heterogranular granonematoblastic texture.

Sandstone and quartzite (19) with intercalations of conglomerate (20) and pelite (21) - "Rosebel/Bonidoro" upper detrital basin

The so-called "Bonidoro" formation (Choubert, 1960, 1974) defined as the Upper Detrital Unit by Milesi *et al*. (1995), occurs in a succession of basins on the northern margin of the Central TTG Complex, and is the equivalent of the Rosebel Formation in Suriname (Bosma *et al*., 1983). It comprises sandstone and quartzite, and both mono- and polygenic conglomerate; these reflect river-type deposits, among which various types have been individualized (Vinchon *et al*., 1988; Ledru *et al.*, 1991, Manier, 1992; Manier *et al*., 1993). Inherited clasts seem to reflect the wide spectrum of regionally contiguous formations (siltite, sandstone, greywacke, volcanite and granitoid, as well as some hydrothermal equivalents). Microgranite sills have been described at the base of the formation.

Considering its significant depth, with a maximum of 5000 m for the western Mana Basin, these structures have been referred to as the North Guiana Trough (Milesi *et al*., 1995). They are interpreted as "pull-apart" basins formed in a sinistral strike-slip context (Ledru *et al*., 1991; Egal *et al*., 1992).

Granitic association and coeval migmatite (10 to 12, 14 to 18)

Previously defined as "Caraïbe"-type granitoid by Choubert (1974), this suite of granite (*sensu lato*) and associated migmatite is well developed in the southern and western parts of French Guiana. The granodioritic terms are also well expressed near the Oyapok River in the eastern part of the country, as well as in the core of the Central TTG Complex (as reflected by the high thorium content shown on the radiometric map - Fig. 3). They comprise K-feldspar (microcline and perthitic orthoclase), quartz, plagioclase, green biotite, green amphibole and titanite. Detailed field work along the Oyapok River, and its related creeks, has revealed many transitional facies between i) true magmatic facies, ii) diatexite, i.e. anatectic granitic melt with weak and vague evidence of centimetre-scale biotite-bearing protolith remnants, and iii) areas of clear protolith melt lithologies that gave rise to the granitic melts. Such protolith remnants include grey gneiss of possible sedimentary origin, tonalite to granodiorite of probable magmatic origin, and basic lenses similar to greenstone-belt metavolcanics. In some cases, the amount of basic lenses in the granodiorite matrix can exceed 60%.

Similar unequivoquial evidence of protolith melting can be seen in the northern TTG coastal area mentioned earlier; in the Laussat quarry, for example, the evidence shows that the migmatisation clearly originated as *in situ* synfolial melting of the metatonalite (Fig. 5b). In the southern part of

French Guiana, the dominant granodiorite, monzogranite and syenite (in part) compositions show strong similarities with metaluminous Mg-K magmatism, as reflected in particular by compositions with amphibole-pyroxene; whenever hyperpotassic mafic end member seems lacking. Other dominant terms of this granite suite (*sensu lato*) are defined in the northern part of the country by porphyritic monzogranite and peraluminous leucogranite, while in the central part of the southern greenstone branch a porphyritic granodiorite, several tens of kilometres long, exhibits a specific horseshoe shape and cuts all the greenstone-belt lithologies. It can be recognised on radiometric map (Fig. 3) where it is enhanced by high Thorium content.

All these varied granitic associations are syn- to late-tectonic as regards the major E-W regional ductile deformation trends. Despite penetrative deformation, some melt layers show locally melt extrusion which suggest way-up criteria (Fig. 5f) (Burg, 1991). Metaluminous monzogranite and pegmatite, best expressed along the Atlantic coast, are considered as late synkinematic magmatic products of these granitic associations (*sensu lato*).

From a geochemical standpoint, the biotite-bearing tonalite and granite show geochemical affinities with the mid-potassic plutonic rocks found in subduction zones (Milesi *et al*., 1995; Vanderhaeghe *et al*., 1998).

Gabbro (13)

Gabbroic plutons, with both amphibole-rich and pyroxene-rich end-members, are exposed within the greenstone belts in the northeastern part of French Guiana. The amphibole-bearing gabbro is weakly foliated and contains green amphibole, plagioclase and biotite. The pyroxene-bearing gabbro is less common and is constituted by recrystallized plagioclase and anhedral orthopyroxene. Coarser-grained facies at Saut Athanase show better preserved magmatic textures.

Rhyolite (9) - “Belvedere Mounts” rhyolite

The rhyolite in the Belvedere Mounts, to the west of the Mana River, corresponds to the Upper Rhyolite Unit mapped by Barruol *et al*. (1978). Although these authors integrated the unit in the greenstone belt, our own observations point to an absence of deformation. Also, a single drill-core observation shows that it cross-cuts the volcanic formations. At regional scale, the inferred area mapped for these formations corresponds to a striking high-K content on the radiometric map (Fig. 3). The limit of this anomaly was therefore used to define the boundary of the Belvedere Mounts rhyolite.

Dolerite/microgabbro dykes (6, 7, 8) - “Apatoe”, “Tampok” and “Comté” dyke swarms

Dyke swarms cut all the above Precambrian lithologies. The major swarm is in the northeasternmost part of French Guiana, close to the mouth of the Oyapok River. A few tens of dykes, 10-50 km long, are characterized on the aeromagnetic map (Fig. 2) by N160° trends; they are also plotted on the 1:500,000-scale geological map (Fig. 4). Farther west, on the northern limb of the Central TTG Complex, we find more widely spaced WNW-ESE-trending dykes, while in the western part of the country, the dykes revert to a more northwesterly trend. Both the NNW-SSE and WNW-ESE trends have been dated at between 190 and 200 Ma (Deckart, 1996; Deckart *et al*., 1997; Nomade *et al*., 2000; Nomade 2001). In other words, most of the dykes exposed on the Atlantic coast are related to the “Central Magmatic Atlantic Province” (Courtillot and Renne, 2003) whose emplacement at the Triassic-Jurassic boundary was linked to the fracturing of Pangea prior to the opening of the Atlantic Ocean. On the basis of paleomagnetic and argon data, which give two groups of magnetic remanences estimated at 198.3 ± 2.0 Ma and 192.3 ± 1.5 Ma, Nomade *et al.* (2000) conclude on the presence of two stages within the 190 - 200 Ma age span. Moreover, by using the anisotropy of magnetic susceptibility fabrics, they suggest that the Early Jurassic dyke swarm may have originated from horizontal magma fluxes from a distant magma source possibly located to the southeast.

Besides these well-known Mesozoic occurrences, which mark the precursor stages of the Atlantic Ocean opening, two other main dolerite trends have been defined in the field:

- a NNE-SSW trend corresponding to the axis of major rivers such as the Comté and the Oyapok. By analogy with the Proterozoic Avanavero dolerite trends from Suriname, this NNE-SSW generation is probably of Paleoproterozoic age, as suggested by weakly constrained Ar-Ar data on biotite (Deckart *et al*., 1997).

- a NW-SE trend of hitherto unknown age, but dated as Neoproterozoic by K-Ar dating in the course of our work (see details in the following section and Appendix B).

Phanerozoic sedimentation (1 to 5)

Quaternary deposits define the Atlantic coast, but their study is beyond the scope of this paper.

Geochronology

More than 100 isotopic investigations were carried out for the new 1:500,000-scale Geological Map of French Guiana - mainly Pb-Pb dating on zircon (TIMS) together with U-Pb dating on zircon (SIMS), U-Th-Pb dating on monazite (EPMA), and Sm-Nd model age determinations on

Number	Age	Reference	Number	Age	Reference	Number	Age	Reference
1	2069 ± 4 Ma $\varepsilon^{2.07} = -0.2$	C3 C4	22	$\varepsilon^{2.14} = +2.0$	C4	45	2156 ± 6 Ma	A2
2	$\varepsilon^{2.14} = +0.8$	C4	23	2141 ± 8 Ma	C3	46	2109 ± 7 Ma $\varepsilon^{2.11} = -1.3$	E2
3	$\varepsilon^{2.14} = +1.6$	C4	24	2124 ± 3 Ma $+0.5 < \varepsilon^{2.13} < +2.0$	C3 C4	47	2163 ± 3 Ma $\varepsilon^{2.17} = +1.8$	D3 CD4
4	2172 ± 2 Ma	D3	25	2137 ± 6 Ma	C3	48	2098 ± 2 Ma	B3
5	$\varepsilon^{2.14} = -3.7$	C4	26	2089 ± 4 Ma	C3	49	[> 2.32 Ga] $\varepsilon^{2.10} = -2.9$	D3 CD4
6	2132 ± 3 Ma $\varepsilon^{2.13} = +0.4$	C3 C4	27	2089 ± 4 Ma	C3	50	2103 ± 12 Ma (2.65 Ga) $\varepsilon^{2.10} = +1.8$	D2 CD4
7	$\varepsilon^{2.14} = -8.6$	C4	28	2202 ± 5 Ma $\varepsilon^{2.20} = -2.2$	E3 E4	51	[2.77 - 3.18 Ga]	B3
8	2060 ± 4 Ma (2.90 Ga) $\varepsilon^{2.06} = +1.1$	A2 AC4	29	2135 ± 2 Ma $\varepsilon^{2.13} = -0.2$	E3 E4	52	[> 2.93 Ga] $\varepsilon^{2.10} = -1.0$	D2 CD4
9	(2.09 - 2.15 Ga)	D3	30	2147 ± 5 Ma	A3	53	$\varepsilon^{2.13} = +3.4$	CD4
10	2152 ± 8 Ma	C3	31	2136 ± 3 Ma $\varepsilon^{2.14} = +1.2$	E3 E4	54	2098 ± 2 Ma	B3
10b	$\varepsilon^{2.14} = -3.3$	C4	32	2149 ± 4 Ma	E3	55	2128 ± 10 Ma $\varepsilon^{2.13} = +0.9$	D2 CD4
11	2146 ± 2 Ma $+2.2 < \varepsilon^{2.15} < +2.3$	F1 F4	33	2148 ± 3 Ma	A3	56	2094 ± 6 Ma	A2
12	2148 ± 4/-3 Ma $+2.2 < \varepsilon^{2.15} < +2.3$	F1 F4	34	2131 ± 6 Ma $\varepsilon^{2.13} = +1.7$	E2 E4	57	$\varepsilon^{2.10} = -0.3$	CD4
12b	> 1800 Ma	F5	35	[2.2 Ga] $\varepsilon^{2.20} = +0.8$	E3 E4	58	$\varepsilon^{2.10} = -1.3$	CD4
13	2208 ± 12 Ma	A2	35b	2155 ± 3 Ma	C3	59	$\varepsilon^{2.10} = +1.6$	CD4
14	2173 ± 2 Ma (2.22 Ga)	A3	36	2112 ± 2 Ma	D3	60	2090 ± 2 Ma	C3
14b	2165 ± 6 Ma	C3	37	809 ± 29 Ma	F5	61	2161 ± 3 Ma	C3
15	2144 ± 2 Ma	A3	38	$\varepsilon^{2.14} = -5.3$	C4	62	2090 ± 8 Ma	A2
16	2132 ± 3 Ma	C3	39	$\varepsilon^{2.14} = -3.4$	C4	63	[2.17 Ga] [2.17 Ga] 2094 ± 7 Ma $\varepsilon^{2.10} = -3.7$	A6 A2 A2 C4
17	2092 ± 3 Ma	A3	40	$\varepsilon^{2.14} = -5.6$	C4			
18	2084 ± 6 Ma	A3	41	$\varepsilon^{2.14} = -10$	C4	64	2100 ± 1 Ma	D3
19	2093 ± 3 Ma	A3	42	$\varepsilon^{2.14} = +1.9$	C4	65	2160 ± 6 Ma	C3
20	2092 ± 4 Ma	C3	43	2138 ± 4 Ma $\varepsilon^{2.14} = +1.9$	C3 C4	66	2183 ± 3 Ma	D3
21	2129 ± 3 Ma	A3	44	$\varepsilon^{2.14} = -0.6$	C4	67	2104 ± 2 Ma	D3
Values given in Ma correspond to the age of rock emplacement. Values given in Ga are for hosted rocks (which age is given in Ma), partially derived from an older rock (which age is given in Ga). ε^{t}_{Nd} values display the $^{143}Nd/^{144}Nd$ evolution of rocks compared to the bulk composition of the Earth (CHUR) at the time of their formation (t). Positive values indicate a juvenile source for the rocks while negative values reveal the presence of a reworked crustal component.						68	2104 ± 2 Ma [2.14 - 2.19 Ga]	D3
						69	2095 ± 6 Ma 2061 ± 15 Ma	A6

GEOCHRONOLOGY AND ISOTOPE GEOCHEMISTRY: Measurements of absolute ages (performed or compiled) are numbered on the map and displayed in the table. Geochronological laboratories and radiometric methods used for dating are listed by a letter and a number,

(A) Alain Cocherie - brgm - Orléans
(B) Valter Gama de Avelar UFPa - Belém
(C) Catherine Guerrot - brgm - Orléans
(D) Jean-Michel Lafon - UFPa - Belém
(E) Jean-Jacques Peucat - Géosciences - Rennes
(F) Available previous data
(1) U-Pb zircon (TIMS)
(2) U-Pb zircon (ion microprobe)
(3) Pb - zircon (evaporation)
(4) Sm-Nd
(5) Ar-Ar and/or K-Ar
(6) Monazite (electron microprobe)

Table 1.- Details of the isotopic data shown on the 2nd edition of the 1:500,000-scale Geological Map of French Guiana.

Tabl. 1.- Liste des données isotopiques utilisées pour l'établissement de la seconde édition de la carte géologique à 1/500 000 de Guyane.

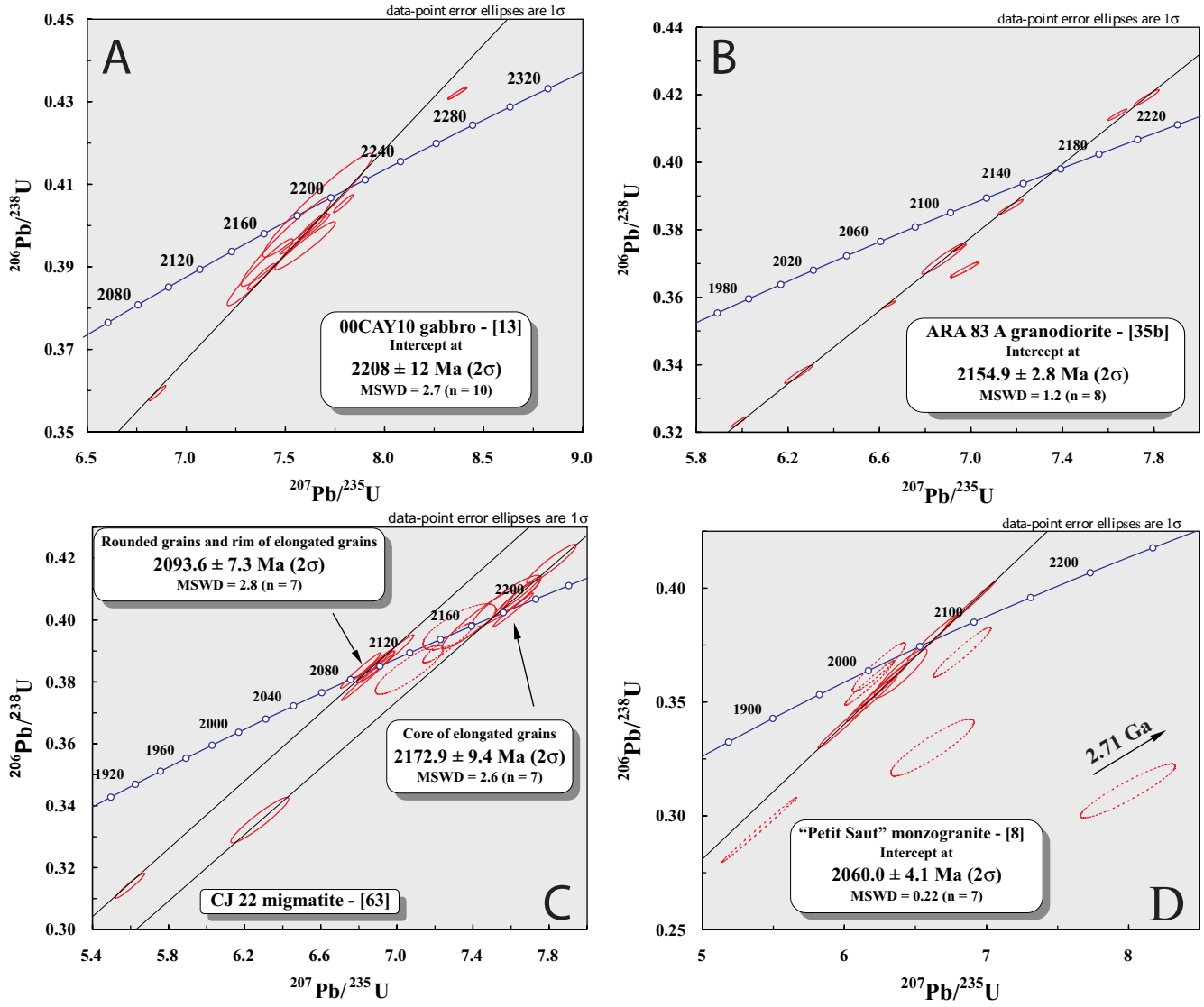

Fig. 6.- Concordia diagrams for the samples dated by the U-Pb method on zircon, using an ion microprobe. A, B, D = U-Pb dating by Cameca IMS 1270; C = U-Pb dating by Shrimp II.

Fig. 6.- Diagramme concordia pour les échantillons datés par la méthode U-Pb sur zircon, par microsonde ionique. A, B, D = Datation U-Pb par Cameca IMS 1270 ; C = Datation U-Pb par Shrimp II.

whole rock. The results are listed in the legend of the geological map (Delor *et al.*, 2001) and are given in Table 1.

Here we use a selected set of 24 representative geochronological results, obtained mainly on magmatic rocks by Pb-evaporation and U-Pb on zircon, U-Th-Pb on monazite and K-Ar on whole rocks, as well as other available ages, to re-assess the absolute chronology of the Paleoproterozoic terrains in French Guiana. The corresponding isotopic data are listed in Tables 2, 3, 4 and 5 respectively for Pb-evaporation on zircon, U-Pb (SIMS) on zircon, U-Th-Pb (EPMA) on monazite, and K-Ar on whole rocks. Full sample descriptions and geochronological results are given in Appendix B, together with a brief description of the experimental procedures. With all the samples, the name is followed by a bracketed number corresponding to its reference number on the geological map. Some of the Pb-evaporation data in table 1 differ slightly from those given on the Geological Map of French Guiana; this is due to a re-appraisal of the data reduction and a re-calculation of the ages, but does not affect the interpretation of the age.

All the isotopic results fall within a range between 2.22 and 2.06 Ga, which confirms that the entire Transamazonian evolution of French Guiana occurred during the Rhyacian.

The U-Pb age of 2208 ± 12 Ma (Fig. 6A) obtained for the crystallization of the "Pointe des Amandiers" Fe-gabbro (00CAY10-[13]) confirms that the "Île de Cayenne" trondhjemite/gabbro complex represents the earliest rock-

forming event of the Transamazonian orogeny. This new result, taken together with i) the age of 2216 ± 4 Ma obtained by Vanderhaeghe *et al*. (1998) on inherited zircons from a 2.17 Ga trondhjemite (CAY18A-[14]), ii) the age of 2202 ± 5 Ma given by detrital zircons from a garnet-bearing mica schist (Z125-[28]) from the southern branch of the greenstone belt, and iii) the age of *ca.* 2.2 Ga yielded by an associated TTG sample (Z263A-[35]), point to a range of 2.22 - 2.20 Ga for the first magmatic episode (Eorhyacian) in the evolution of the eastern Guiana Shield, rather than *ca*. 2.17 Ga proposed by Vanderhaeghe *et al.* (1998) on the basis of the age obtained on "Île de Cayenne" trondhjemite.

Dating of 10 granitoids showing TTG magmatic features and of one metaandesite from the greenstone belt, furnished ages ranging from 2183 ± 3 Ma to 2132 ± 3 Ma. However, the ages of the dated granitoids are not evenly distributed within this range – seven yielded Pb-evaporation and U-Pb ages between 2183 ± 3 Ma and 2154.9 ± 2.8 Ma (fig. 6B: ARA83A-[35b]; fig. 7A: 74-98OY-[66]; fig. 7B: 40-98OY-[61]; fig. 7C: 50-98OY-[65]; fig. 7D: B107-[47]; fig. 7E: Laussat-[4]; fig. 7F: 00CAY9f-[14b]), and three, plus the metaandesite sample, gave ages between 2141 ± 8 Ma and 2132 ± 3 Ma (fig. 7G: CG60-[23]; fig. 7H: GC269-[25]; fig. 7I: DAC147-[16]; fig. 7J: MA29A-[6]). The results indicate a main period of TTG magmatism at *ca.* 2.18 - 2.16 Ga and 2.14 - 2.13 Ga with a lack of geochronological values in the 2.16 - 2.14 Ga range. This gap suggests a quiescent period of about 20 Ma between the older and the younger magmatic episodes, although taking the errors on the ages into consideration, we could be considering a period of only 5 Ma and, therefore, one that is only apparent.

A significant number of geochronological results from other TTG granitoids in French Guiana (plotted on the geological map) give ages in the 2.18 - 2.13 Ga range. This is exemplified by the Pb-evaporation age of 2138 ± 4 Ma obtained on zircon in a metarhyolite (INI42-[43]) from the Camopi River and the U-Pb (SIMS) zircon age of 2128 ± 10 Ma displayed by a granodiorite (B64a-[55]) from the Oyapock River, upstream the Camopi River. It is also exemplified by the U-Pb (SIMS) zircon age of 2131 ± 6 Ma and the Pb-evaporation zircon age of 2136 ± 3 Ma yielded respectively by a tonalite (Degrad-R-[34]) and a monzogranite (Z136-[31]) from the southwest of the country.

Values between 2.16 Ga and 2.14 Ga have also been observed in this dataset. For example, U-Pb (TIMS) zircon ages of 2146 ± 2 Ma and 2148 +4/-3 Ma from a metarhyolite and a granodiorite, respectively, in the St Elie district (Lafrance *et al.*, 1999), a U-Pb (SHRIMP) zircon age of 2156 ± 6 Ma from a metarhyolite (L213-[45]) in southeastern French Guiana, and Pb-evaporation ages of 2144 ± 6 Ma on zircon from a tonalite (Cay12A-[15]) close to Cayenne (Vanderhaeghe *et al*., 1998), and of 2152 ± 8 Ma on a rhyolite (Cr.Infirme-[10]) from northwestern French Guiana. A banded orthogneiss from northern French Guiana, close to the Atlantic coast, also belongs to the TTG magmatism, but its age of emplacement is not well constrained - Pb-evaporation dating furnished values between 2.09 and 2.15 Ga (sample Remy - [9]).

The above results reinforce the hypothesis that the lack of ages between 2.16 Ga and 2.14 Ga, is only apparent and that the geochronological data would be better explained by a multi-pulse or protracted model for the 2.18 - 2.13 Ga magmatism. That this TTG magmatism may have continued slightly longer, i.e. until 2.12 Ga, is suggested by the Pb-evaporation zircon age of 2124 ± 3 Ma obtained on a granodiorite (GC27-[24]) from the central-western part of the country. Vanderhaeghe *et al*. (1998) also indicated the existence of tonalite as young as 2115 ± 7 Ma, with inherited zircons at about 2129 ± 6 Ma (sample Reg27-[21] - Pb-evaporation on zircon), but as the calc-alkaline pluton is located in the northeastern part of the country, which underwent migmatization at about 2.10 Ga (see later), the younger age of the tonalite may represent a resetting by migmatization and the older age (*ca*. 2.13 Ga) a magmatic age for the zircons. Finally, a Pb-evaporation zircon age of 2135 ± 3 Ma has been obtained for a Fe-hastingsite-bearing syenogranite (Z132-[29]) related to the Tampok basic-ultrabasic suite.

The distribution of the ages of the TTG magmatism seems to be roughly dependent on the geographical location of the dated rocks. The 2.18 - 2.16 Ga ages were mostly obtained on granitoids from the northern and the south-central parts of the country, while ages in the 2.15 - 2.13 Ga range are dominant in the Central TTG Complex. Such a geographical pattern in the ages, with older northern and southern domains surrounding a younger central area, is significant from a geodynamic standpoint and is discussed later in a specific chapter.

The Sm-Nd age of 2.11 Ga obtained by Gruau *et al*. (1985) from komatiite and andesite in the southern branch of the greenstone belt, and the Rb-Sr age of 2.00 ± 0.07 Ga obtained on associated granitoid, are significantly lower than those available in the northern branch, suggesting a southward younging trend for the greenstone belt. However, the large error on the Sm-Nd (± 90 Ma) and Rb-Sr (± 70 Ma) ages, as well as the fact that the rocks have been metamorphosed - which may have affected the Sm-Nd isotopic system - do not allow us to conclude on this hypothesis. Nevertheless, the existence of detrital zircon as young as 2090 ± 8 Ma in an enclave of magnetite-bearing quartzite (JM18-[62] - U-Pb (SIMS) zircon age) within TTG granitoid from southwestern French Guiana indicates that the hypothesis of the existence of late Rhyacian greenstone belt cannot be discarded.

Basic and ultrabasic magmatism also occurred during Mesorhyacian times (cf. the basic-ultrabasic Tempok suite),

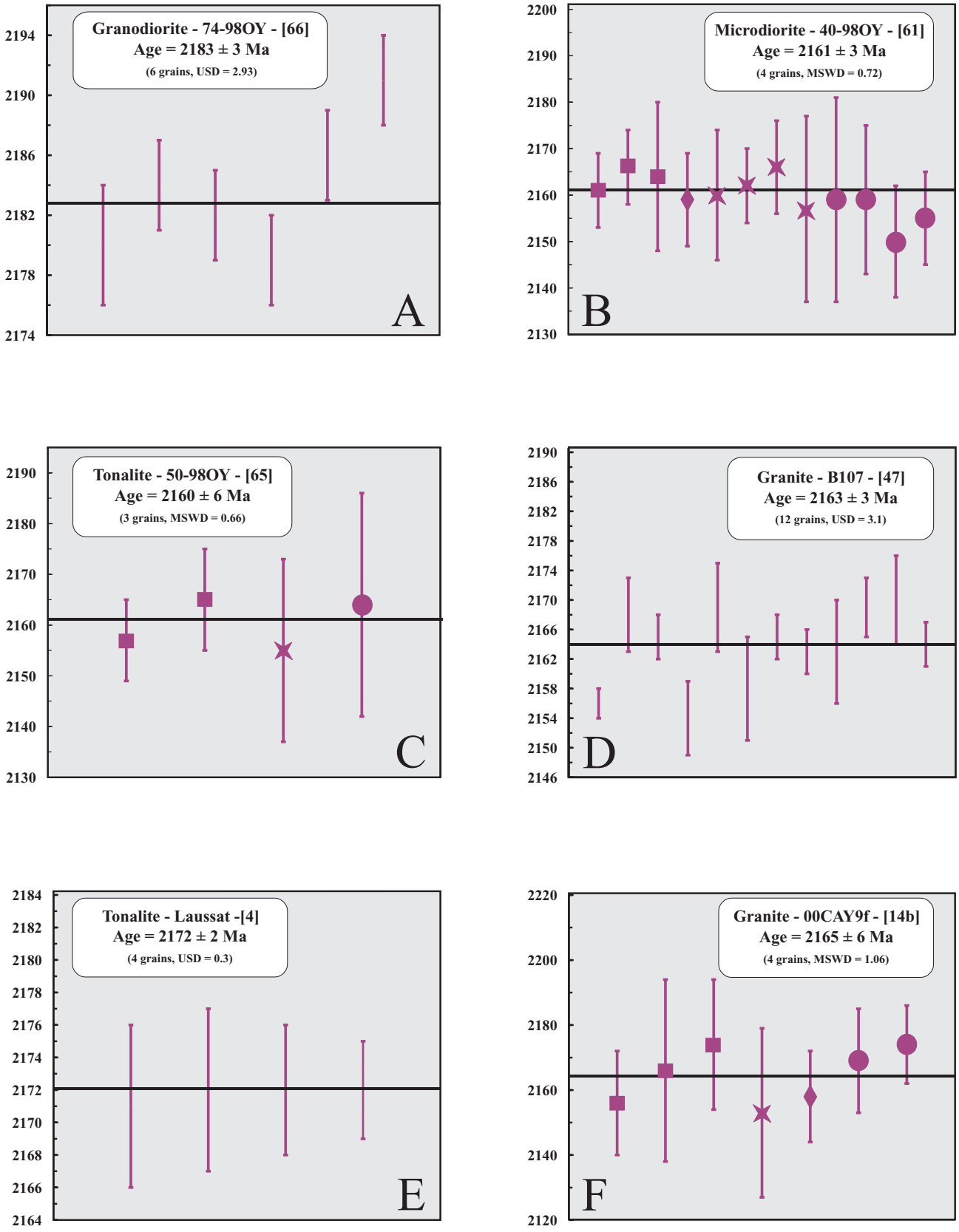

Fig. 7.- Pb-evaporation diagrams for the dated samples from French Guiana. For the samples dated at the Belém laboratory, the error bars correspond to the mean age value on each zircon. For the samples dated at the BRGM laboratory, the error bars correspond to the mean value on each step. The different step-heating of each grain are identified by the same symbol.

Fig. 7.- Diagramme d'évaporation du Plomb pour les échantillons datés de Guyane. Pour les échantillons datés au laboratoire de Belém, les barres d'erreur correspondent à la valeur moyenne pour chaque zircon. Pour les échantillons datés au BRGM, les barres d'erreur correspondent à la valeur moyenne pour chaque étape d'évaporation. Les différentes étapes d'évaporation pour un même zircon sont identifiées par un même symbole.

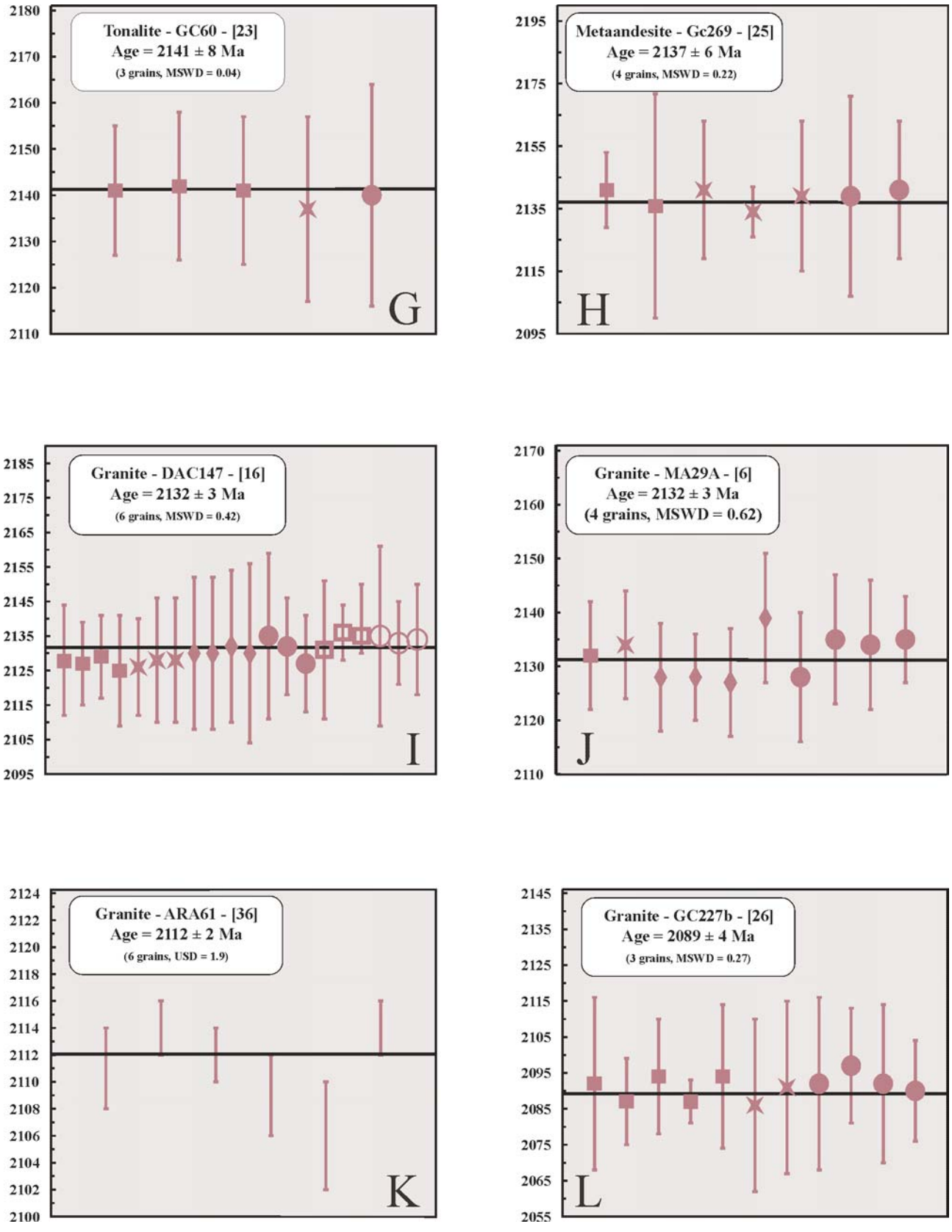

Fig. 7.- Suite/continued.

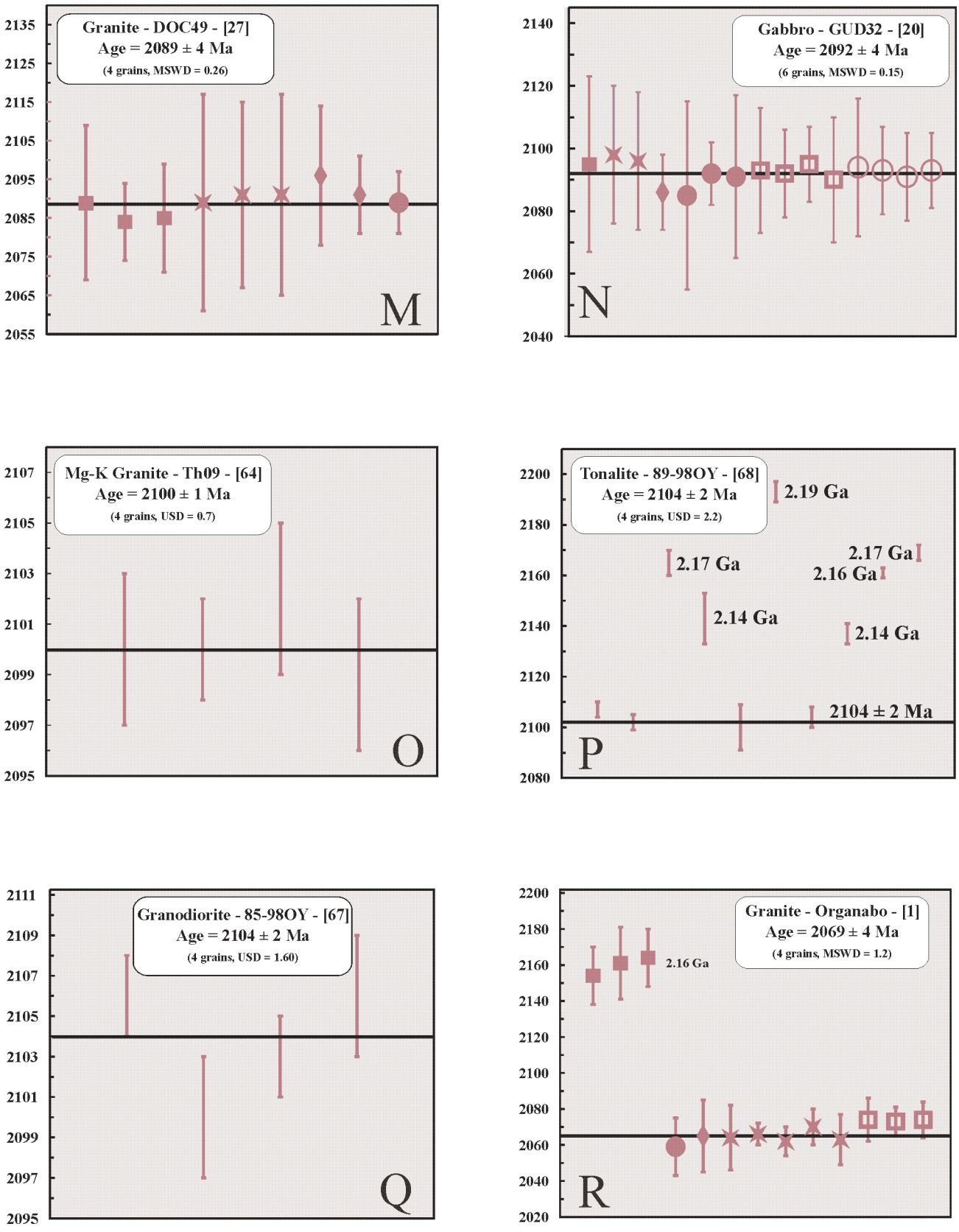

Fig. 7.- Suite/continued.

mainly in the southern part of the country where it is spatially associated with the greenstone belt. A diorite associated with this basic - ultrabasic magmatism in southwestern French Guiana provided a Pb-evaporation zircon age of 2147 ± 5 Ma (ITA40A-[30]).

The Pb-evaporation method on zircons from another generation of granitoids, with petrological and geochemical characteristics differing from those of the 2.18-2.13 Ma TTG granitoids, provided a range of ages between 2.11 Ga and 2.08 Ga. Most of these younger ages are interpreted as magmatic ages defining a main magmatic episode during Neorhyacian times. The older granite, which furnished an age of 2112 ± 2 Ma (ARA61-[36] - Fig. 7K), also yielded a slightly older U-Th-Pb (EPMA) age of 2127 ± 10 Ma on monazite (Fig. 8A). Whether the true crystallization age is 2112 Ma or 2127 Ma cannot, at present, be determined. The younger granitoids (GC227b-[26] - Fig. 7L; DOC49-[27] - Fig. 7M) yielded the same age of 2089 ± 4 Ma. Different kinds of magmatic rock were produced during this episode, as shown by the age of 2092 ± 4 Ma for a gabbro (GUD32-[32] - Fig. 7N) from the Approuague River, the age of 2109 ± 7 Ma for a biotite-amphibole-bearing granodiorite (M76-[46]) from the horseshoe body that cross-cuts the southern branch of the greenstone belt in its central part, and the age of 2100 ± 1 Ma for a Mg-K-rich granite (TH09-[64] - Fig. 7O) from the southwesternmost part of French Guiana.

The other dated granitoids are of peraluminous granite, considered to be derived from the partial melting of Paleoproterozoic continental crust. This episode has been well documented by Pb-evaporation zircon results obtained by Vanderhaeghe *et al*. (1998) on samples from northeastern French Guiana (e.g. Maripa-[17]: 2094 ± 5 Ma; Reg 25-[19]: 2093 ± 8 Ma; Reg26-[18]: 2084 ± 8 Ma, as well as by other U-Pb and Pb-Pb zircon dating on rocks from southeastern French Guiana, mainly along the Oyapok River, such as the gabbroic body close to Camopi village (B91-[54]: 2098 ± 2 Ma) and the amphibole-bearing syenite in the extreme southeast of the country (35-98OY-[60] - 2090 ± 2 Ma) or that in the extreme southwest (Z206-[56] - 2094 ± 6 Ma). This magmatic episode, within the range of 2.11 - 2.08 Ga, has also been recognized by Pb-evaporation dating on zircon from rocks in the neighbouring region in Brazil (northern Amapá State) where Avelar (2002) and Avelar *et al.* (2002) published ages around 2.11 Ga and 2.09 Ga on similar granitic rocks. Pegmatites were also produced during this magmatic episode, as shown by the U-Th-Pb (EPMA) age of 2095 ± 6 Ma obtained on monazite from a pegmatite (89-98RC1-[69]; Fig. 8B) in the Roche Corail area of northeastern French Guiana. However, the existence of one grain with a younger age of 2061 ± 15 Ma (Fig. 8C) suggests that the pegmatite crystallization may be younger, i.e. about 2.06 Ga, and due to the melting of 2.11 - 2.08 Ga granite. At present we have no field constraints for determining whether 2095 Ma or 2061 Ma represents the true age of crystallization.

Migmatization at about 2.10 Ga was also associated with this magmatic event. For example, a migmatitic granodiorite (B85-[50]) yielded a U-Pb (SIMS) zircon age of 2103 ± 12 Ma, which could correspond to either the crystallization age of the magmatic protolith or the age of the migmatitic event, and a granodioritic orthogneiss (85-98OY-[67] - Fig. 7Q) along the Oyapok River in southeasternmost French Guiana furnished a similar Pb-evaporation zircon age of 2104 ± 2 Ma. A tonalite (89-98OY-[68] - Fig. 7P) from the same area in southeasternmost French Guiana is considered to have undergone a melting event dated at 2104 ± 2; older ages between 2.14 Ga and 2.19 Ga obtained on inherited zircons from this rock indicate that the tonalitic protolith belonged to the Mesorhyacian TTG magmatism. The existence of coeval granite (85-98OY-[67] - Fig. 7Q) with the same age as the migmatization event suggests that the migmatization and the formation of the peraluminous granite belong to the same melting event.

The migmatization event has also been registered by zircon from a migmatite (CJ22-[63]) in southwestern French Guiana, which furnished a U-Pb (SHRIMP) age of 2093.6 ± 7.3 Ma (Fig. 6C); the protolith, supposedly of metasedimentary origin, was dated by another population of zircons from the same rock at 2173 ± 9.4 Ga. Monazites from the same rocks do not registered this migmatization event, but furnished U-Th-Pb (EPMA) ages of 2167 ± 19 Ma (melanosomes; Fig. 8D) and 2172 ± 4 Ma (paleosome; Fig. 8E) interpreted in the same way as the zircon ages.

Two samples of tonalitic–granodioritic orthogneiss, which intrudes the metasedimentary sequences from the western part of the southern branch of the greenstone belt and occurs in a migmatitic context, provided Pb-evaporation zircon ages of 2149 ± 4 Ma (ITA46-[32]) and 2148 ± 3 Ma (ITA64b-[33]). These values are considered as the magmatic age of the zircon rather than the age of the migmatitic event. The age of migmatization is therefore not constrained by the isotopic results, which constitute further evidence of the Mesorhyacian TTG magmatic event. A phase of regional sinistral deformation is associated with this magmatic / metamorphic episode, as shown by the Pb-evaporation age of 2098 ± 2 Ma given by zircons extracted from a syntectonic vein within migmatitic granodiorite (B102-[48]) from the Oyapok River, close to Camopi village.

A late generation of meta-aluminous monzogranite has provided the youngest magmatic ages in French Guiana, as shown i) by the 2069 ± 4 Ma age obtained by Pb evaporation on zircon from the “Organabo” biotite granite (Organabo-[1] - Fig. 7R) and ii) by the age of 2060 ± 4 Ma obtained by U-Pb (SIMS) on zircon from the “Petit Saut” two-mica granite (Petit Saut-[8] - Fig. 6D), both located in the northern part of the country. A similar age of 2059 ± 23 Ma was obtained by U-Th-Pb (EPMA) on monazite extracted from the same “Petit Saut” granite (Fig. 8F).

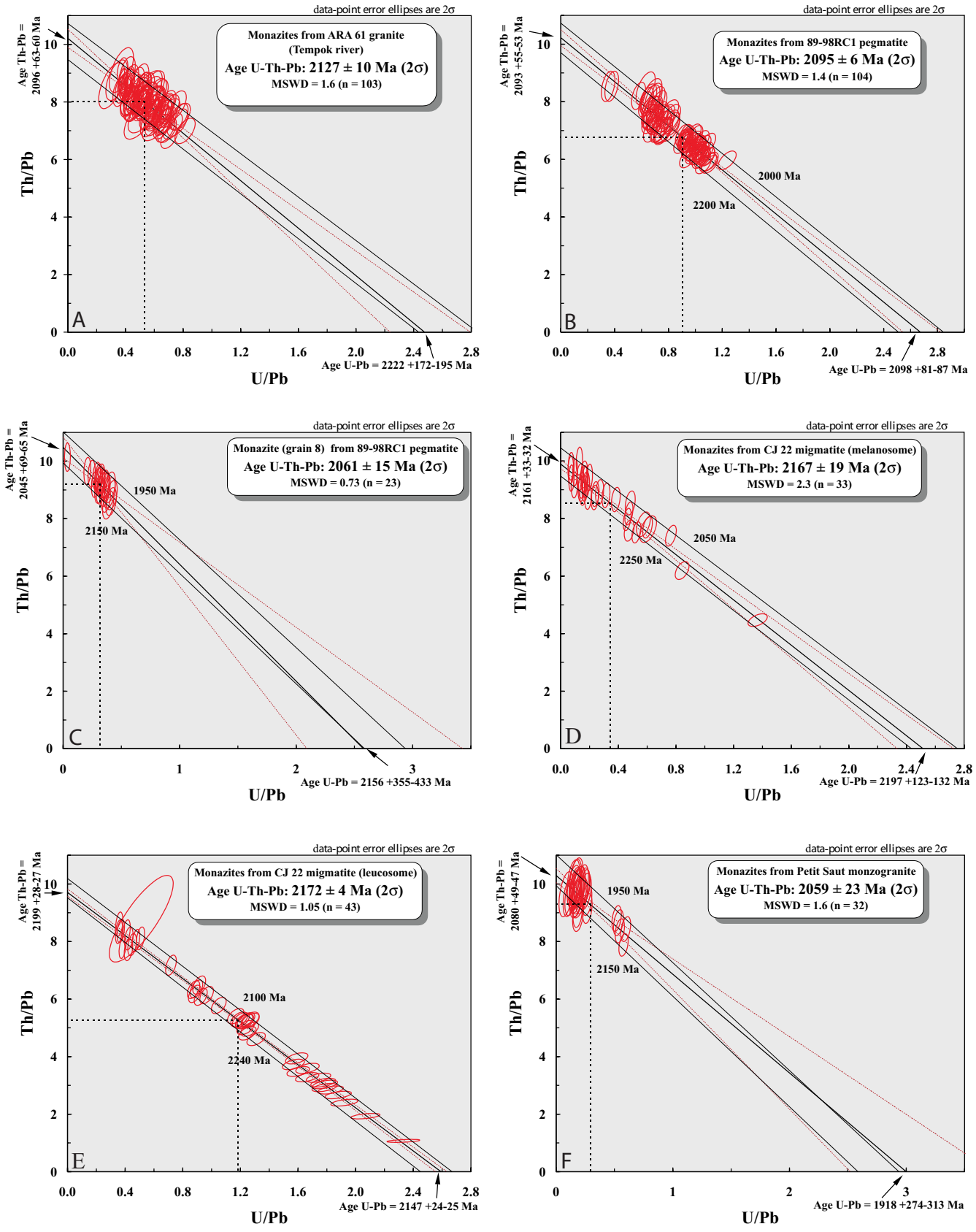

Fig. 8.- Th/Pb versus U/Pb diagrams for monazite dated by the U-Th-Pb (EPMA) method.

Fig. 8.- Diagrammes Th/Pb versus U/Pb pour les monazites datées par la méthode U-Th-Pb (méthode EPMA).

Zircons from the two granites have also indicated the existence of an inherited lead component, or inherited zircon (Figs. 7R and 6D). In the case of the "Organabo" granite, the inherited lead component displayed an $^{207}Pb/^{206}Pb$ age of 2.16 Ga, suggesting a Mesorhyacian age for the source of the granite, while in the case of the "Petit Saut" granite, the participation of an Archean source in its genesis is indicated by the $^{207}Pb/^{206}Pb$ minimum age of 2.71 Ga furnished by one of the zircons. Note that this is the first occurrence of an isotopic Archean signature in zircon from rocks of northern French Guiana. An Archean inheritance in zircon from Paleoproterozoic rocks had so far been identified only in paragneiss (B68a-[52] with an age of at least 2.93 Ga) and in quartzite (B73f-[51] with 3.19-2.77 Ga ages) from along the Camopi River in southeastern French Guiana (Avelar *et al.*, 2003), while preserved Archean rocks are known only in central Amapá State, several hundred kilometres to the south (João and Marinho, 1982; Montalvão and Tassinari, 1984; Avelar *et al.*, 2003).

Sm-Nd results obtained on several samples of metasediments and magmatic rocks are listed on the 1:500,000-scale geological map. For example, intermediate to acid metavolcanic rocks from the southern branch of the greenstone belt displayed positive $\varepsilon_{(Nd)t}$ values at the time of crystallization (Mar15a-[22] with +0.2, and INI42-[43] with +1.9). In the northern branch, Lafrance *et al*. (1999) obtained $\varepsilon_{(Nd)t}$ values of around +2.2 ± 2.4 for rhyolite at St Elie (sample [11]). These positive values, together with the corresponding Rhyacian T_{DM} model ages confirm the juvenile character of the greenstone belt, in good agreement with the previous Sm-Nd results of Gruau *et al*. (1985) on the metavolcanic series, and exclude any significant participation of a crustal component during magma formation. Associated TTG granitoids also display systematically positive $\varepsilon_{(Nd)t}$ values (+2.3 ± 0.4) and T_{DM} model ages not older than 2.35 Ga, again precluding the involvement of a significant amount of pre-Transamazonian crust during magma genesis.

Metagreywacke and pelite investigated from the southern and northern branches of the greenstone belt give contrasting Nd isotopic signatures, indicating distinct origins. Three samples of metagreywacke (MA16b-[2], MA21a-[3], and INI34-[42]) provided positive $\varepsilon_{(Nd)t}$ values of +0.8, +1.6 and +1.9, repectively, whereas the metapelite from both branches yielded negative $\varepsilon_{(Nd)t}$ values as low as -10 - i.e. MA28-[5], MA33-[7] and MA46-[10b] from the northern branch with -3.7, -8.6 and -3.3, respectively, and INI12-[38], INI20-[39] nad INI19A-[40] and 29-[41] along the Camopi River in the southern branch with -5.3, -3.4, -5.6 and -10, respectively. An origin from the erosion of the TTG granitoids may account for the juvenile isotopic signature of the metagreywacke, whereas pre-Transamazonian crustal sources are needed to explain the negative $\varepsilon_{(Nd)t}$ values of the metapelite.

Finally, metagranitoid (B99-[49], B34-[57] and B25a-[59]), paragneiss (B20-[58] and B68a-[52]), amphibolite (INI69-[44] and B67-[53]) and migmatite (B85-[50]) from the Camopi and Oyapok regions, have provided both positive or negative $\varepsilon_{(Nd)t}$ values and T_{DM} model ages between 2.24 and 2.58 Ga, showing that these rocks originated from a juvenile mantle-derived source, as well as from mixed sources including an Archean crustal component; the results are discussed in detail by Avelar *et al.* (2003). In the case of the "Petit Saut" granitoid in northern French Guiana (Petit Saut-[8]) and the migmatitic granodiorite from the Camopi River (B85-[50]), the positive $\varepsilon_{(Nd)t}$ value and Rhyacian T_{DM} model age contrast with the presence of Archean inherited zircons as old as 2.71 Ga and 2.65 Ga, respectively. This indicates that the participation of small amounts of a reworked Archean component, even in granitoid displaying a juvenile Nd isotopic signature, cannot be discarded.

Although no geochronological investigation on the cooling of the Transamazonian orogeny was made during the preparation of the second edition of the 1:500,000-scale Geological Map of French Guiana, Nomade *et al.* (2000) obtained a set of Ar-Ar data on biotite and amphibole from magmatic rocks along the Oyapok River, which indicates that temperature decreased from 550 °C to 350 °C between 2.05 Ga and 1.93 Ga in the Camopi area, and between 1.99 Ga and 1.93 Ga in the southeasternmost part of the country. This cooling history cannot be extended to the other areas of French Guiana, where geochronological results are lacking.

The age of 809 ± 29 Ma, obtained for the dolerite dyke (ARA60-[37]) in the western part of central French Guiana, is significantly older than the ages obtained from the Jurassic dolerite dykes in the northern part of the country, i.e. *ca*. 198-192 Ma (Deckart *et al*., 1997). It points to the presence of a Neoproterozoic generation of dykes, which tends to be confirmed by paleomagnetic poles inconsistent with younger Mesozoic generations (Théveniaut and Delor, 2003). The existence of yet another generation of dolerite, this time Paleoproterozoic in age, has been suggested by the Ar-Ar age older than 1800 Ma that was obtained by Deckart (1996) on a dyke from the Comté River, in northeastern French Guiana.

Tectonism

Two major tectonic phases, D1 and D2, have so far been documented in the metavolcanites and metasediments of the greenstone sequences (Lasserre *et al*., 1989; Ledru *et al.*, 1991; Egal *et al*., 1992; Milesi *et al*., 1995). The relationships between these deformation events and the recognition (and labelling) of successive S1 and S2 structures is not straightforward, although broadly argued in the literature. For example, the individualization of S0 (stratification) and S1 and S2 foliations, both in the greenstone sequences and in the

Upper Detrital Unit, requires precise formulations that take into account the unconformable position of the Upper Detrital Unit above the greenstone sequences. In the following sections we shall discuss S1 foliations exclusively in relation to the greenstones, while S2 evidence will be discussed with reference to both the greenstone deformation planes and the Upper Detrital Unit. This definition will have critical implications when discussing the tectonometamorphic evolution.

Northern greenstone branch

- D1, in the western Mana and Maroni formations, is only evidenced as S1 microlithons in a dominant S2 foliation. Moreover, biotite and garnet overprint S1, but predate S2 (Lasserre *et al*., 1989), thus pointing to the clear individualization of separate D1 and D2 tectonic steps. Our own observation on the southern limb of a colombo-tantalite granite intruding metasediments along the Mana River clearly concludes as to the presence of biotite-staurolite thermal aureoles with a downdip lineation along an S1 marked by these minerals. The 2132 ± 3 Ma age obtained for the granite (sample MA29A-[6]), is the oldest age obtained for D1 syntectonic plutonism in northwestern French Guiana. In the eastern domain, near Regina, Milesi *et al*. (1995) report that D1 was contemporaneous with contact metamorphism under low- to intermediate-pressure conditions that successively gave pre- to syn-S1 biotite, syn- to post-S1 amphibole and late-S1 andalusite and staurolite. D1 is mainly subvertical with a variably plunging lineation. No proof of thrusting or strike-slip tectonism can be determined (Milesi *et al*., 1995).

- D2, which has been described both in the greenstone belt and in the Upper Detrital Unit, is characterized by a vertical foliation along which a horizontal mineral lineation is developed. It is heterogeneous and best developed in the east of the country, where sinistral criteria have been documented in the Upper Detrital Unit. In most cases, only a single schistosity related to the D2 event is observed in the Upper Detrital Unit, although several steps have been identified locally (Egal *et al*., 1995; Donzeau and Vanderhaeghe *in* Milesi *et al*., 1995). This argument has been used to emphasize the post-D1 character of the detrital deposits; moreover, the arrangement of the detrital basin is interpreted in terms of a pull-apart basin opening during D2 (Ledru *et al*., 1991; Egal *et al.*, 1992).

In the course of our mapping study we obtained evidence for a two-step evolution comprising:

i) a main D2a stage, marked by major sinistral deformation trends contemporaneous with the granitic suite dated at *ca*. 2.10 Ga and pull apart basin opening,

and ii) a D2b stage that is well identified in northern French Guiana as late WNW-ESE dextral strike-slip corridors (Fig. 4a) along which late metaluminous monzogranite, dated at 2.07 - 2.06 Ga, was emplaced. Its regional emplacement along these WNW-ESE directions is confirmed at a mesoscopic scale by co-eval melt vein development along N145 shear planes dissecting the main migmatitic foliation in northern TTG complex (Fig. 5b). These D2b shear planes clearly exhibit dominant dextral component with minor normal fault component. The observation of identical melt paragenesis collected along the main D2a foliation and infilling the dissecting dextral vein tends to indicate a D2a-b thermotectonic continuum.

Southern greenstone branch and surrounding gneiss

- Early structures referring to a D1 event have been described by Marot (1988) in migmatite, tonalitic orthogneiss and metatexite terrain in southern French Guiana. The S1 is marked by a continuum of increasing metamorphic conditions from a northern epizonal (sericite-chlorite) domain to a southern mesozonal (garnet-sillimanite gneiss and migmatite) domain. Probable D1-related microstructures in greenstone formations are best preserved north of the Ouaqui River in southwestern French Guiana. The lithological formations exhibit a north-south, vertical to subvertical, foliation with a rough downdip stretching mineral lineation. Stratification, where visible, is transposed into the foliation planes. From mesoscopic to macroscopic scale, the deformation seems to result from flattening, with little or no evidence of rotational criteria (Kerbaol, 1997). D1 foliation in the greenstone formations is wrapped around the imbricated plutons of the Central TTG Complex, which would suggest a syn- to late-tectonic emplacement of the plutons during an earlier D1 event. Because both the plutons and the greenstone formations are dated at *ca*. 2.16-2.13 Ga, this isotopic date can be considered as the age of the D1 event in a global context dominated by TTG diapirism in the surrounding greenstones. Thermal aureoles around the Tampok gabbro, which is coeval with this second TTG magmatism, are characterized by andalusite blastesis (Bemba *et al.*, 1978; Marot, 1988) pointing to a low-pressure type metamorphism during D1.

This entire set of observations and the new isotopic constraints are at considerable variance with the main conclusions proposed by Jegouzo *et al.* (1990) farther south along the Ouaqui River. On the basis of classical "S/C"-type shearing kinematics criteria, these authors argue for dominant northward thrusting. Our own observations do not support such a conclusion, although local thrusting cannot be discarded in a global process dominated by TTG diapirism. Similar localized evidence was reported by Kerbaol (1997), who remarks that magmatic amphiboles locally show rotation with asymmetric pressure shadows indicating a relative upward movement of the western compartment.

- The onset of D2 event in the southern greenstone branch is individualised progressively when moving southwards from the southern limb of the central TTG complex. The S1 foliations characterising the TTG-greenstone veer progressively until they are parallel to the major trends of the Ouaqui River. A subhorizontal mineral stretching lineation is observed on the vertical foliation planes, with a development of secondary vertical shear planes. The sigmoidal shape of the foliation between shear planes argues for a sinistral sense of movement. These structures can be followed eastward over several tens of kilometres, and reflect major strike-slip crustal shear zones in the southern parts of the country (Fig. 4a). The shear zone has reworked the Degrad Roche orthogneiss, which bears evidence of mylonitic foliation consisting of biotite, quartz and feldspar.

The foliation trends in the succession of granitic to dioritic amphibolite and migmatitic gneiss along the Marouini River are varied, but most commonly present a high dip and a dominant N-S direction. These structures tend to curve until they reach E-W trends along the contacts with the Tampok gabbro. One notes rapid transitions from migmatitic gneiss with well-expressed schistosity and mineral lineations, to granitoid where either schistosity or mineral lineation is predominant. The mineral lineations are marked by micas and amphiboles.

In southern French Guiana, the D2 event was followed by deformation under a lower-temperature ductile regime marked by mylonitic textures, rounded feldspar porphyroclasts, kink bands in the biotite, and strong quartz recrystallization. Such textures have been described at neosome / paleosome contacts in migmatitic facies (Marot *et al.*, 1983). These late structures, which have not been studied in detail, are related to a brittle-ductile context and are considered as reflecting the waning thermotectonic stages of Transamazonian cooling.

Metamorphism in the greenstone belt

The metamorphic grades, especially in the metasedimentary sequences, have been documented by various authors from the early pioneering days (Choubert, 1974) to more recent regionally-focused studies in both the northern (Milesi *et al.*, 1995; Vanderhaeghe *et al.*, 1998) and southern (Marot, 1988) domains.

Northern domain

According to Milesi *et al.* (1995), metamorphism in the northern domain is irregularly developed and very commonly observed as a static recrystallization of biotite, amphibole, andalusite and staurolite; similar observations have also been made in the contiguous terrains of Suriname (Bosma *et al.*, 1983). Milesi *et al.* (op. cit.) interpret such recrystallization as the fingerprint of a thermal metamorphism due to the abundant granitoid intrusions. Sericite and chlorite blastesis, and the syntectonic crystallization of biotite and amphibole, can similarly be related to intrusion emplacement. Our data on the northwestern series of pelite and greywacke show an increase in higher-grade index minerals (e.g. garnet, biotite, garnet andalusite and staurolite) towards the plutons, together with steeply plunging staurolite blastesis near certain plutons. This entire set of data is best interpreted in terms of thermal aureoles.

Kyanite- and chloritoid-bearing associations in the Upper Detrital Unit were reported and interpreted by Milesi *et al.* (1995) as the result of a prograde metamorphism culminating at 550 - 600 °C and 5-6 kb (Tegyey, 1993). The presence of these minerals in some parageneses, together with the Na content in muscovite, has been used to establish P-T conditions of the alumino silicate-bearing assemblages, with maximum pressure conditions of about 7 kb (Vanderhaeghe *et al.*, 1998). However, attentive revisiting of the plots of various paragonite-bearing muscovites in the NaK^{-1} diagram (Chatterjee and Froese, 1975) shows that the best fit of probe analyses with immiscibility gap curve limits are obtained for pressure conditions closer to 4 kb rather than 7 kb, and with temperature conditions below 550 °C. Such upper temperature limit is constrained by the striking absence of staurolite (Vanderhaeghe *et al.*, 1998). At the preferred 4 kb pressure estimate, the crystallization of kyanite after andalusite (Ledru *et al.*, 1991; Egal *et al.*, 1995) does not need a significant increase in pressure during the D2 event (Fig. 9). Instead, a rather isobaric cooling path best fits the inferred crossing of the andalusite/kyanite stability field. Moreover, the late recrystallization of kyanite during the post-S2 crenulation stage (Egal *et al.*, 1995) would favour a protracted kyanite blastesis during the waning stages of metamorphism.

The petrological conclusions of Vanderhaeghe *et al.* (1998) emphasising crustal thickening therefore need to be reconsidered. In view of the absence of earlier kyanite or sillimanite blastesis prior to andalusite formation, the pressure-temperature (P-T) path reconstructed for the Upper Detrital Unit is better interpreted as a succession of i) increasing P-T conditions during burial, down to the andalusite stability field, followed by ii) isobaric cooling towards the kyanite stability field, and iii) final exhumation in the kyanite field. Both an initial gradient towards andalusite and isobaric cooling are consistent with close relationships between basin opening and anomalous high geothermal gradients enhanced by pluton emplacement. The overall apparent counterclockwise P-T path (fig. 9), already suggested by Vanderhaeghe *et al.* (op. cit.; see their Fig. 13), needs further support from more precise thermobarometric constraints coupled with precise isotopic dating of the metamorphism. However, it must be pointed out that similar evidence of a counterclockwise P-T path

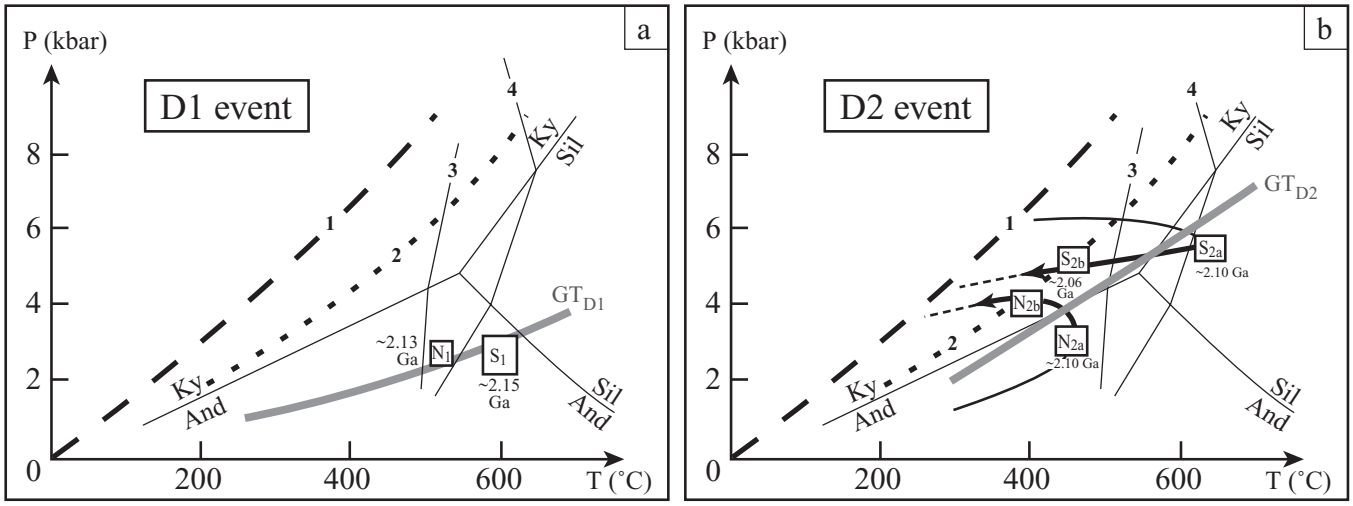

Fig. 9.- P-T evolution of French Guiana metasedimentary formations respectively for D1 event (a) and D2 event (b). Reaction 1 and 2 refer to present day stable geotherm (1) and inferred archaic type geotherm (2) according to Lambert (1976). Staurolite in produced by chloritoide breakdown (3), staurolite out (4) and andalusite/kyanite/sillimanite (And/Ky/Sil) stability fields are from Powell *et al.* (1998). For D1 event, N and S abbreviations in PT boxes refer to northern and southern greenstone belt branches. For D2 event S refer to southern greenstone belt branch while N concerns specifically detrital basins in northern domain.

Fig. 9.- Evolution P-T des formations métasédimentaires de Guyane respectivement pour l'épisode D1 (a) et l'épisode D2 (b). Les réactions 1 et 2 font référence aux géothermes stable actuelle (1) et de type archaïque (2) de Lambert (1976). Les réactions d'apparitions du staurotide à partir du chloritoïde (3) et de déstabilisation du staurotide (4) sont de Powell et al. *(1998), de même que le champ de stabilité de andalousite/disthène/sillimanite (And/Ky/Sil). Pour l'événement D1 les abbréviations N et S dans les boites P-T se refèrent respectivement aux domaines Nord et Sud des ceintures de roches vertes. Pour l'évènement D2, S se réfère au domaine sud de ceinture de roches vertes alors que N concerne spécifiquement les bassins détritiques du domaine nord.*

has recently been argued for the ultrahigh-temperature metamorphism of the Bakhuis belt in Suriname, which was dated at 2.07-2.05 Ga (de Roever *et al*., 2003b).

Southern domain

The metamorphic parageneses on the southern limb of the Central Guiana Complex are constituted mainly by amphibolitic schist, mica schist and micaceous quartzite with fine-grained banding. The banding is highlighted by quartzofeldspathic layers and micaceous layers with chlorite, chloritoid and paragonite. This paragenesis is symptomatic of greenschist facies.

This metamorphism progressively increases south of lat. 3°30' N, and is observed both in gabbroic massifs and in the surrounding greenstone belt.

The Tampok gabbro exhibits a granoporphyroblastic texture, commonly with polygonal recrystallization and poikiloblastic amphibole enclosing pyroxene, plagioclase and quartz. Further evidence of mesozonal metamorphism is better seen in the greenstone belt formations.

In the rocks of intermediate composition, the metamorphism is marked by dominant two-mica -amphibole gneiss - a foliated, well-banded rock with a rather heterogranular granonematoblastic texture. The metamorphic paragenesis consists of green hornblende, biotite, muscovite, chlorite, sphene, epidote, plagioclase, K-feldspar and quartz.

The amphibolite shows a granonematoblastic texture, their paragenesis include quartz, andesine, Fe-hornblende, biotite, sphene, epidote and ilmenite.

The metasediments are characterized by the successive appearance of biotite, garnet and sillimanite. The common highest-grade assemblages are represented by biotite-garnet ± sillimanite exhibiting a granonematoblastic texture. The presence of kyanite, although commonly found in stream-sediment samples, is not reported in rock samples by Marot (1988). However, kyanite-bearing assemblages were found during our recent sampling in the Araoua area for the 1:500,000-scale geological map. According to Kerbaol (1997) they comprise muscovite + biotite + garnet + sillimanite + kyanite gneiss with a granoporphyroclastic texture. The sillimanite crystallizes as pluri-centimetric blasts enclosing an earlier crystallization of biotite, muscovite and plagioclase. The matrix consists of garnet + biotite + plagioclase + muscovite + quartz and opaque minerals. Biotite and muscovite do not show significant variations, either as an armoured relict in garnet or in the matrix; they are in equilibrium with garnet, which in turn locally forms corona around sillimanite blasts. Kyanite crystallizes as small crystals inside sillimanite blasts. Muscovite is clearly a secondary mineral.

Considering the probable proximity of primary kyanite-bearing source rocks, given the numerous kyanite-bearing stream samples, Marot (1988) concluded on a probable

kyanite-in isograd between a garnet-in and a sillimanite-in isograd in the greenstones. The overall succession of these isograds in the eastern Araoua area (Bemba *et al.*, 1978; Marot, 1988) is inferred to be E-W, concordant with the dominant regional S2 foliations. To the west, these isograds about against the Tampok gabbro and its andalusite thermal aureoles.

Two conflicting set of arguments have been put forward to advocate the time relationships between the Tampok gabbro and the regional metamorphism associated with the penetrative E-W deformation trends. According to Marot (1988), the succession of the garnet-in to sillimanite-in synfolial regional isograds is dissected by the main Tampok gabbro intrusion and its coeval andalusite thermal aureole; this would imply that the Tampok gabbro suite postdates the regional (D2) tectonometamorphic event. The second hypothesis takes into account the observations of Bemba *et al.* (1978), who point to significant Tampok gabbro recrystallization during later regional metamorphism, suggesting reworking by D2 metamorphism.

The *ca.* 2.15 Ga emplacement age inferred for the Tampok gabbro suite, and our field and isotopic evidence pointing to S2 syntectonic upper-amphibolite metamorphism and migmatization at *ca* 2.10 Ga, would seem to confirm the hypothesis of Bemba *et al.* (1978). It can even be refined in a geological scenario with gabbro emplacement at *ca.* 2.15 Ga during a D1 event, and subsequent reworking at *ca*. 2.10 Ga by a D2 event.

Pressure-Temperature estimates of the metamorphism of successive D1 and D2 tectonothermal events in southern French Guiana can tentatively be inferred on the basis of index metamorphic minerals and limited petrological studies. For the D1 event, the development of andalusite-bearing thermal aureoles around the Tampok gabbro argue for low-pressure metamorphic conditions during D1 (Fig. 9). For the D2 event metamorphic conditions at 700 °C and <5-6 kb for the earliest D2 stage would explain the absence of garnet in the greenstone metabasic assemblages (Fig. 9). More quantitative temperature estimates for the D2 regional event were made on the basis of the biotite-garnet mineral pairs by Kerbaol (1997) using the Kleeman and Reinhardt (1994) calibration because of the significant amount of MnO (3-6.5%). They estimated that temperatures decreased from 680 °C to 600 °C from garnet core to garnet rim, with estimated maximum pressures of 5-6 kb. These records of decreasing temperature are supported by the successive crystallization of sillimanite and then kyanite, and therefore reflect a cooling path above the aluminosilicate triple point around 4 kb (Fig. 9). A clockwise P-T path can be proposed for D2 in the southern domain.

It is worth noting that despite the higher metamorphic conditions registered in southern French Guiana, our study does not support the recent conclusions of Voicu *et al*. (2001) who advocate the development of granulite metamorphism in the area. Our observations of localised orthopyroxene recrystallization within the Tampok gabbro (Kerbaol, 1997) and minor, regionally associated, charnockite are better interpreted as an annealing process during cooling, and/or localized high-temperature thermal (re)heating, during the course of successive and interfering emplacements of Tampok gabbro plutons.

Conclusion on thermotectonic regimes

The thermotectonic evolution of French Guiana can be described in terms of two main thermotectonic events: D1 and D2. From a petrological standpoint, and despite a clearer high-temperature imprint in the southern terrains, the metamorphic gradients during D1 and D2 are symptomatic of medium- to low-pressure types, with an inferred D2 counterclockwise P-T path, in both the northern and southern greenstone terrains. The cause of metamorphism during the successive D1 and D2 thermotectonic events was due mainly to TTG- and granitic-type plutonism, with evidence of thermal aureoles, in a global context of low to moderate crustal thickening.

Fig. 9 is synthetising such a P-T evolution both for the northern and southern greenstone branches:

- Andalusite-bearing thermal aureoles (Saut Tamanoir - Mana River, Tampok gabbros) are pointing to an anomalously high geothermal gradient during D1, in conjunction with a dominant period of Mesorhyacian TTG magmatism, which in turn is driving gravity driven deformations of volcano-sedimentary formations around plutonic bodies. No significant evidence of tangential tectonics and associated crustal thickening can be demonstrated.

- Andalusite-kyanite and sillimanite-kyanite transition are witnessed respectively in the northern Upper Detrital Unit and southern greenstone domains, during D2, in conjunction with a dominant period of Neorhyacian granite suite magmatism and associated migmatisation, dated at *ca*. 2.1-2.06 Ga. Early D2a andalusite (north) or sillimanite (south) parageneses are developing during the onset of a sinistral transcurrent structural stage corresponding to the opening of pull-apart basins and to the main granite magmatism. On the basis of a D2b metaluminous monzogranite age emplacement, a further counterclockwise P-T evolution towards the kyanite stability field can tentatively be estimated at *ca.* 2.08-2.06 Ga, by analogy with the co-eval counterclockwise P-T path in the Bakhuis granulite belt from Suriname (2.07-2.05 Ga). The inferred thermotectonic continuum from D2a andalusite stage to D2b kyanite stage is compatible by structural observation on melt genesis during D2a-D2b continuum in northern Laussat migmatitic complex (Fig. 5b).

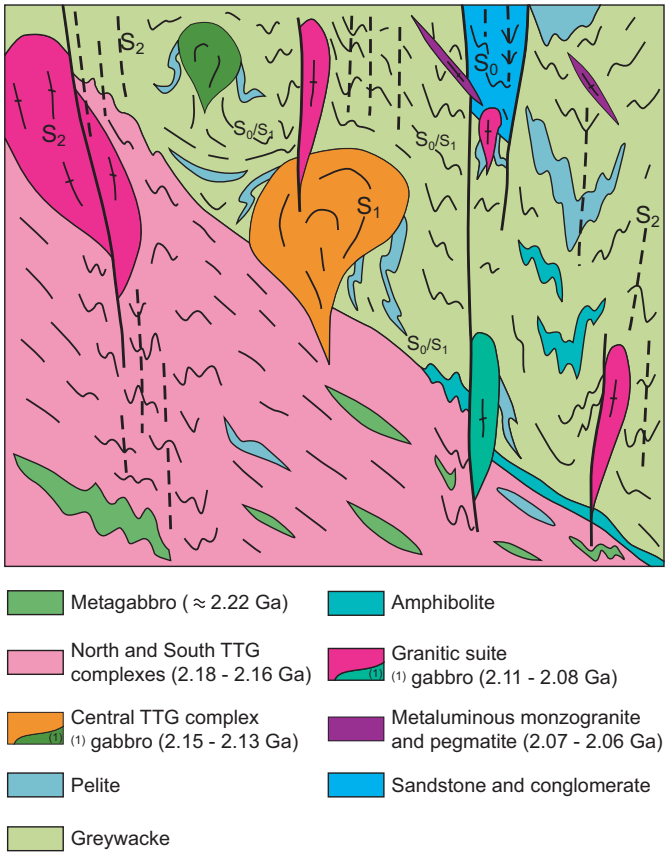

Fig. 10.- Litho-chronological diagram of French Guiana Paleoproterozoic formations.

Fig. 10.- Diagramme litho-chronologique des formations paléoprotérozoïques de Guyane.

Integration of lithostructural and isotopic data in a regional framework

On the basis of the geological, geophysical, lithological, geochronological, tectonic and metamorphic data presented above, Figure 10 presents the overall relationships between the formations of French Guiana in the form of a diagrammatic S-N lithochronological figure integrating the major rock types and their relative chronology. Further detailed vertical views of the relationships of the geological units can be inferred from the geological cross-section given in Figure 11, which has been drawn from south to north along the western border of French Guiana - its trace is indicated on Figure 4a - and takes into account all the geological units along its trace, using the same colour codes and index numbers as the geological map. The cross section highlights the location of the northern and southern Mesorhyacian TTG, with ages between 2.18 and 2.16 Ga. The Mesorhyacian Central TTG Complex, dated at 2.15-2.13 Ga, is represented as a set of imbricated plutons, partly intrusive in the greenstone belt where the dating of some volcanic formations indicates ages as old as 2.16 Ga. In the northern part of the cross section, the Upper Detrital Unit is illustrated as a basin deposit having unconformable relationships with the greenstone belt, although tectonic contacts are inferred at both the northern and southern boundaries of the basin. Granitic suite plutons are emplaced within all formations, except the Upper Detrital Unit.

Figure 12 is a regional-scale lithostructural sketch map of French Guiana that includes Suriname to the west and the Brazilian States of Amapá and Pará to the south and east. This synthetic view of the eastern part of the Guiana Shield takes into account the results discussed in this study, together with much of the recent field and isotopic data obtained in contiguous countries (Lafon *et al.*, 1998; Norcross *et al.*, 1998; 2000; Voicu *et al.*, 1999, 2001; Nogueira *et al.*, 2000; Ricci *et al.*, 2001; Avelar *et al.*, 2001, 2003; Avelar, 2002; Delor *et al.*, 2003; de Roever *et al.*, 2003a, b; Rosa Costa *et al.*, 2003).

The whole of the Paleoproterozoic TTG and greenstone terrains define a WNW-ESE-trending "lens" centred on French Guiana, with its external northern and southern parts being limited by the northern and southern Mesorhyacian TTG domains, dated at 2.18-2.16 Ga.

The northern Mesorhyacian TTG domain is broadly parallel to the Atlantic coastline. Its extension east of French Guiana is poorly constrained, although we assume that it could progressively bend towards the Amazon River mouth, like the regional foliation trends of the contiguous granite suite. West of French Guiana, it continues into Suriname with a few NE-SW sinistral offsets of inferred Mesozoic age. Its extension west of the Bakhuis belt is unknown.

The southern Mesorhyacian TTG domain extends eastward into Amapá State (Brazil) and has been traced out to near the Amazon delta. To the west, it is dissected by a later granitic suite, but reappears close to the Bakhuis belt.

Between these two Mesorhyacian TTG domains, the greenstone belt is wrapped around the Mesorhyacian Central TTG Complex within which D1 greenstone synform are preserved from D2 reworking.

Figure 12 clearly shows that the Neorhyacian granitic suite is well developed in two elongate NW-SE and W-E domains, respectively east and south of French Guiana. The eastern domain forms most of the northern part of Amapá State, while the southern domain extends into Suriname with progressive bending from N100°-oriented trends to almost N-S oriented trends.

In Amapá and Suriname, these granite suite domains are abutting against high grade (*pro parte* granulite facies) metamorphic domain : i) In Amapá the merging of Neorhyacian NW-SE and W-E elongate granitic domain coincide with an arcuate zone of flat lying to shallowly

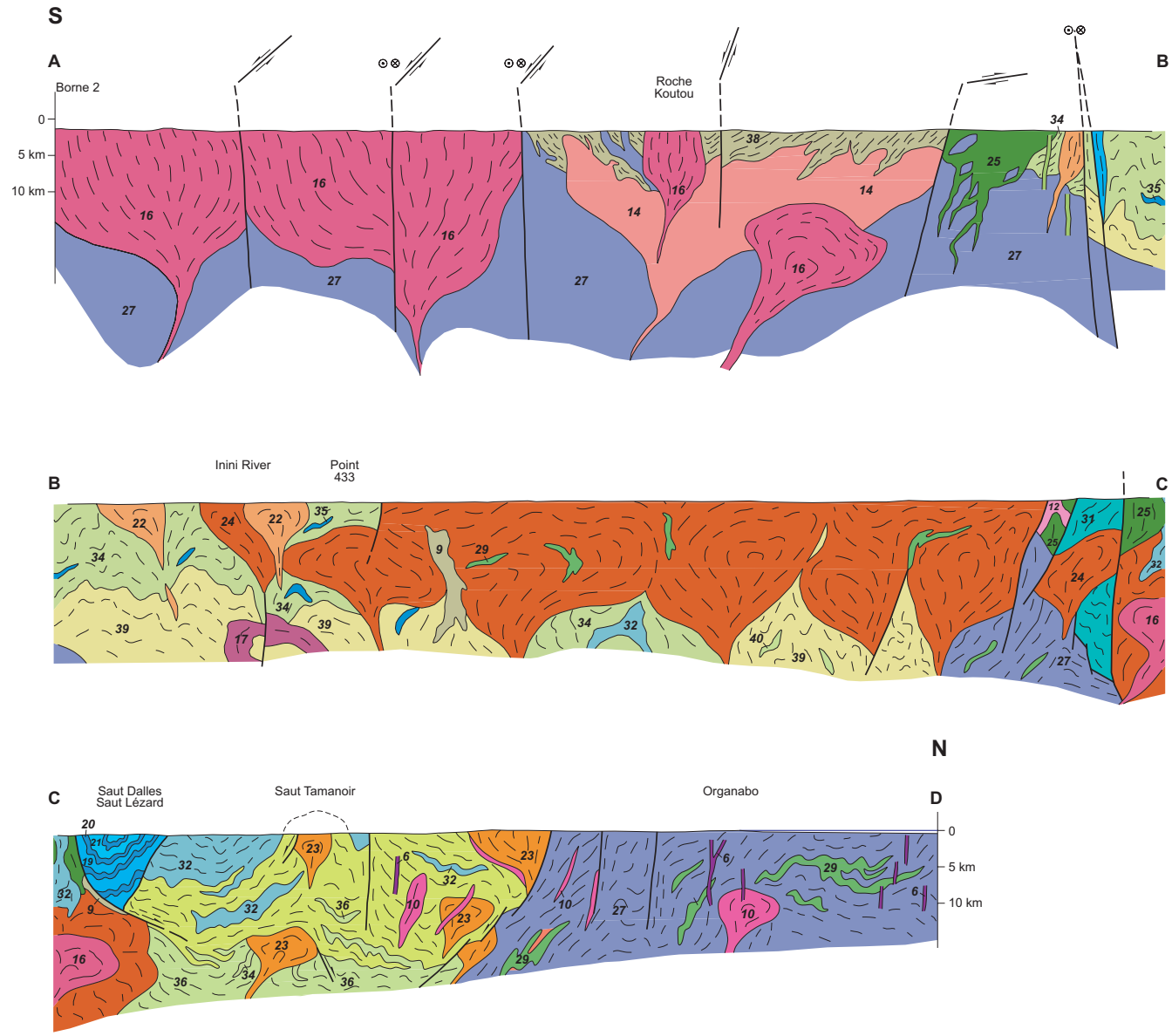

Fig. 11.- S-N geological cross-section (see Figure 4a for the trace). Colours and formation code numbers as for fig.4a.

Fig. 11.- Coupe géologique N-S (voir son tracé sur la figure 4a). Couleurs et numéros de formations identiques à ceux des figures 4a, b.

dipping foliations that include esposures of charnockite dated at 2.05 Ga (Avelar, 2002), with more evidence of granulitic rocks (João and Marinho, 1982; Lafon *et al.*, 1998). ii) In Suriname the limit of granite suite is highlited by the Neorhyacian Bakhuis granulite belt (2.07-2.05 Ga) and the younger high-grade metamorphics and acid volcanics of inferred Orosirian age (*ca.* 2.01-1.96 Ga). More details of the Suriname Paleoproterozoic domain are given in de Roever *et al*. (2003a, b) and Delor *et al*. (2003), with special reference to granulitic metamorphism genesis in a revised Guiana shield framework.

The Archean basement is restricted in Amapá. Although exposed, its recognized extension needs to be taken into account because it could explain the presence of inherited Archean protolith in the greenstone metasediments and granitic suite, as revealed in this study on Sm-Nd and Pb-Pb isotopic grounds.

Post-Paleoproterozoic formations are restricted to dolerite dykes of various ages, and to Paleozoic and Mesozoic cover rocks related to the Amazon Basin and Atlantic Ocean opening. The overall framework of French Guiana and its contiguous countries, therefore, appears essentially to result essentially from the Paleoproterozoic tectonometamorphic event for which a geodynamic scenario is proposed below.

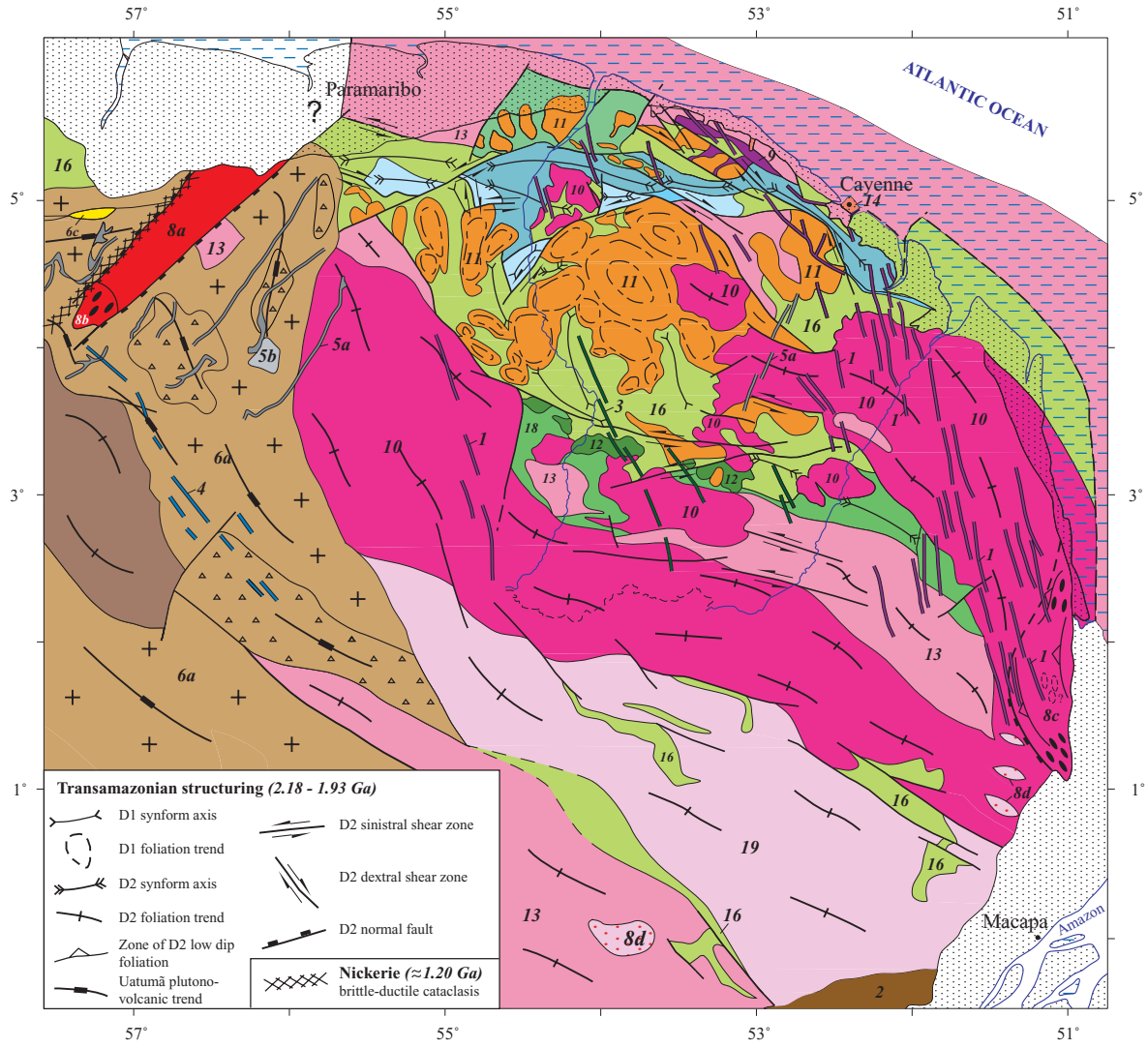

CENOZOIC

Continental cover

Marine cover

MESOZOIC

1 "Apatoe" dolerite *(200-195 Ma)*

PALEOZOIC

2 North Amazonian cover

NEOPROTEROZOIC

3 "Tampok" dolerite *(809 Ma)*

MESOPROTEROZOIC

4 "Kayser" dolerite *(1.5 Ga)*

PALEOPROTEROZOIC

5a "Avanavero"/"Comté" dolerite *(1.8 Ga)*

5b "Tafelberg" sandstone

PALEOPROTEROZOIC

Late Transamazonian acid plutono-volcanic event

(Orosirian : ≈2.01 - 1.96 Ga, pro parte "Uatumã")

6a, 6b, 6c a) Biotite granite, two-mica granite
b) Acid volcanism and hypovolcanic plutonism, c) conglomerate

Late Transamazonian tectonometamorphic and magmatic event

(Late Rhyacian to Orosirian : 2.07 - 1.93 Ga)

7 Granulite and migmatite *(≈ 2.00 Ga)* : Coeroeni gneis

8 a, b, c, d Granulite *(2.07 - 2.05 Ga)* :
a) Banded granulite; b) Charnockite, gabbro;
c) Charnockite intrusion among granite; d) Reworking of Archean protolith

9 Metaluminous monzogranite *(2.07 - 2.06 Ga)*

Main Transamazonian event *(2.26 - 2.08 Ga)*

10 Neorhyacian granitic plutonism in part Mg-potassic *(2.11 - 2.08 Ga)*

11, 12 a, 13 Mesorhyacian TTG plutonism
Central complex *(2.15 - 2.13 Ga)* a) Gabbro
N and S complexes *(2.18 - 2.16 Ga)*

14 Eorhyacian tholeiitic magmatism in an oceanic domain *(~2.26 - 2.20 Ga)*

15 Pull-apart detrital basin synchronous with the sinistral transcurrent tectonism

16, 17 a, b, c, 18 Greenstone belt
a) low-to intermediate-pressure thermal aureole
b) intermediate-pressure metamorphism
c) Archean derived pelitic sediments

ARCHEAN

19 Mesoarchean basement *(3.30 - 2.90 Ga)* reactivated by Transamazonian event

Fig. 12.- Structural sketch map of French Guiana in its lithostructural setting at regional scale, including Suriname to the west and Amapá and Pará States (Brazil) to the south and east.

Fig. 12.- Schéma structural replaçant la Guyane dans son cadre régional lithostructural, incluant le Suriname à l'ouest et les états du Pará et de l'Amapá (Brésil) au sud et à l'est.

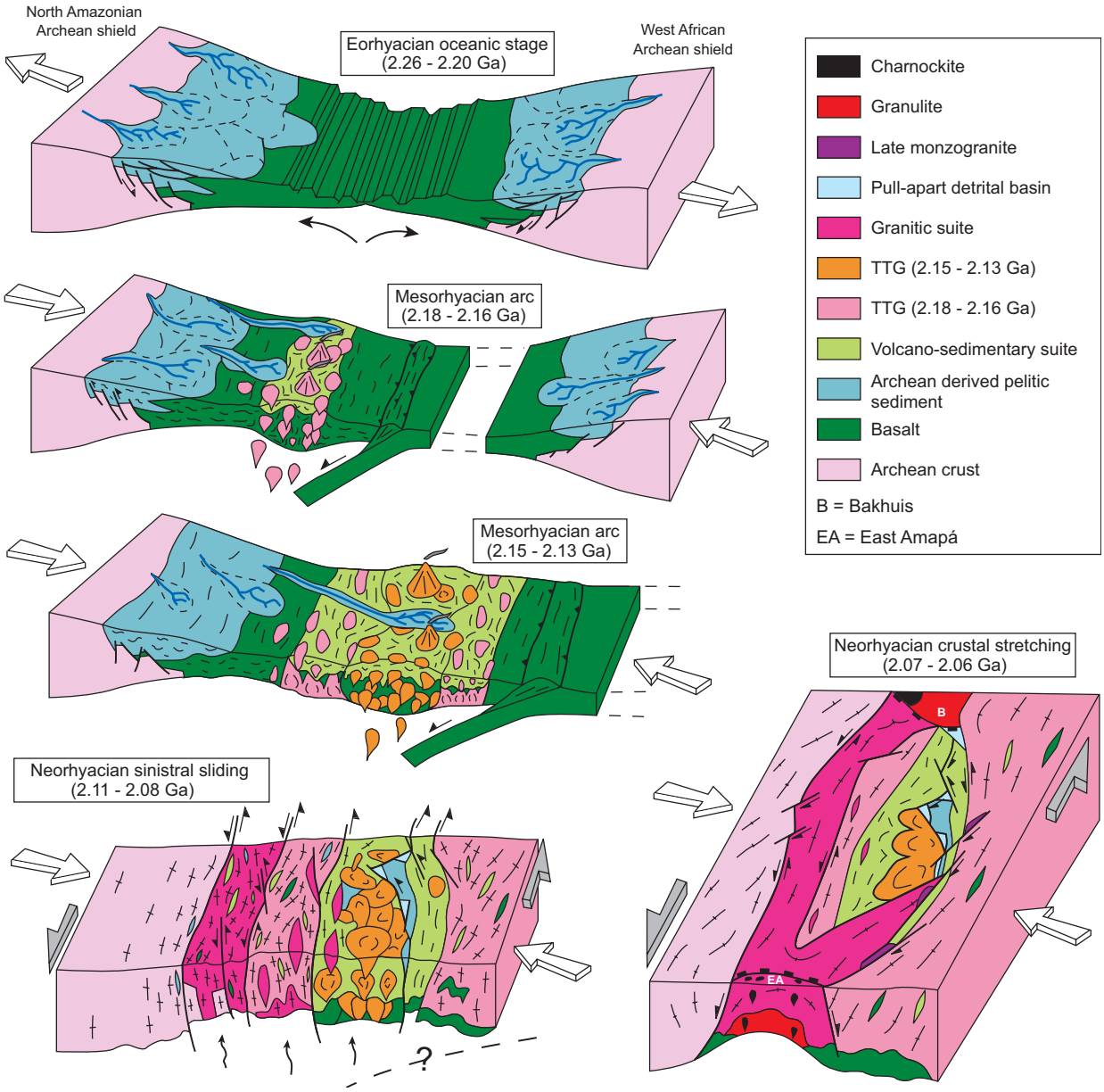

Fig. 13.- A geodynamic evolution model for French Guiana Paleoproterozoic terrains.

Fig. 13.- Evolution géodynamique des terrains paléoprotérozoïques de Guyane.

Geodynamic discussion

Previous models

Various tectonic models have been proposed for the geodynamic evolution of the Guiana Shield. Of special interest for the northeastern position of French Guiana is the concept of the Maroni-Itacaiúnas Province (MIP; see Fig. 1A) introduced by Cordani *et al*. (1979) and Cordani and Neves (1982) to represent a Paleoproterozoic belt accreted to an Archean block (Central Amazonian Province) during a collisional orogeny at *ca*. 2.22-1.95 Ga; the orogeny corresponds to a major period of crustal growth. In the Amazonian context, this Rhyacian time span is consistently acknowledged as the earliest orogenic belt, south of which further younging crustal growth and reworking down to *ca*. 1.1 Ga is documented (Fig. 1; Tassinari *et al*., 2000; Santos *et al*., 2000). In French Guiana, further structural tectonic analyses have been provided by Ledru *et al*. (1994) and Vanderhaeghe *et al.* (1998). Following the formation of an oceanic crust, these authors propose a two-stage model for the Transamazonian, with a first stage of "crustal growth by magmatic accretion", and a second stage of "crustal recycling and tectonic accretion" during oblique convergence between juvenile blocks. The second stage was responsible for the formation of foreland basins in a pull-apart system, and the emplacement of high-K

granite at *ca*. 2.09 Ga. The final transcurrent tectonism resulted in lateral block extrusion and burial of the foreland basins.

A revised geodynamic model

By integrating the entire set of available petrostructural and isotopic data, and on the basis of our detailed structural sketch map (Fig. 12) and previous synthesis (Delor *et al*., 2000), we propose a revised geological model for the Guiana Shield, focusing on the main Paleoproterozoic tectonothermal stages (Fig. 13). We refer to the IUGS Paleoproterozoic sub-eras (Plumb, 1991) and give the inferred ages in brackets for a better geological understanding.

Eorhyacian: juvenile oceanic crust (2.26-2.20 Ga)

The juvenile character of the Paleoproterozoic crust, plus the tholeiitic affinities of its earliest remnants, strongly suggest major mantle extraction processes, starting at 2.26 Ga, between the once contiguous southern (Amazonian) and northern (African) Archean plates.

The oldest Paleoproterozoic basement dated in French Guiana is along the Atlantic coast where some "Île de Cayenne" gabbro and trondhjemite, derived from mid-oceanic tholeiitic magma, have provided zircon ages as old as 2.21-2.22 Ga. On the southern limb of the French Guiana TTG-greenstone domain, inherited ages in migmatitic gneiss point to protolith ages as old as *ca*. 2.2 Ga. Sm-Nd data for the Ipitinga greenstones (MacReath and Faraco, 1997) point to Eorhyacian crust as old as 2.26-2.20 Ga. Therefore, such dismembered and highly reworked juvenile crust remnants are interpreted as the product of mantle extraction at 2.26-2.20 Ga, with a subsequent stage of oceanization. To that end, our interpretation moves the rifting of the Archean plates to 50 Ma before the date proposed by Vanderhaeghe *et al*. (1998). Further geochemical studies would be necessary to infer the possible involvement of a mantle plume, as suggested in the coeval West African Birimian terrains (Abouchami *et al.*, 1990; Boher *et al.*, 1992).

Mesorhyacian: D1 convergence versus multi-pulse TTG accretion (2.18-2.13 Ga)

Two processes can be inferred for the earliest stages of Paleoproterozoic magmatism in order to account for the huge volume of early Paleoproterozoic TTG batholiths: the one in terms of archaic mantle upwelling leading to progressive oceanic crust melting at its base, and the other in terms of modern subduction processes. With both interpretations, the production of dominant TTG melts would have resulted from the melting of a basaltic juvenile crust, either through underplating or through plate consumption. The first hypothesis, which has been tentatively proposed for the West African Shield (Delor *et al.*, 1994; Vidal *et al*., 1996) as well as for the early crustal growth of the Guiana Shield (Delor *et al.*, 1998b), could explain the absence of any high-pressure eo-Transamazonian metamorphic products, while the second hypothesis has been repeatedly advocated on geochemical grounds. In the absence of specific geochemical arguments to strengthen the first hypothesis, we propose a crustal growth scenario where the TTG products result from a subduction process, respecting the specific constraints given by our mapping and isotopic data on TTG domains.

We have determined that the TTG diachronous pulses in French Guiana occurred between 2.18 Ga and 2.13 Ga, with an apparent internal younging direction of accretion, i.e. 2.15-2.13 Ga in the central domain bordered by 2.18-2.16 Ga in the northern and southern domains. This relative TTG geometry can be interpreted in terms of a progressive consumption of juvenile crust during N-S convergence of the Amazonian and African Archean blocks resulting from a major southward-directed subduction; this would have led to a first TTG magmatic arc at 2.18-2.16 Ga, and then to a second TTG magmatic arc at 2.15-2.13 Ga emplaced in the middle of the first one. Further studies are needed to assess whether this apparent two-step TTG accretion is valid or whether we are dealing with a protracted TTG process operating relatively continuously from 2.18 Ga to 2.13 Ga. Whatever the case, our data and interpretations differ significantly from those of Vanderhaeghe *et al*. (1998), who concluded on a progressive southerly TTG younging related to several subduction zones between 2.14 and 2.0 Ga. Our preferred geodynamic subduction model needs to be tested against further data on other prominent TTG areas in Suriname, Guyana, Venezuela and Amapá.

In addition, the presence of a significant Archean heritage (based mainly on Sm-Nd isotopic data) in the pelitic sedimentary terms of the greenstone belt contrasts with the juvenile character of the TTG magmatism, volcanism and even metagreywacke sedimentary end-members; this also has to be integrated into our geodynamic model. In the light of available data, we consider that these Archean signatures reflect specific stage(s) of Archean basement erosion and basin deposition.

Neorhyacian: D2a sinistral sliding versus granitic magmatism and detrital basin opening (2.11-2.08 Ga)

Granitic domains form the second type of dominant Paleoproterozoic crustal lithology emplaced between 2.10 and 2.08 Ga. Such syntectonic granitic accretion reflects a blockage of early plate convergence (D1) and its development into sinistral sliding (D2a) of the southern Amazonian and northern African Archean plates. Sinistral shearing is prominant at regional scales from the development of sigmoidal foliation trajectories (see Fig. 4a,

south of 3° latitude). Evidence of *in situ* melting contemporaneous with this granitic suite has been observed in the field in the northern TTG coastal area (Laussat Complex), in the southern Tamouri Complex, and in the northern Oyapok River in the eastern part of French Guiana. Such TTG crustal melting under low- to moderate-pressure conditions, as deduced for the coeval metamorphism, implies the participation of anomalous thermal gradients in depth, which is best interpreted in terms of mantle perturbation. The local occurrence of Mg-K magmatism (amphibole- and/or pyroxene-bearing granite/granodiorite), and its regional individualization in southern French Guiana and central Suriname, could reflect mantle-crust interactions as being responsible for such high-temperature granites. Indeed, as advocated by Moyen *et al*. (1997, 2001) for the late Archean. Closepet granite of South India, such peculiar granite magmatism contains some juvenile products and is not solely enhanced by intracrustal reworking, as frequently assumed.

As demonstrated by Vandergaeghe *et al*. (1998), the formation of pull-apart basins have been initiated during the D2 sinistral deformation event, to which we refer as D2a.

Neorhyacian: D2b strike-slip corridors versus late monzogranite emplacement and detrital basin metamorphism (2.07-2.06 Ga)

With respect to the global D2 tectonic continuum, the production of late metaluminous monzogranite emplaced along WNW-ESE dextral strike-slip corridors in northern French Guiana is marking further stage of oblique plate convergence, i.e. between 2.07 and 2.06 Ga. This D2b shearing postdates the formation of pull-apart basins, as already pointed by Vanderhaeghe *et al*. (1998). Our updated geological framework for the Guiana Shield emphasizes the chronological relationships of the D2b event with the UHT granulite metamorphism in Suriname, and charnockite magmatism in Amapà, both dated as Neorhyacian. The D2b tectonic stage was thus synchronous with this UHT metamorphism in Suriname which is thought to be due to mantle upwelling enhanced by continental scale crustal stretching (Delor *et al.*, 2003). Further evidence for the synchronous timing of the metamorphism in i) the pull-apart basins of French Guiana and ii) the UHT granulite in Suriname, is given by the counterclockwise P-T path obtained for the late D2 metamorphic history of both domains. As advocated by Delor *et al*. (2003), such counterclockwise P-T path related to a mantle perturbation witnesses high-thermal gradient during burial and subsequent isobaric cooling, which in turn point to the absence of significant crustal thickening. Such a metamorphic evolution does not fit with the previous geodynamic model of foreland basin evolution where clockwise P-T path is expected in the course of subsequent burial, crustal thickening and late exhumation (Ledru *et al*., 1997; Vanderhaeghe *et al*., 1998).

In the light of such an infered late-Transamazonian mantle driven thermal perturbation, the significance of the Belvédère rhyolite is still to be deciphered: Neorhyacian ? or even Orosirian ? volcanic activity, possibly linked with the precursor stages of the so-called "Uatumã" volcanism? Further studies should take this point into account. Indications of late-Transamazonian (Orosirian) deep-seated basic magma sources could be the late NNE-SSW dolerite dykes found in the Comté River (Delor *et al*., 2001), and possibly along the Oyapok River, in French Guiana. In that respect the rather linear NNE-SSW trend of the Dachine diamond-bearing volcaniclastic komatiites would gain to be re-assessed from a chronostructural standpoint. Morever, the NNE-SSW fault trends which dissect the whole of French Guiana, as can be seen on the geological map (Fig. 4a) and the radiometric map (Fig. 3), could witness at a broader scale the waning stage of Transamazonian thermotectonic activity in French Guiana.

Conclusions

On the basis of recent airborne geophysics, field geological investigations and about 100 new isotopic (Pb-Pb and Sm-Nd) data, we are able to provide a comprehensive and detailed overview for the wide spectrum of Paleoproterozoic terrains in French Guiana. We consider the complex geological evolution in terms of dualistic crustal growth, with both Archean recycling and juvenile Paleoproterozoic crustal accretion, resulting from mantle extraction processes that began, at the earliest, at 2.26 Ga. Our data point to the formation of juvenile oceanic crust (2.25 -2.20 Ga) on the basis of lithological and isotopic data from the "Île de Cayenne Complex". The dominant tonalitic magmatism and regionally associated greenstone belt (2.18 -2.13 Ga) are interpreted within a scenario of island-arc plutonovolcanism in response to a main southward-directed subduction during a D1 event related to N-S convergence of the African and Amazonian Archean cratons. Two major pulses of tonalitic magmatism are indicated at 2.18 - 2.16 Ga and 2.15 - 2.13 Ga, with an intra-arc younging direction that resulted in the older 2.18 - 2.16 Ga migmatized TTG being exposed in northern and southern French Guiana, while the younger 2.15-2.13 Ga generation occupies an inner position. Granitic magmatism and migmatization of earlier TTG-greenstones at *ca*. 2.11-2.08 Ga occurred in response to the closure of the island-arc basins, with an evolution from southward-directed subduction to sinistral wrenching (D2a), but without significant crustal thickening of volcano-sedimentary sequences. Detrital basin opening occurs during D2a and seems to be located in areas where crustal stretching was maximum (pull-apart basins). Further crustal stretching leads to dextral shearing and co-eval leucogranite emplacement during late D2 deformation. This D2b stage, dated at 2.07 - 2.06 Ga in French Guiana, is amplified farther west in Suriname, where it culminates with the production of the Bakhuis granulite belt dated at *ca*. 2.07 - 2.05 Ga. The similar counterclockwise P-T path found in

both the French Guiana detrital basins and the Suriname granulite, argues for an anomalously high geotherm during burial, followed by isobaric cooling. Such a metamorphic signature, together with the abundant granite magmatism produced by the melting of TTG-greenstone facies at moderate pressures, is correlated with mantle upwelling during prolonged stretching of the Transamazonian crust.

Acknowledgements

The study was supported by BRGM from 1996 to 2000 as part of the French Guiana mapping project, and also benefited from further specific BRGM support under *the Projet Centre Guyane*. The work is also associated with the Pronex Project of the Geosciences Centre of the UFPa (Pronex Project no. 420.00/00 *Magmatismo, Metalogênese e Evolução Crustal da Província Mineral de Carajás e Províncias Adjacentes*). We are particularly indebted to J.P. Richard (BRGM Guyane) for organizing the many field trips, to the French Army (9th RIMA) for its logistical support for a Tumuc Humac field trip, and to all collaborators of the French Guiana geological mapping project for help in sampling.

The airborne geophysical survey was achieved with great skills by Geoterrex under BRGM supervision. Claude Delor and Cathy Truffert adress their warmfull thanks to José Perrin, Philippe Bernard, Jean-Marc Miehe, Evgenii Burov and Fawsia Asfirane for their dedicated full-time implication during the airborne campaign in French Guiana and/or further data interpretation in Orléans.

For the geological data acquisition, as well as for subsequent scientific investigations and discussions, we give special thanks to:

- José Maria de Azevedo and Maria Telma Lins Faraco (CPRM, Geological Survey of Brazil) who surveyed the transboundary area along the Oyapock River jointly with the BRGM field geologists;

- Ramon Capdevila and Jean-Jacques Peucat (University of Rennes) for their stimulating discussions and for having contributed to field petrostructural (RC) and isotopic data acquisition (JJP) in the southern part of French Guiana;

- the University of Orléans research scientists Yan Chen, Olivier Monod, André Pouclet, Max Vidal, and their postgraduate PhD student Sébastien Nomade and MSc students Dominique Herpin, François Kerbaol, Cécile Rigollet and Cédric Vaumoron;

- the mining compagnies for stimulating discussions. We are particularly indebted to C.A. Bertoni (Guyanor S.A.) who provided us a detailed map of diamond-bearing volcaniclastic komatiites.

Despite these very helpful recent contributions, our study would not have reached the present level of knowledge without the tremendous mapping efforts achieved by many geologists throughout the past century. We would like to mention specifically, in chronological order, the systematic pioneering mapping of Boris Choubert and co-workers covering the whole of French Guiana, the subsequent detailed mapping of the southern greenstones by Alain Marot and co-workers, and the harsh and impressive stream-sediment sampling achieved by many geologists during the course of the Mining Inventory Programme of French Guiana from 1975 to 1995.

We also thank Pierre Jézequel for his invaluable expertise in mineral processing at BRGM, and Magali Portheault (Géo-Hyd) for her cheerfull availability and efficiency in the realization of geological figures for this article.

Finally, we are grateful to Renaud Caby, Joël Le Métour, Patrick Ledru and Emond de Roever for having helped in so many ways to improve this paper. Any infelicities and misinterpretations are entirely our responsibility.

References

Abouchami W., Boher M., Michard A., Albarède F. (1990) - A major 2.1 Ga old event of mafic magmatism in West Africa: an early stage of crustal accretion. *J. Geophys. Res.*, **95**, 17605-17629.

Avelar V.G. de (2002) - Geocronologia Pb-Pb em zircão e Sm-Nd em rocha total da porção centro-norte do Estado do Amapá - Brasil: implicações para a evolução do setor oriental do Escudo das Guianas. Belém, CPGG-UFPA, PhD thesis, 212 p.

Avelar V.G. de, Lafon J.M., Delor C. (2001) - Geocronologia Pb-Pb em zircão e Sm-Nd em rocha total da porção centro-norte do Amapá. Implicações para a evolução geodinâmica do Escudo das Guianas. *In*: Simpósio de Geologia da Amazônia, 7, Belém, SBG-NO. Resumos Expandidos (CD-ROM).

Avelar V.G. de, Lafon J.M., Delor C. (2002) - Revisão geocronológica da porção centro–norte do Estado do Amapá: Implicações geodinâmicas. *In*: Congresso Brasileiro de Geologia, 41. João Pessoa - PB. SBG. Anais de resumos, p. 291

Avelar V.G. de, Lafon J.M., Delor C., Guerrot C., Lahondère D. (2003) - Archean crustal remnants in the easternmost part of the Guiana Shield: Pb-Pb and Sm-Nd geochronological evidence for Mesoarchean versus Neoarchean signatures. *Géologie de la France*, **2-3-4**, 83-99.

Barruol J., Brosse J.M., Langevin E. (1978) - SAÜL, carte géologique de la France à 1/100 000, département de la Guyane, BRGM, Orléans.

Bemba G., Hocquard C., Schmitt J-M. (1978) - Prospection générale et cartographie géologique de la feuille à 1/100 000 Araoua. BRGM Report 78 GUY 008.

Boher M., Abouchami W., Michard A., Albarède F., Arndt T.N. (1992) - Crustal growth in West Africa at 2.1 Ga. *J. Geophys. Res.*, **97**, 345-369.

Bosma W., Kroonenberg S.B., Maas K., Roever E.W.F. de (1983) - Igneous and metamorphic complexes of the Guiana Shield in Surinam. *Geol. Mijnbouw*, **62**, 241-254.

Burg J.P. (1991) - Syn-migmatization way-up criteria. *J. structural geol.*, **13(6)**, 617-623.

Capdevila R., Arndt N., Letendre J., Sauvage J. (1999) - Diamonds in volcaniclastic komatiite from French Guiana. *Nature* (London), **399**, 6735, 456-458.

Chaterjee N.D., Froese E. (1975) - A thermodynamic study of the pseudobinary, join muscovite-paragonite in the system $KalSi_3O_8$-$NaAlSi_3O_8$-Al_2O_3-SiO_2-H_2O. *Amer. Mineral*., **60**, 985-993.

Choubert B. (1960) - Carte géologique de la Guyane Française à l'échelle du 1/500 000 (2 sheets, North and South). Serv. Carte géol. Fr., Paris.

Choubert B. (1964) - Âges absolus du Précambrien guyanais. *C.R. Acad. Sci., Paris*, t. **258**, groupe 9, 631-634.

Choubert B. (1974) - Le Précambrien des Guyanes. Mém. BRGM, Orléans, 81, 213 p.

Cocherie A., Albarède F. (2001) - An improved U-Th-Pb age calculation for electron microprobe dating of monazite. *Geochim. Cosmochim. Acta*, **65**, 24, 4509-4522.

Cocherie A., Guerrot C., Rossi Ph. (1992) - Single-zircon dating by step-wise evaporation: comparison with other geochronological techniques applied to the Hercynian granites of Corsica, France. *Chemical Geology* (Isotope Geocience Section), **101**, 131-141.

Cocherie A., Legendre O., Peucat J-J., Kouamelan A.N. (1998) - Geochronology of polygenetic monazites constrained by *in situ* electron microprobe Th-U-total Pb determination: implications for lead behaviour in monazite. *Geochim. Cosmochim. Acta*, **62**, 2475-2497.

Cocherie A., Rossi Ph., Legendre O., Lafon J.M., Delor C., Jezequel P. (2000) - Systematic dating on monazite and zircon by EPMA, a tool for geochronological surveying and mapping of Precambrian basements: the example of French Guiana. 31st Intern. Geol. Congr., Rio de Janeiro, Brazil, August 6-17, 2000.

Cocherie A., Be Mezeme E., Legendre O., Fanning C.M. (2002) - Electron microprobe dating as a tool for understanding closure of the U-Th-Pb system in monazite : examples from migmatite. GSA 2002 Denver Annual Meeting (october 27-30, 2002).

Cocherie A., Be Mezeme E., Legendre O., Fanning C.M., Faure M., Rossi Ph. (2004) - Electron-microprobe dating as a tool for determining the closure of Th-U-Pb systems in migmatitic monazites. *Amer. Mineral*., in press.

Compston W., Williams I.S., Clement S.W. (1982) - U-Pb ages within single zircons using a sensitive high mass-resolution ion microprobe. American Society for Mass Spectrometry Conference 30th, Honolulu, p. 593-595.

Cordani U.G., Neves B.B.B. (1982) - The geologic evolution of South America during the Archean and Early Proterozoic. *Rev. Bras. Geoc*., **12**, 78-88.

Cordani U.G., Tassinari C.C.G., Teixeira W., Basei M.A.S., Kawashita K. (1979) - Evolução tectônica da Amazônia com base nos dados geocronológicos. II Congresso Geológico Chileno. Arica. Chile, Actas, p. 137-148.

Courtillot V., Renne P.R. (2003) – On the age of flood basalt events. *C.R. Geoscience*, **335** (2003), 113-140.

Deckart K. (1996) –-Etude du magmatisme associé au rifting de l'Atlantique central et Sud : géochronologie $^{40}Ar/^{39}Ar$ et géochimie sur les intrusions jurassiques de Guinée et de Guyane française/Suriname, et crétacées du Brésil. PhD thesis, University of Nice Sophia-Antipolis, 221 p.

Deckart K., Feraud G., Bertrand H. (1997) - Age of Jurassic continental tholeiites of French Guyana, Surinam and Guinea: implications for the initial opening of the Central Atlantic Ocean. *Earth Planet. Sci. Lett*., **150**, 205-220.

Delor C., Simeon Y., Kouamelan A.N., Peucat J.-J. (1994) - Persistance de processus de création crustale au Birrimien (Paléoprotérozoïque) en Côte d'Ivoire (Afrique de l'Ouest). 15ème Réunion des Sciences de la Terre Nancy - France. Comptes Rendus, p. 10.

Delor C., Perrin J., Truffert C. (1997) - Campagne de géophysique aéroportée en Guyane française. Magnétisme et radiométrie spectrale. BRGM Report R 39625, 102 p. (Ed. BRGM).

Delor C., Perrin J., Truffert C. (1998a) - Images géophysiques de socle. *Géochronique*, **67**, 7-12

Delor C., Rossi Ph., Cocherie A., Capdevilla R., Peucat J.J., Vidal M. (1998b) - The French Guyana basement revisited: new petrostructural and geochronological results, and correlations with the West African shield. *In:* Congresso Brasileiro de Geologia, 40 ; Belo Horizonte. Anais, p. 49.

Delor C., Faraco M.T., Fraga L., Lafon J.M., de Roever E., Rossi P., Vidal M. (2000) - Synthesis of the North Amazonian Precambrian Shield (SYNAPS) and trans-atlantic correlations: a geological framework for the analysis of Precambrian crustal growth. General Symposia no. 9-2 "Continental Growth (or Survival) in the Precambrian" (CD-ROM).

Delor C., Lahondère D., Egal E., Marteau P. (2001) - Carte géologique de la Guyane à 1/500 000, 2nd edition, BRGM.

Delor C., Roever E.W.F. de, Lafon J.M., Rossi P., Cocherie A., Guerrot C., Potrel A. (2003) - The Bakhuis ultrahigh-temperature granulite belt (Suriname): II. implications for late Transamazonian crustal stretching in a revised Guiana shield framework. *Géologie de la France*, **2-3-4**, 207-230.

Deloule E., Alexandrov P., Cheilletz B., Laumonier B., Barbey P. (2003) - In-situ U-Pb zircon ages for early Ordovician magmatism in the eastern Pyrenees, France: the Canigou orthogneisses. *Inter. J. Earth Sci*., in press.

Egal E., Mercier D., Itard Y., Mounie F. (1992) - L'ouverture de bassins en pull-apart ou Protérozoïque inférieur : nouveaux arguments dans le nord du craton guyanais 1992. *C.R. Acad. Sci. Paris*, **314**, II, 1499-1506.

Egal E., Milesi J.P., Ledru P., Cautru J.P., Freyssinet P., Thiéblemont D., Vernhet Y., Cocherie A., Hottin A.M., Tegyey M., Vanderhaeghe O. (1994) - Ressources minérales et évolution minière de la Guyane. Carte thématique minière à 1/100 000. Feuille Cayenne : carte et notice. BRGM Report R 38019, 59 p.

Egal E., Milesi J.P., Vanderhaeghe O., Ledru P., Cocherie A., Thiéblemont D., Cautru J.P., Vernhet Y., Hottin A.M., Tegyey M., Martel-Jantin B. (1995) - Ressources minérales et évolution minière de la Guyane. Carte thématique minière à 1/100 000. Feuille Régina : carte et notice. BRGM Report R 38458, 64 p.

Gaudette H.E., Lafon J.M., Macambira M.J.B., Moura C.A.V., Scheller T. (1998) - Comparison of single filament Pb evaporation/ionization zircon ages with conventional U-Pb results: examples from the Precambrian of Brazil. *J. South Amer. Earth Sci.*, **11**(4), 351-363.

Gibbs A.K., Barron C.N. (1983) - The Guiana Shield Reviewed. *Episodes*, Ottawa, **2**, 7-14.

Gibbs A.K., Barron C.N. (1993) - The Geology of the Guiana Shield. Oxford Monographs on Geology and Geophysics, **22**, 246 p.

Gruau G., Martin H., Leveque B., Capdevila R., Marot A. (1985) - Rb-Sr and Sm-Nd geochronology of Lower Proterozoic granite-greenstones belts terrains in French Guiana, South America. *Precambrian Res*., **30**, 63-80.

Jegouzo P., Ledru P., Marot A., Capdevila A. (1990) - Processus collisionnels d'âge paléoprotérozoïque dans le bouclier guyanais. 13ème réunion des Sciences de la Terre, Grenoble, Soc. géol. de France, Paris, p. 71.

João X.S.J., Marinho P.A.C. (1982) - Catametamorfitos Arqueanos da região centro-este do Território Federal do Amapá. *In*: Simp. Geol. Amaz. 1, Belem. Anais Belem. SBG. 2, 207-228.

Kerbaol F. (1997) - Relations entre les séries épizonales de Maripasoula-Inini et les séries à métamorphisme de haute température de l'Alitany et du Tampoc de part et d'autre de l'accident du Ouaqui (Sud de la Guyane française) dans les formations paléoprotérozoïques du Bouclier des Guyanes. Mémoire de DEA, University of Orléans, 40 p.

Kleenman U., Reinhardt J. (1994) - Garnet-biotite thermometry revisited : The effect of Al(VI) and Ti in biotite. *Eur. J. Mineral.*, **6**, 925-941.

Kober B. (1986) - Whole grain evaporation for $^{207}Pb/^{206}Pb$ age investigations on single zircons using a double filament source. *Contrib. Mineral. Petrol.*, **93**, 482-490.

Kober B. (1987) - Single grain evaporation combined with Pb^{+} emitter bedding for $^{207}Pb/^{206}Pb$ investigations using thermal ion mass spectrometry, and implications for zirconology. *Contrib. Mineral. Petrol.*, **96**, 63-71.

Lafon J.M., Rossi P., Delor C., Avelar V.G., Faraco M.T.L. (1998) - Novas testemunhas de relíquias arqueanas na crosta continental paleoproterozóica da Província Maroni-Itacaiúnas (Sudeste do Escudo das Guianas). *In:* Congresso Brasileiro de Geologia, 40, Belo Horizonte. Anais p. 64.

Lafrance J., Bardoux M., Voicu G., Stevenson R., Machado N. (1999) - Geological and metallogenic environments of gold deposits of the Guiana Shield: a comparative study between St-Elie (French Guiana) and Omai (Guyana). *Explor. Mining Geol.*, **8** (1 & 2), 117-135.

Lambert R St. J. (1976) - In the early history of the earth, ed. BF Windley, 363-373.

Lasserre J.L., Ledru P., Manier E., Mercier D. (1989) - Le Protérozoïque de Guyane. Révision lithostructurale. Implications pour la formation détritique Orapu et la gîtologie de l'or. BRGM Report 89 GUF023, 52 p.

Ledru P., Lasserre J.L., Manier E., Mercier D. (1991) – Le Protérozoïque inférieur nord guyanais : révision de la lithologie, tectonique transcurrente et dynamique des bassins sédimentaires. *Bull. Soc. géol. Fr.*, **162-4**, 627-636.

Ledru P., Johan V., Milesi J.P., Tegyey M. (1994) – Markers of the last stages of the Palaeoproterozoic collision: evidence for a 2 Ga continent involving circum-South Atlantic provinces. *In*: T. Onstott (Editor), Proterozoic Paleomagnetism and Paleogeography. *Precambrian Res.*, **69**, 169-191.

Ledru P., Milesi J.P., Johan V., Sabaté P., Maluski H. (1997) - Foreland basins and gold-bearing conglomerates: a new model for the Jacobina Basin (São Francisco province, Brazil). *Precambrian Res.*, **86**, 155-176.

Ludwig K.R. (1999) - Isoplot/Ex version 2.06 : A Geochronological Toolkit for Microsoft Excel. Berkeley Geochronology Center, Special Publication N° 1a. 49 p.

Ludwig K.R. (2001) - Users manual for ISOPLOT/EX, version 2.49 A geochronological toolkit for Microsoft Excel. Berkeley Geochronology Center. Special Publication 1a, 43 p.

Manier E. (1992) - Les conglomérats aurifères de Guyane française (Protérozoïque inférieur) : dynamique des bassins sédimentaires et contrôles des minéralisations. Ecole Nationale Supérieure des Mines de Paris, Mém. Sci. de la Terre, 17, 176 p.

Manier E., Mercier D., Ledru P. (1993) - Sedimentary dynamics of Lower Proterozoic alluvial deposits in French Guyana. Gold mineralisation in proximal facies. *Int. Assoc. Sedimentol. Spec. Publ.*, **17**, 553-568

Marot A. (1988) - Carte géologique du Sud de la Guyane à 1/500 000 et notice, BRGM Ed.., 86 p.

Marot A., Bemba G., Sempere T. (1979) - Prospection générale et cartographie géologique de la feuille à 1/100 000 Haute Ouaqui. BRGM Report 79 GUY 002.

Marot A., Bemba G., Boulanger P. (1983) - Prospection générale et cartographie géologique de la feuille à 1/100 000 Itany. BRGM Report BRGM GU 26.

McDougall I. (1985) – K-Ar and $^{40}Ar/^{39}Ar$ dating of the hominid-bearing Pliocene-Pleistocene sequence at Koobi Fora, Lake Turkana, northern Kenya. *Geol. Soc. Amer. Bull*., **96**, 159-175.

McReath I., Faraco M.T.L. (1997) - Sm/Nd and Rb/Sr systems in parts of the vila Nova metamorphic suite, northern Brazil. *In*: South American sysmposium on Isotope Geology, 1, campos de Jordão. Extended abstracts, 194-196.

Milesi J.P., Egal E., Ledru P., Vernhet Y., Thiéblemont D., Cocherie A., Tegyey M., Martel-Jantin B., Lagny Ph. (1995) - Les minéralisations du Nord de la Guyane française dans leur cadre géologique. *Chronique de la Recherche Minière, Fr*., **518**, 5-58.

Montalvão R.M.G., Tassinari C.C.G. (1984) - Geocronologia pré-cambriana do Território Federal do Amapá (Brasil). *In:* Simp. Amaz., 2 Manaus. *Anais Manaus*, MME-DNPM, 54-57.

Montgomery C., Hurley P.M. (1978) - Total U-Pb and Rb-Sr systematics in the Imataca series, Guyana shield, Venezuela. *Earth Planet. Sci. Lett*., **39**, 281-290.

Moyen J.F., Martin H., Jayananda M. (1997) - Origin of the late-Archaean granite of Closepet, South India: information from geochemical modeling of trace element behaviour. *C.R. Acad. Sci. Paris* - Series IIA, **325**(9), 659-664.

Moyen J.F., Martin H., Jayananda M. (2001) - Multi-element geochemical modelling of crust–mantle interactions during late-Archaean crustal growth: the Closepet granite (South India). *Precambrian Res.*, **112** (1-2), 87-105

Nomade S. (2001) - Evolution géodynamique des cratons des Guyanes et d'Afrique de l'Ouest. Apport des données paléomagnétiques, géochronologiques ($^{40}Ar/^{39}Ar$) et géochimiques en Guyane et Côte-d'Ivoire. PhD thesis, University of Orléans, France.

Nomade S., Théveniaut H., Chen Y., Pouclet A., Rigollet C. (2000) - Paleomagnetic study of French Guyana Early Jurassic dolerites: hypothesis of a multistage magmatic event. *Earth Planet. Sci. Lett.*, **184**, 155-168.

Nomade S., Chen Y., Féraud G., Pouclet A., Théveniaut H. (2001) - First Palaeomagnetic and $^{40}Ar/^{39}Ar$ study of Palaeoproterozoic rocks from the French Guiana (Camopi and Oyapok rivers), northeastern Guiana Shield. *Precambrian Res*., **109**, 239-256.

Norcross C.E., Davis D.W., Spooner E.T.C. (1998) - U-Pb geochronology of the Omai intrusão hosted Au-quartz vein deposit and host rocks, Guyana, South America. *In*: GSA ANNUAL MEETING, Toronto, Ontario, p. A-127.

Norcross C.E., Davis D.W., Spooner E.T.C., Rust A. (2000) - U-Pb and Pb-Pb age constrainsts on Paleoproterozoic magmatism, deformation and gold mineralization in the Omai area, Guyana Shield. *Precambrian Res*., **102**, 69-86.

Picot J.C. (1982) - Indice diamantifère de IT 33 (Haut Inini), Inventaire minier du département de la Guyane. BRGM Report 82 GUY 004.

Plumb K.A. (1991) - New Precambrian time scale. *Episodes*, **14** (2), 139-140.

Pommier A., Cocherie A., Legendre O. (2003) - "EPMA dating": a program for age calculation from electron microprobe measurements of U-Th-Pb. EGS-AGU-EUG. Nice, France, 6-11 April 2003.

Powell R., Holland T., Worley B. (1998) - Calculating phase diagrams involving solid solutions via non-linear equations, with examples using THERMOCALC. *J. Metamorphic Geol.*, **16**, 577-588.

Ricci P.S.F., Carvalho J.M.A., Rosa-Costa L.T. (2001) - Diferentes terrenos, com embasamentos geocronologicamente distintos, justapostos por megaestruturas regionais na fronteira Pará/Amapá. *In:* Simpósio de Geologia da Amazônia, 7, Belém, SBG-NO, Resumos Expandidos (CD-ROM).

Rosa-Costa L.T., Ricci P.S.F., Lafon J.M., Vasquez M.L., Carvalho J.M.A., Klein E.L., Macambira E.M.B. (2003) - Geology and geochronology of Archean and Paleoproterozoic domains of the Southwestern Amapá and Northwestern Pará, Brazil, Southeastern Guiana Shield. *Géologie de la France*, **2-3-4**, 101-120.

Roever E.W.F. de, Kroonenberg S.B., Delor C., Phillips D. (2003) - The Käyser dolerite, a Mesoproterozoic alkaline dyke suite from Suriname. *Géologie de la France*, **2-3-4**,161-174.

Roever E.W.F. de, Lafon J.M., Delor C., Cocherie A., Rossi P., Guerrot C., Potrel A. (2003) - The Bakhuis ultrahigh-temperature granulite belt (Suriname): I. petrological and geochronological evidence for a counterclockwise P-T path at 2.07-2.05 Ga. *Géologie de la France*, **2-3-4**, 207-230.

Santos J.O.S., Hartmann L.A., Gaudette H.E., Groves D.I., McNaughton N.J., Fletcher I.R. (2000) - A new understanding of the provinces of the Amazon Craton based on integration of field mapping and U-Pb and Sm-Nd geochronology. *Gondwana Res*., **3** (4), 453-488.

Schuhmacher M., Chambost E. de, McKeegan K.D., Harrison T.M. (1993) - In situ U-Pb dating of zircon with the CAMECA IMS1270. SIMS IX Proceeding.

Streckeisen A.L. (1967) - Classification and nomenclature of igneous rocks. *Neues Jb. Mineral., Monatsh., Abh*., **107**, 144-214.

Streckeisen A.L. (1976) - To each plutonic rock its proper name. *Earth Sci. Rev*., **12**, 1-33.

Suzuki K., Adachi M. (1991) - Precambrian provenance and Silurian metamorphism of the Tsubonosawa paragneiss in the South Kitakami terrane, Northeast Japan, revealed by the chemical Th-U-total Pb isochron ages of monazite, zircon and xenotime. *Geochem. J.*, **25**, 357-376.

Tassinari C.C.G., Bettencourt J.S., Geraldes M.C., Macambira M.J.B., Lafon J.M. (2000) - The Amazonian Craton. *In:* Tectonic Evolution of South America, Cordani U.G., Milani E.J., Thomaz Filho A., Campos D.A. (eds.), 31st Int. Geological Congress, 2000, 41-96.

Tassinari C.C.G., Macambira M.J.B. (1999) - Geochronological provinces of the Amazonian craton. *Episodes*, **22(3)**, 174-182.

Tassinari C.C.G., Teixeira W., Nutman A.P., Szabó G.A., Mondin M., Sato K. (2001) - Archean crustal evolution of the Imataca Complex, Amazonian Craton: Sm-Nd, Rb-Sr & U-Pb (SHRIMP) evidences. *In:* Simpósio de Geologia da Amazônia, 7. Belém. (CD-ROM).

Tegyey M. (1993) - Evolution métamorphique des roches détritiques aurifères du Sillon Nord-Guyanais « Orapu » (région de Cayenne-Régina, Guyane française). BRGM Report 36858, 43 p.

Teixeira W., Ojima G.K., Kawashita K. (1984) - A evolução geocronológica de rochas metamórficas e ígneas da Faixa móvel Maroni-Itacaiúnas, na Guiana francesa. *In*: Simpósio Amazônico, 2, Manaus. MME-DNPM, Anais. p. 81-86.

Teixeira W., Kawashita K., Taylor P.N., Ojima S.J., Viera A.G. (1985) – Reconhecimento geocronológico da Guyana francesa: novos dados, integração e implicações tectônicas. Simpósio Geológico da Amazonia, 2. Belém. Anais. Belém. Sociedade Brasileira de Geociências, **1**, 194-207.

Théveniaut H., Delor C. (2003) - Le paléomagnétisme du bouclier des Guyanes : état des connaissances et analyse critique des données. *Géologie de la France*, **2-3-4**, 59-82.

Vanderhaeghe O., Ledru P., Thiéblemont D., Egal E., Cocherie A., Tegyey M., Milési J.P. (1998) - Contrasting mechanism of crustal growth. Geodynamic evolution of the Paleoproterozoic granite-greenstone belts of French Guiana. *Precambrian Res.*, **92**, 165-193.

Vernhet Y., Milesi J.P., Ledru P., Plat R., Egal E. (1992) - Carte des minéralisations du Nord de la Guyane Française. *In*: Milesi *et al*., 1995.Ed. BRGM.

Vidal M., Delor C., Pouclet A., Simeon Y. (1996) - Evolution de l'Afrique de l'Ouest entre 2.2 et 2 Ga : le style « archéen » des ceintures vertes et des ensembles sédimentaires birimiens du Nord-Est de la Côte d'Ivoire. *Bull. Soc. géol. Fr.*, **167** (3), 307-319.

Vinchon C., Manier E., Lasserre J.L., Milesi J.P., Ledru P. (1988) - Etude sédimentologique des grès Orapu. Application à l'étude des gîtes d'or. BRGM Report 88 GUF GEO, 9 p.

Voicu G., Bardoux M., Jébrak M., Crépeau R. (1999) - Structural, mineralogical, and geochemical studies of the Paleoproterozoic Omai gold deposit, Guiana Shield. *Canad. Mineral.,* **37** (3), 559-573.

Voicu G., Bardoux M., Stevenson R. (2001) - Lithostratigraphy, geochronology and gold metallogeny in the northern Guiana Shield, South America: a review. *Ore Geology Review*, **18**, 211-236.

Williams I.S. (1998) - U-Th-Pb Geochronology by Ion Microprobe. *Rev. Econ. Geol.*, **7**, 1-35.

Appendix A
Aerogeophysical survey acquisition

The 1996 airborne geophysical survey over French Guiana simultaneously recorded the earth's magnetic field and gamma-ray spectra on 256 channels, using modern positioning techniques (GPS, radar and laser altimetry). The data-acquisition work was entrusted to *Compagnie générale de géophysique* (CGG) on the basis of a call for tenders. Two Cessna Titan 404 aircraft were used, both equipped with a sophisticated navigation system (video radar, altimeter, laser altimeter, barometers and GPS), a magnetometer and a gamma-ray spectrometer.

The flight specifications for the survey were 120 m above the forest canopy at a speed of about 260 km/h so as to provide a spatial resolution of the order of 7 m for the magnetic data and 70 m for the spectrometric data. The measurements were recorded along 130,000 line kilometres oriented N030° with a line spacing of 500 or 1000 m, and more rarely of 250 m.

The quality and contractual character of the measured parameters were controlled throughout the programme by two BRGM geophysicists. The results of the airborne campaign were presented in a synthesis report accompanied by eight thematic (magnetic and gamma-ray radiation) maps at 1:500,000 scale that are available from the BRGM in both paper and digital format (Delor *et al*., 1997).

Appendix B
Geochronology - analytical procedures and isotopic results

Analytical procedures

Pb-evaporation on zircon (TIMS): The Pb-Pb data used in this paper are unpublished results obtained by the Pb-evaporation method of Kober (1986, 1987) at the BRGM and UFPa geochronological laboratories, and earlier results from Vanderhaeghe *et al.* (1998). The isotopic results are displayed in Table 2.

The Pb-Pb analyses on zircon performed at the BRGM Geochronological laboratory followed the experimental procedure described in Cocherie *et al*. (1992). However, weighted mean values of the $^{207}Pb/^{206}Pb$ ages and corresponding errors were recalculated using the Ludwig (1999 and 2001) Isoplot software. The samples analysed at the BRGM laboratory were microdiorite (40-98OY-[61]), tonalite (50-98OY-[65]), granite (00CAY9f-[14b], GC60-[23], DAC147-[16], MA29A-[6], GC227b-[26], DOC49-[27], Organabo-[1]), metaandesite (GC269-[25]), and gabbro (GUD32-[20]).

For the Pb-evaporation analyses performed at the UFPa laboratory, the weighted means and errors on the age were calculated according to Gaudette *et al.* (1998). The samples dated at the UFPa (Pará-Iso) laboratory were granodiorite (74-98OY [66], 85-98OY-[67]), granite (B107-[47], ARA61-[36]), tonalite (Laussat-[4], 89-98OY-[68]), and Mg-K granite (TH09-[64]).

A test by the UFPa laboratory of data reduction with the Isoplot program of Ludwig (2001) furnished results that are statistically indistinguishable from the calculations obtained following Gaudette *et al*. (1998). Consequently, the results from the BRGM and Belém laboratories are directly comparable, despite being calculated using different procedures. The geochronological results have been plotted in age diagrams using the Isoplot program (Ludwig, 2001), independently of the calculation procedure for the age (Fig. 7).

The final value for the samples dated at the UFPa laboratory is calculated by the weighted average of the mean value for each grain, wereas for those dated at the BRGM laboratory, its is calculated by the weighted average of the mean value for each step of all the grains.

U-Pb on zircon by ion microprobe: Four samples were analysed for U-Pb dating by ion microprobe (SIMS). Three of these - a gabbro (00CAY10-[13]), a granodiorite (ARA83-[35b]) and a monzogranite (Petit Saut-[8]) - were dated by the U-Pb method on zircon at CNRS - CRPG in Nancy using a Cameca IMS1270 ion microprobe. The characteristics and design of the Cameca IMS1270 are described by Schuhmacher *et al*. (1993). The experimental procedure for the sample preparation and the instrumental parameters for the U-Pb isotope determinations of the studied samples are presented by Deloule *et al*. (2003).

The fourth sample - a migmatite (CJ 22) [63] - was analysed using the Shrimp II of the Research School of Earth Sciences (Australian National University, Canberra). The analytical procedures are described in detail by Compston *et al*. (1982) and Williams (1998).

Zircon	Temp. T°C	Number of ratios	206Pb/ 204Pb	208Pb/ 206Pb	207Pb*/ 206Pb*	2σ	Age (Ma) step	2σ	Age (Ma) Grain	2σ
Granodiorite - 74-98OY - [66]										
74-98OY/1	*1450*	*84*	*13158*	*0,085*	*0,13464*	*37*	*2160*	*5*		
	1500	*18*	*> 1000000*	*0,059*	*0,13543*	*55*	*2170*	*7*	***2170***	*7*
74-98OY/2	*1450*	*36*	*9174*	*0,068*	*0,13159*	*95*	*2120*	*13*		
	1500	*90*	*142857*	*0,072*	*0,13184*	*24*	*2123*	*3*		
	1550	*18*	*> 1000000*	*0,085*	*0,13195*	*61*	*2124*	*8*	***2123***	*3*
74-98OY/3	*1450*	*88*	*28571*	*0,082*	*0,13544*	*21*	*2170*	*3*		
	1500	84	40000	0,098	0,13622	35	2180	4	**2180**	**4**
74-98OY/4	*1450*	*16*	*11628*	*0,124*	*0,13480*	*86*	*2162*	*11*		
	1500	78	19231	0,107	0,13654	21	2184	3	**2184**	**3**
74-98OY/5	*1450*	*80*	*7634*	*0,095*	*0,13326*	*33*	*2142*	*4*		
	1500	88	30303	0,131	0,13640	21	2182	3	**2182**	**3**
74-98OY/6	*1450*	*18*	*4505*	*0,061*	*0,13295*	*59*	*2137*	*8*	***2137***	***8***
74-98OY/7	1450	86	31250	0,080	0,13554	39	2171	5		
	1500	86	166667	0,050	0,13609	24	2178	3		
	1550	90	> 1000000	0,048	0,13630	30	2181	4	**2179**	**3**
74-98OY/8	*1450*	*54*	*23810*	*0,061*	*0,13389*	*33*	*2150*	*4*		
	1480	*89*	*142857*	*0,065*	*0,13577*	*21*	*2174*	*3*		
	1520	90	166667	0,078	0,13670	20	2186	3	**2186**	**3**
74-98OY/9	*1450*	*84*	*50000*	*0,057*	*0,13417*	*21*	*2153*	*3*		
	1550	*90*	*10417*	*0,043*	*0,13415*	*24*	*2153*	*3*	***2153***	***2***
74-98OY/10	*1450*	*89*	*23810*	*0,124*	*0,13514*	*33*	*2166*	*4*		
	1550	90	34483	0,131	0,13705	25	2191	3	**2191**	**3**
74-98OY/11	*1450*	*36*	*21739*	*0,115*	*0,13545*	*31*	*2170*	*4*		
	1500	*88*	*30303*	*0,108*	*0,13601*	*21*	*2177*	*3*	***2177***	***3***
74-98OY/12	*1450*	*19*	*8000*	*0,111*	*0,13275*	*23*	*2135*	*3*	***2135***	***3***
	Mean (6 grains 3+4+5+7+8+10, 692 ratios, USD=2.93)								**2183**	**3**
Microdiorite - 40-98OY - [61]										
Zr A	1440	64	37950	0.119	0.13475	62	2161	8		
	1460	61	101740	0.171	0.13517	66	2166	8		
	1480	65	46000	0.176	0.13497	124	2164	16	**2163**	**10**
Zr B	*1440*	*12*	*9100*	*0.045*	*0.13100*	*120*	*2111*	*16*		
	1460	34	52520	0.101	0.13465	82	2159	10	**2159**	**10**
Zr C	*1420*	*57*	*33510*	*0.060*	*0.13272*	*94*	*2134*	*12*		
	1440	65	36940	0.134	0.13470	102	2160	14		
	1460	56	40440	0.174	0.13484	66	2162	8		
	1500	58	39620	0.180	0.13519	74	2166	10		
	1560	45	21590	0.194	0.13446	154	2157	20	**2162**	**12**
Zr D	1420	19	11330	0.088	0.13458	168	2159	22		
	1440	60	36640	0.102	0.13460	118	2159	16		
	1460	68	35240	0.131	0.13394	94	2150	12		
	1500	53	34170	0.145	0.13431	72	2155	10	**2155**	**14**
	Mean (grains A+B+C+D, 648 ratios, 12 steps, MSWD=0.72)								**2161**	**3**
Tonalite - 50-98OY - [65]										
Zr A	*1440*	*60*	*13590*	*0.094*	*0.13141*	*78*	*2117*	*10*		
	1460	*9*	*3220*	*0.162*	*0.13454*	*206*	*2158*	*26*		
	1480	65	31870	0.173	0.13448	62	2157	8		
	1500	42	9400	0.213	0.13505	70	2165	10	**2160**	**8**
Zr C	*1420*	*15*	*8370*	*0.077*	*0.13105*	*162*	*2112*	*22*		
	1440	64	22530	0.144	0.13428	138	2155	18	**2155**	**18**
Zr D	*1400*	*70*	*6910*	*0.117*	*0.13032*	*158*	*2102*	*22*		
	1420	29	6750	0.175	0.13503	174	2164	22	**2164**	**22**
	Mean (grains A+C+D, 200 ratios, 4 steps, MSWD=0.66)								**2160**	**6**

Table 2.- Pb-Pb isotopic data on zircons from the samples dated by the Pb-evaporation method. In italic: data not included in the mean age calculation of the grain. *: radiogenic.

Tabl. 2.- Données isotopiques Pb-Pb sur zircons pour les échantillons datés par la méthode d'évaporation du plomb.

Granite - B107 - [47]										
B107/1	*1500*	*90*	*16667*	*0,094*	*0,13319*	*22*	*2141*	*3*		
	1520	86	34483	0,103	0,13439	18	2156	2		
	1550	52	21277	0,100	0,13436	30	2156	4	**2156**	**2**
B107/2	1500	52	250000	0,118	0,13531	38	2168	5	**2168**	**5**
B107/3	*1450*	*52*	*4016*	*0,091*	*0,12806*	*33*	*2072*	*5*		
	1500	84	33333	0,121	0,13508	20	2165	3	**2165**	**3**
B107/5	*1450*	*36*	*32258*	*0,084*	*0,13204*	*34*	*2126*	*5*		
	1500	86	37037	0,113	0,13423	40	2154	5	**2154**	**5**
B107/6	*1450*	*16*	*41667*	*0,090*	*0,13318*	*48*	*2141*	*19*		
	1500	86	111111	0,107	0,13535	47	2169	6	**2169**	**6**
B107/7	*1450*	*18*	*7092*	*0,083*	*0,12892*	*44*	*2084*	*6*		
	1500	50	32258	0,110	0,13448	56	2158	7	**2158**	**7**
B107/8	*1450*	*82*	*25000*	*0,098*	*0,13161*	*25*	*2120*	*3*		
	1500	90	83333	0,111	0,13500	23	2164	3		
	1550	16	> 1000000	0,110	0,13530	72	2168	9	**2165**	**3**
B107/9	*1450*	*18*	*3571*	*0,070*	*0,12810*	*115*	*2072*	*16*		
	1500	*78*	*50000*	*0,101*	*0,13409*	*18*	*2152*	*2*		
	1500	*49*	*83333*	*0,101*	*0,13375*	*22*	*2148*	*3*		
	1550	88	200000	0,111	0,13488	21	2163	3	**2163**	**3**
B107/10	*1500*	*18*	*4386*	*0,060*	*0,12926*	*75*	*2088*	*10*		
	1500	*68*	*17544*	*0,094*	*0,13350*	*19*	*2145*	*3*		
	1550	19	37037	0,105	0,13487	54	2163	7	**2163**	**7**
B107/11	*1450*	*84*	*38462*	*0,094*	*0,13450*	*18*	*2158*	*2*		
	1500	88	27778	0,104	0,13518	20	2167	3		
	1550	80	20408	0,110	0,13553	22	2171	3	**2169**	**4**
B107/13	*1450*	*45*	*11905*	*0,082*	*0,12949*	*17*	*2091*	*2*		
	1500	88	76923	0,125	0,13532	23	2169	3		
	1550	36	58824	0,136	0,13582	39	2175	5	**2170**	**6**
B107/14	*1500*	*86*	*45455*	*0,113*	*0,13383*	*21*	*2149*	*3*		
	1550	88	66667	0,117	0,13497	25	2164	3	**2164**	**3**
	Mean (12 grains 1+2+3+5+6+7+8+9+10+11+13+14, 1089 ratios, USD=3.1)								**2163**	**3**
Tonalite - Laussat - [4]										
LAUSS/2	*1450*	*84*	*21739*	*0,059*	*0,13439*	*23*	*2156*	*3*		
	1500	*96*	*66667*	*0,087*	*0,13480*	*39*	*2162*	*5*		
	1550	34	23256	0,088	0,13550	35	2171	5	**2171**	**5**
LAUSS/3	1500	93	4651	0,136	0,13556	41	2172	5	**2172**	**5**
LAUSS/4	*1450*	*50*	*25641*	*0,085*	*0,13403*	*23*	*2152*	*3*		
	1500	70	333333	0,101	0,13561	31	2172	4	**2172**	**4**
LAUSS/5	*1450*	*54*	*25000*	*0,050*	*0,13127*	*40*	*2115*	*5*		
	1500	86	62500	0,098	0,13559	22	2172	3	**2172**	**3**
	Mean (4 grains 2+3+4+5, 283 ratios, USD=0.3)								**2172**	**2**
Granite - 00CAY9f - [14b]										
Zr A	*1380*	*14*	*1040*	*0.06*	*0.12416*	*438*	*2017*	*62*		
	1400	*23*	*1880*	*0.06*	*0.13130*	*226*	*2115*	*30*		
	1420	27	6540	0.08	0.13435	124	2156	16		
	1460	64	5150	0.11	0.13517	220	2166	28		
	1480	15	5340	0.12	0.13578	154	2174	20	**2165**	**28**
Zr B	*1380*	*7*	*880*	*0.06*	*0.12622*	*1220*	*2046*	*166*		
	1400	*60*	*17080*	*0.08*	*0.13273*	*146*	*2134*	*20*		
	1420	69	9000	0.08	0.13417	202	2153	26		
	1460	*7*	*8080*	*0.09*	*0.13456*	*542*	*2158*	*70*	**2153**	**26**

Table 2.- Suite/Continued.

Zr C	*1380*	*61*	*4320*	*0.10*	*0.12799*	*136*	*2071*	*18*		
	1400	*58*	*10580*	*0.10*	*0.13272*	*60*	*2134*	*8*		
	1420	70	23420	0.10	0.13457	100	2158	14	**2158**	**14**
Zr D	1460	57	8620	0.03	0.13120	166	2114	22		
Zr E	*1400*	*67*	*14830*	*0.08*	*0.13354*	*74*	*2145*	*10*		
	1420	63	15600	0.10	0.13542	126	2169	16		
	1460	15	4520	0.11	0.13578	100	2174	12	**2170**	**16**
	Mean (grains A+B+C+E, 448 ratios, 7 steps, MSWD=1.06)								**2165**	**6**
Granite - GC60 - [23]										
Zr A	1440	100	19300	0.095	0.13326	102	2141	14		
	1460	48	36090	0.093	0.13331	122	2142	16	**2141**	**14**
	1500	63	68860	0.099	0.13323	130	2141	16		
Zr B	1580	41	11020	0.105	0.13297	146	2137	20	**2137**	**20**
Zr D	1600	48	6510	0.106	0.13314	176	2140	24	**2140**	**24**
	Mean (grains A+B+D, 300 ratios, 5 steps, MSWD=0.04)								**2141**	**8**
Metaandesite - GC269 - [25]										
Zr B	1560	24	10760	0.183	0.13323	92	2141	12		
	1580	14	11700	0.184	0.13285	276	2136	36	**2139**	**24**
Zr C	1520	55	5410	0.230	0.13324	166	2141	22		
	1560	58	17580	0.261	0.13270	60	2134	8		
	1580	32	4530	0.248	0.13308	184	2139	24	**2138**	**20**
Zr D	*1520*	*8*	*3410*	*0.112*	*0.13164*	*518*	*2120*	*68*		
Zr E	1560	32	8860	0.107	0.13309	242	2139	32	**2139**	**32**
Zr F	1560	42	4100	0.118	0.13322	164	2141	22	**2141**	**22**
	Mean (grains B+C+D+F, 257 ratios, 7 steps, MSWD=0.22)								**2137**	**6**
Granite - DAC147 - [16]										
Zr C*	*1500*	*16*	*6380*	*0.082*	*0.13125*	*166*	*2115*	*22*		
analyse	1520	29	10440	0.080	0.13227	118	2128	16		
1997	1560	63	16400	0.086	0.13214	92	2127	12		
	1580	58	20550	0.092	0.13235	90	2129	12		
	1600	46	20560	0.110	0.13201	120	2125	16	**2127**	**14**
Zr A	1420	14	9220	0.073	0.13209	108	2126	14		
	1460	33	19710	0.076	0.13222	130	2128	18		
	1480	41	9300	0.082	0.13223	144	2128	18	**2127**	**18**
Zr B	1420	20	8740	0.084	0.13238	162	2130	22		
	1460	29	9250	0.097	0.13240	170	2130	22		
	1480	15	10820	0.132	0.13251	162	2132	22		
	1500	57	11610	0.149	0.13240	204	2130	26		
	1520	*8*	*13800*	*0.154*	*0.13262*	*168*	*2133*	*22*	**2130**	**24**
Zr C	1420	57	7780	0.144	0.13274	180	2135	24		
	1460	68	10530	0.123	0.13252	100	2132	14		
	1480	68	6610	0.162	0.13216	110	2127	14	**2131**	**18**
Zr D	1420	31	8980	0.071	0.13251	158	2131	20		
	1460	63	8280	0.089	0.13288	78	2136	8		
	1480	41	6400	0.139	0.13318	76	2140	10	**2136**	**14**
Zr E	1420	22	5300	0.055	0.13276	192	2135	26		
	1460	65	15110	0.067	0.13262	96	2133	12		
	1480	52	10840	0.091	0.13273	120	2134	16	**2134**	**16**
	Mean (grains A+B+C+D+E, 872 ratios, 20 steps, MSWD=0.423)								**2132**	**3**

Table 2.- Suite/Continued.

Granite - MA29A - [6]										
Zr A	*1440*	*62*	*29140*	*0.041*	*0.13005*	*36*	*2099*	*4*		
	1460	*58*	*49650*	*0.045*	*0.13136*	*36*	*2116*	*4*		
	1480	69	81530	0.049	0.13255	76	2132	10	**2132**	**10**
Zr B	*1440*	*67*	*6820*	*0.086*	*0.12949*	*102*	*2091*	*14*		
	1460	55	21980	0.115	0.13269	78	2134	10	**2134**	**10**
Zr C	*1400*	*15*	*6280*	*0.070*	*0.13091*	*324*	*2110*	*44*		
	1420	35	10990	0.048	0.13225	76	2128	10		
	1440	56	19200	0.047	0.13224	62	2128	8		
	1460	37	19010	0.054	0.13218	82	2127	10		
	1480	22	24250	0.058	0.13307	84	2139	12	**2129**	**10**
Zr D	1400	34	13000	0.054	0.13224	98	2128	12		
	1420	70	26080	0.047	0.13281	92	2135	12		
	1440	63	29820	0.049	0.13274	84	2134	12		
	1460	55	32060	0.058	0.13278	62	2135	8	**2134**	**10**
	Mean (grains A+B+C+D, 630 ratios, 10 steps, MSWD=0.62)								**2132**	**3**
Granite - ARA61 - [36]										
ARA61/1	*1450*	*52*	*3106*	*0,109*	*0,13017*	*31*	*2101*	*4*		
	1500	90	50000	0,136	0,13097	19	2111	3	**2111**	**3**
ARA61/2	1500	90	71429	0,221	0,13116	19	2114	2		
	1550	36	125000	0,254	0,13122	33	2115	4	**2114**	**2**
ARA61/3	*1450*	*84*	*6536*	*0,132*	*0,12818*	*27*	*2074*	*4*		
ARA61/4	1450	90	5650	0,153	0,13105	23	2112	3		
	1500	84	7092	0,224	0,13095	22	2111	3	**2112**	**2**
ARA61/5	1450	86	7299	0,185	0,13081	22	2109	3	**2109**	**3**
ARA61/6	1500	82	10204	0,122	0,13055	26	2106	4	**2106**	**4**
ARA61/7	*1450*	*46*	*10526*	*0,059*	*0,13132*	*79*	*2116*	*11*		
	1500	*82*	*200000*	*0,042*	*0,13183*	*24*	*2123*	*3*		
ARA61/8	1450	90	25641	0,217	0,13107	17	2113	2		
	1550	82	45455	0,231	0,13125	19	2115	3	**2114**	**2**
	Mean (6 grains 1+2+4+5+6+8, 730 ratios, USD=1.9)								**2112**	**2**
Granite - GC227b - [26]										
Zr A	1380	32	3900	0.131	0.12954	172	2092	24		
	1400	65	13020	0.119	0.12916	82	2087	12		
	1420	59	18030	0.128	0.12973	118	2094	16		
	1460	60	28300	0.133	0.12918	48	2087	6		
	1480	12	14040	0.136	0.12972	156	2094	20	**2090**	**14**
Zr C	1460	29	4290	0.128	0.12915	174	2086	24		
	1480	18	3530	0.124	0.12948	172	2091	24	**2088**	**24**
Zr D	1380	35	2200	0.115	0.12958	176	2092	24		
	1420	58	2020	0.144	0.12996	176	2097	16		
	1460	62	10270	0.145	0.12956	156	2092	22		
	1480	61	7800	0.174	0.12939	106	2090	14	**2093**	**18**
	Mean (grains A+C+D, 491 ratios, 11 steps, MSWD=0.27)								**2089**	**4**
Granite - DOC49 - [27]										
Zr D*	1520	19	18930	0.073	0.12934	148	2089	20		
analyse	1560	64	27400	0.080	0.12900	72	2084	10		
1997	1580	61	34020	0.087	0.12906	96	2085	14	**2085**	**14**
Zr B	*1400*	*12*	*550*	*0.153*	*0.12954*	*284*	*2092*	*38*		
	1420	44	680	0.137	0.12932	232	2089	28		
	1460	53	2410	0.099	0.12950	172	2091	24		
	1480	21	2660	0.086	0.12951	196	2091	26	**2090**	**28**
Zr C	1460	54	8480	0.132	0.12986	138	2096	18		
	1480	64	7720	0.127	0.12946	74	2091	10	**2093**	**16**
Zr E	*1380*	*5*	*1130*	*0.153*	*0.12555*	*182*	*2037*	*26*		
	1400	*7*	*1560*	*0.129*	*0.12963*	*240*	*2093*	*32*		
	1460	68	21150	0.130	0.12937	60	2089	8	**2089**	**8**
	Mean (grains B+C+D+E, 448 ratios, 9 steps, MSWD=0.256)								**2089**	**4**

Table 2.- Suite/Continued.

Gabbro - GUD32 - [20]										
Zr A	1500	49	8980	0.215	0.12978	208	2095	28	**2095**	**28**
Zr B	1500	89	22060	0.199	0.13000	164	2098	22		
	1520	59	16780	0.204	0.12985	162	2096	22	**2097**	**20**
Zr C	1500	66	12560	0.189	0.12912	88	2086	12	**2086**	**12**
Zr D	1480	38	10690	0.174	0.12904	222	2085	30		
	1500	68	29550	0.207	0.12956	74	2092	10		
	1520	16	12010	0.219	0.12949	192	2091	26	**2090**	**22**
Zr E	1500	46	11960	0.202	0.12963	148	2093	20		
	1520	61	53230	0.208	0.12956	104	2092	14		
	1560	67	56330	0.203	0.12978	90	2095	12	**2094**	**16**
Zr F	1500	63	30120	0.201	0.12941	148	2090	20		
	1520	66	23390	0.198	0.12971	162	2094	22		
	1560	65	51010	0.189	0.12964	102	2093	14		
	1580	71	60050	0.194	0.12949	100	2091	14		
	1600	*10*	*20000*	*0.188*	*0.13104*	*286*	*2112*	*38*		
	1680	27	7990	0.185	0.12963	178	2093	12	**2092**	**18**
	Mean (grains A+B+C+D+E+F, 851 ratios, 15 steps, MSWD=0.15)								**2092**	**4**
Mg-K granite - TH09 - [64]										
TH09/1	*1450*	*88*	*9804*	*0,088*	*0,12939*	*19*	*2090*	*3*		
	1470	84	43478	0,078	0,13	37	2098	5		
	1490	88	37037	0,085	0,13018	23	2101	3	**2100**	**3**
TH09/2	1450	88	5000	0,140	0,13009	31	2100	4		
	1470	88	11765	0,157	0,1301	22	2100	3		
	1550	86	5376	0,194	0,13021	22	2101	3	**2100**	**2**
TH09/3	*1470*	*86*	*125000*	*0,182*	*0,12982*	*23*	*2096*	*3*		
	1480	82	100000	0,221	0,13022	29	2101	4		
	1550	90	200000	0,241	0,13034	27	2103	4	**2102**	**3**
TH09/4	1450	36	90909	0,114	0,13006	69	2099	9		
	1480	90	34483	0,227	0,13004	27	2099	4	**2099**	**3**
	Mean (4 grains 1+2+3+4, 732 ratios, USD=0.7)								**2100**	**1**
Tonalite - 89-98OY - [68]										
89-98OY/1	1450	86	18182	0,138	0,13041	24	2104	3		
	1480	86	50000	0,184	0,13056	20	2106	3		
	1520	90	31250	0,199	0,13083	19	2109	3	**2107**	**3**
89-98OY/2	*1450*	*16*	*6135*	*0,068*	*0,12904*	*66*	*2085*	*9*		
	1480	86	16393	0,151	0,13013	19	2100	3		
	1500	88	16667	0,185	0,13042	18	2104	2		
	1550	18	16667	0,198	0,12997	53	2098	7	**2102**	**3**
89-98OY/3	*1450*	*32*	*6211*	*0,052*	*0,13263*	*96*	*2133*	*13*		
	1550	86	27778	0,052	0,13506	36	2165	5	**2165**	**5**
89-98OY/4	*1450*	*16*	*2762*	*0,061*	*0,12847*	*55*	*2077*	*7*		
	1550	14	2994	0,062	0,13335	77	2143	10	**2143**	**10**
89-98OY/6	1450	70	9524	0,065	0,13015	65	2100	9	**2100**	**9**
	1500	*88*	*14286*	*0,060*	*0,13433*	*23*	*2155*	*3*		
89-98OY/7	*1450*	*88*	*3247*	*0,071*	*0,13555*	*28*	*2172*	*4*		
	1500	70	4386	0,055	0,13728	29	2193	4	**2193**	**4**
89-98OY/8	1450	90	3344	0,065	0,13044	26	2104	4	**2104**	**4**
89-98OY/9	1450	86	9804	0,055	0,13293	34	2137	4	**2137**	**4**
89-98OY/11	*1450*	*88*	*8065*	*0,055*	*0,13447*	*17*	*2157*	*2*		
	1500	88	8850	0,053	0,13472	18	2161	2	**2161**	**2**
89-98OY/12	*1450*	*86*	*9174*	*0,055*	*0,13451*	*19*	*2158*	*3*		
	1500	80	3846	0,059	0,13534	22	2169	3	**2169**	**3**
	Mean (4 grains 1+2+6+8, 614 ratios, USD=2.2)								**2104**	**2**
	Inheritance: 2137 - 2193 Ma (6 grains)									

Table 2.- Suite/Continued.

Granodiorite - 85-98OY - [67]										
85-98OY/1	1480	84	1000000	0,104	0,13051	20	2105	3		
	1510	84	> 1000000	0,110	0,13054	18	2106	2		
	1550	88	125000	0,109	0,13081	39	2109	5	**2106**	**2**
85-98OY/2	*1450*	*84*	*19608*	*0,080*	*0,12975*	*35*	*2095*	*5*		
	1480	88	83333	0,097	0,13009	39	2100	5		
	1520	84	55556	0,106	0,13015	22	2100	3	**2100**	**3**
85-98OY/3	*1450*	*88*	*18868*	*0,078*	*0,12946*	*27*	*2091*	*4*		
	1480	88	> 1000000	0,070	0,13038	18	2103	2		
	1520	90	> 1000000	0,070	0,13038	21	2103	3	**2103**	**2**
85-98OY/4	1470	86	200000	0,093	0,13054	20	2106	3	**2106**	**3**
	Mean (4 grains 1+2+3+4, 692 ratios, USD=1.60)								**2104**	**2**
Granite - Organabo - [1]										
Zr A	*1380*	*45*	*11840*	*0.031*	*0.12914*	*124*	*2086*	*18*		
	1400	*45*	*6150*	*0.046*	*0.13188*	*162*	*2123*	*22*		
	1420	*58*	*17840*	*0.055*	*0.13246*	*192*	*2131*	*26*		
	1460	63	5690	0.085	0.13423	116	2154	16		
	1480	63	16820	0.089	0.13479	160	2161	20		
	1500	60	11080	0.103	0.13502	128	2164	16	***2159***	***20***
Zr C	*1460*	*49*	*2700*	*0.069*	*0.12504*	*140*	*2029*	*20*		
	1480	*72*	*5270*	*0.077*	*0.12630*	*72*	*2047*	*10*		
	1500	45	6470	0.080	0.12714	116	2059	16	**2059**	**16**
Zr D	*1420*	*59*	*2600*	*0.078*	*0.12499*	*104*	*2029*	*14*		
	1460	65	6240	0.081	0.12762	146	2065	20		
	1480	*52*	*2330*	*0.089*	*0.12318*	*82*	*2003*	*12*		
	1500	*27*	*2190*	*0.089*	*0.12350*	*210*	*2007*	*30*	**2065**	**20**
Zr E	1460	60	13790	0.051	0.12751	132	2064	18		
	1480	56	13450	0.058	0.12766	44	2066	6		
	1500	62	11750	0.062	0.12739	58	2062	8		
	1520	61	23440	0.064	0.12797	72	2070	10		
	1580	55	12060	0.061	0.12742	96	2063	14	**2065**	**10**
Zr F	*1420*	*68*	*6330*	*0.069*	*0.12543*	*90*	*2035*	*12*		
	1460	58	39190	0.055	0.12828	84	2074	12		
	1480	58	45360	0.056	0.12816	58	2073	8		
	1500	56	48220	0.058	0.12826	68	2074	10	**2074**	**10**
	Mean (grains C+D+E+F, 576 ratios, 10 steps,MSWD=1.2)								**2069**	**4**
	Inheritance: 2.16 Ga (1 grain A, 3 steps)									

Table 2.- Suite/Continued.

The analytical results are given in Table 3 and shown on Figure 6.

U-Th-Pb on monazite (EPMA): Four samples of monazite, two extracted from granite (Petit Saut-[8]; ARA61-[36]), one from pegmatite (89-98RCI-[69]) and one from migmatite (sample CJ22-[63]), were analysed at the BRGM laboratory by electron probe microanalyzer (EPMA), which enables high spatial resolution dating together with systematic and detailed studies of small minerals. After the pioneer studies of Suzuki and Adachi (1991), recent improvements in the statistical treatment of a large number of *in situ* data now make it possible to decipher the related thermal events and so obtain reliable and precise ages (Cocherie *et al*., 1998; Cocherie and Albarède, 2001). In the case of monazites exhibiting significant Th/U ratio variation, data reduction in the Th/Pb = f(U/Pb) diagram commonly allows a precision of ± 5-10 Ma to be achieved at the 2σ level (Cocherie *et al*., 2002; Cocherie *et al*., in press). The combined use of the Isoplot (Ludwig, 2001) and EPMA dating (Pommier *et al*., 2003) programs enables one to statistically reduce a large number of data in a reproducible way. Table 4 and Fig. 8 give the analytical results.

Grain spot	U ppm	Th ppm	Th/U	Pb* ppm	$^{204}Pb/^{206}Pb$	f_{206} %	$^{206}Pb^*/^{238}U$	±	$^{207}Pb^*/^{235}U$	±	$^{207}Pb^*/^{206}Pb^*$	±	age $^{206}Pb^*/^{238}U$	±	age $^{207}Pb^*/^{235}U$	±	age $^{207}Pb^*/^{206}Pb^*$	±	Conc. %
Ile de Cayenne gabbro (00CAY10)																			
1,1	47	41	0,88	16	0,000030	0,043	0,4000	0,0025	7,639	0,058	0,13849	0,00018	2169	12	2189	7	2208	2	98
1,2	27	40	1,45	8	0,000045	0,067	0,3594	0,0015	6,854	0,035	0,13833	0,00013	1979	7	2093	5	2206	2	90
2,1	20	29	1,43	7	0,000102	0,150	0,3947	0,0013	7,522	0,041	0,13823	0,00030	2145	6	2176	5	2205	4	97
3,1	24	36	1,49	8	0,000090	0,132	0,3997	0,0025	7,644	0,065	0,13872	0,00029	2168	12	2190	8	2211	4	98
3,2	40	51	1,29	13	0,000044	0,065	0,3951	0,0047	7,600	0,125	0,13950	0,00063	2147	22	2185	15	2221	8	97
4,1	79	65	0,83	27	0,000057	0,083	0,4049	0,0103	7,663	0,226	0,13726	0,00057	2192	47	2192	26	2193	7	100
5,1	30	36	1,19	10	0,000069	0,102	0,3887	0,0066	7,372	0,135	0,13755	0,00018	2117	31	2158	16	2197	2	96
6,1	46	46	1,00	15	0,000038	0,056	0,3876	0,0026	7,377	0,056	0,13802	0,00014	2112	12	2158	7	2203	2	96
7,1	32	37	1,18	11	0,000058	0,086	0,3962	0,0089	7,506	0,188	0,13740	0,00034	2152	41	2174	22	2195	4	98
8,1	*63*	*61*	*0,98*	*23*	*0,000033*	*0,048*	*0,4321*	*0,0012*	*8,367*	*0,039*	*0,14045*	*0,00027*	*2315*	*5*	*2272*	*4*	*2233*	*3*	*104*
9,1	109	60	0,55	38	0,000012	0,018	0,4053	0,0018	7,792	0,041	0,13944	0,00012	2193	8	2207	5	2220	2	99
Granodiorite ARA 83 A																			
1,1	605	29	0,05	168	0,000035	0,051	0,3231	0,0012	5,986	0,027	0,13437	0,00010	1805	6	1974	4	2156	1	84
2,1	388	73	0,19	138	0,000011	0,016	0,4140	0,0014	7,639	0,035	0,13382	0,00017	2233	6	2189	4	2149	2	104
2,2	*189*	*27*	*0,14*	*45*	*0,000486*	*0,724*	*0,2773*	*0,0090*	*4,991*	*0,181*	*0,13054*	*0,00050*	*1578*	*45*	*1818*	*30*	*2105*	*7*	*75*
3,1	71	45	0,64	23	0,000024	0,035	0,3746	0,0009	6,948	0,026	0,13452	0,00019	2051	4	2105	3	2158	3	95
4,1	*184*	*21*	*0,12*	*42*	*0,000375*	*0,554*	*0,2622*	*0,0039*	*4,876*	*0,087*	*0,13487*	*0,00039*	*1501*	*20*	*1798*	*15*	*2162*	*5*	*69*
4,2	77	37	0,49	25	0,000068	0,101	0,3715	0,0038	6,881	0,079	0,13435	0,00017	2036	18	2096	10	2156	2	94
5,1	246	45	0,18	71	0,000151	0,223	0,3372	0,0022	6,247	0,051	0,13436	0,00020	1873	11	2011	7	2156	3	87
6,1	84	52	0,62	26	0,000037	0,054	0,3578	0,0009	6,641	0,025	0,13462	0,00016	1972	4	2065	3	2159	2	91
7,1	67	38	0,57	22	0,000045	0,067	0,3867	0,0018	7,173	0,045	0,13453	0,00021	2108	8	2133	6	2158	3	98
8,1	76	27	0,36	27	0,000066	0,098	0,4191	0,0020	7,767	0,046	0,13442	0,00015	2256	9	2204	5	2157	2	105
9,1	*255*	*25*	*0,10*	*81*	*0,000631*	*0,929*	*0,3682*	*0,0019*	*6,973*	*0,050*	*0,13736*	*0,00030*	*2021*	*9*	*2108*	*6*	*2194*	*4*	*92*

Table 3.- U-Pb zircon results for the dated samples from French Guiana. In italic: data not included in the average age of the zircons from a given rock sample. A: samples dated by IMS 1270 (gabbro 00CAY10; granodiorite ARA 83A; "Petit Saut" monzogranite. B: sample dated by SHRIMP II (migmatite CJ 22). Uncertainties given at the one sigma level; f206 % denotes the percentage of 206Pb that is common Pb; Correction for common Pb made using the measured $^{204}Pb/^{206}Pb$; for % Conc., 100 % denotes a concordant analysis.

Tabl. 3.- Résultats U-Pb sur zircons concernant les échantillons de Guyane. En italique : données non utilisées pour le calcul de la moyenne d'âge des zircons pour un échantillon donné. A: échantillons datés par IMS 1270 (gabbro 00CAY10; granodiorite ARA 83A; monzogranite "Petit Saut"). B: échantillon daté par SHRIMP II (migmatite CJ 22). Incertitudes fournies à 1 sigma. f_{206} % indique le pourcentage de ^{206}Pb, provenant du Pb commun.. Corrections du plomb commun utilisant les rapports $^{204}Pb/^{206}Pb$; pour le % conc., 100 % indique une analyse concordante.

Grain spot	U ppm	Th ppm	Th/U	Pb* ppm	$^{204}Pb/^{206}Pb$	f_{206} %	$^{206}Pb^*/^{238}U$	±	$^{207}Pb^*/^{235}U$	±	$^{207}Pb^*/^{206}Pb^*$	±	age $^{206}Pb^*/^{238}U$	±	age $^{207}Pb^*/^{235}U$	±	age $^{207}Pb^*/^{206}Pb^*$	±	Conc. %
Petit Saut monzogranite																			
2,1	*45*	*27*	*0,60*	*15*	*0,00083*	*1,232*	*0,3719*	*0,0089*	*6,829*	*0,165*	*0,13318*	*0,00090*	*2038*	*42*	*2089*	*21*	*2140*	*12*	*95*
3,1	*88*	*44*	*0,50*	*40*	*0,00016*	*0,221*	*0,3109*	*0,0097*	*7,995*	*0,273*	*0,18648*	*0,00243*	*1745*	*48*	*2231*	*31*	*2711*	*21*	*64*
3,2	*46*	*26*	*0,56*	*17*	*0,00086*	*1,246*	*0,3300*	*0,0102*	*6,619*	*0,239*	*0,14548*	*0,00231*	*1838*	*49*	*2062*	*32*	*2294*	*27*	*80*
5,1	42	28	0,68	14	0,00008	0,115	0,3626	0,0088	6,396	0,152	0,12793	0,00130	1994	41	2032	21	2070	18	96
6,1	*38*	*25*	*0,66*	*12*	*0,00006*	*0,095*	*0,3652*	*0,0088*	*6,244*	*0,152*	*0,12400*	*0,00104*	*2007*	*41*	*2011*	*21*	*2015*	*15*	*100*
7,1	244	60	0,25	79	0,00001	0,022	0,3563	0,0087	6,260	0,151	0,12744	0,00036	1964	41	2013	21	2063	5	95
7,2	228	54	0,24	73	0,00006	0,091	0,3781	0,0081	6,617	0,142	0,12693	0,00046	2067	38	2062	19	2056	6	101
7,3	297	70	0,24	96	0,00003	0,049	0,3931	0,0084	6,889	0,147	0,12710	0,00022	2137	39	2097	19	2058	3	104
8,1	52	38	0,73	17	0,00005	0,079	0,3515	0,0081	6,192	0,144	0,12778	0,00056	1942	39	2003	20	2068	8	94
13,1	*39*	*20*	*0,52*	*12*	*0,00008*	*0,118*	*0,3582*	*0,0079*	*6,176*	*0,140*	*0,12504*	*0,00061*	*1974*	*38*	*2001*	*20*	*2029*	*9*	*97*
14,1	210	318	1,52	68	0,00004	0,058	0,3580	0,0079	6,284	0,138	0,12733	0,00035	1973	38	2016	19	2061	5	96
14,2	*110*	*160*	*1,45*	*37*	*0,00002*	*0,026*	*0,2938*	*0,0116*	*5,400*	*0,213*	*0,13331*	*0,00041*	*1660*	*58*	*1885*	*34*	*2142*	*5*	*78*
15,1	38	24	0,62	12	0,00007	0,111	0,3394	0,0079	5,986	0,140	0,12793	0,00048	1884	38	1974	20	2070	7	91
Migmatite CJ 22																			
1,1	618	74	0,12	205	-	<0.01	0,3814	0,0061	6,845	0,112	0,1302	0,0002	2083	29	2092	15	2100	3	99
2,1	163	322	1,97	85	0,000028	0,04	0,4061	0,0068	7,577	0,148	0,1353	0,0011	2197	31	2182	18	2168	14	101
3,1	79	96	1,22	35	-	<0.01	0,4000	0,0076	7,427	0,156	0,1347	0,0009	2169	35	2164	19	2160	12	100
4,1	*48*	*52*	*1,09*	*20*	*0,000157*	*0,23*	*0,3839*	*0,0065*	*7,065*	*0,145*	*0,1335*	*0,0013*	*2095*	*30*	*2120*	*18*	*2144*	*17*	*98*
5,1	678	546	0,80	279	0,000003	<0.01	0,4032	0,0045	7,610	0,087	0,1369	0,0003	2184	20	2186	10	2188	3	100
6,1	425	308	0,72	174	0,000007	0,01	0,4088	0,0043	7,652	0,086	0,1358	0,0004	2210	20	2191	10	2174	5	102
6,2	193	154	0,80	80	0,000004	0,01	0,4071	0,0047	7,632	0,096	0,1360	0,0005	2202	22	2189	11	2176	6	101
7,1	283	157	0,55	93	0,000076	0,11	0,3353	0,0060	6,279	0,124	0,1358	0,0009	1864	29	2016	18	2175	11	86
7,2	1535	50	0,03	409	0,000014	0,02	0,3142	0,0033	5,598	0,063	0,1292	0,0004	1761	16	1916	10	2088	5	84
8,1	*116*	*111*	*0,96*	*48*	*0,000061*	*0,09*	*0,3927*	*0,0053*	*7,272*	*0,110*	*0,1343*	*0,0007*	*2135*	*25*	*2145*	*14*	*2155*	*9*	*99*
9,1	664	105	0,16	223	0,000010	0,02	0,3837	0,0047	6,810	0,087	0,1287	0,0003	2093	22	2087	11	2081	4	101
10,1	589	203	0,34	208	0,000014	0,02	0,3855	0,0041	6,883	0,076	0,1295	0,0003	2102	19	2097	10	2091	4	101
11,1	*733*	*144*	*0,20*	*155*	*0,000227*	*0,33*	*0,2302*	*0,0043*	*4,422*	*0,139*	*0,1394*	*0,0032*	*1335*	*23*	*1717*	*26*	*2219*	*40*	*60*
12,1	542	172	0,32	192	0,000004	0,01	0,3897	0,0045	6,985	0,086	0,1300	0,0004	2122	21	2110	11	2098	5	101
13,1	*136*	*103*	*0,76*	*54*	*0,000010*	*0,02*	*0,3978*	*0,0061*	*7,328*	*0,156*	*0,1336*	*0,0018*	*2159*	*28*	*2152*	*19*	*2146*	*23*	*101*
13,2	667	128	0,19	226	0,000003	0,01	0,3847	0,0042	6,887	0,081	0,1298	0,0004	2098	20	2097	11	2096	6	100
14,1	166	129	0,78	70	0,000100	0,15	0,4181	0,0052	7,812	0,107	0,1355	0,0006	2252	24	2210	12	2171	8	104
14,2	667	63	0,09	221	0,000021	0,03	0,3849	0,0042	6,891	0,080	0,1299	0,0004	2099	20	2098	10	2096	5	100

Table 3.- Suite continued

K-Ar on whole rock: Dolerite sample ARA 60-[37] was prepared for a conventional K-Ar analysis as described by McDougall (1985). The analysis was performed at the Research School of Earth Sciences (Australian National University, Canberra). Separate aliquots of the sample were selected for duplicate potassium and argon analyses. The aliquots for potassium analyses were ground into a powder to improve dissolution. The powdered aliquots were dissolved in sulphuric acid and hydrofluoric acid and the potassium concentrations were determined by standard flame photometric methods. A second weighted aliquot of the sample was loaded into a degassed Mo bucket and placed into a glass bottle connected to a high vacuum system. The sample was heated by radio-frequency induction to a temperature of ~1450 °C to ensure complete outgassing. Argon measurements were carried out using an MS10 mass spectrometer and standard isotope dilution methods with a ^{38}Ar spike. The K-Ar analytical results for dolerite sample ARA 60-[37] are detailed in Tables 1 and 5.

Pb (ppm) ± σ	U (ppm) ± σ	Th (ppm) ± σ	**Isochron age ± 2σ Ma**
Granite ARA61 (13 grains)			
5022 ± 1172	2690 ± 640	40280 ± 10800	**2127 ± 10** (n = 103)
Pegmatite 89-98RC1 (4 grains)			
7113 ± 2555	6419 ± 3130	48242 ± 14898	**2095 ± 6** (n = 104)
Pegmatite 89-98RC1 (1 grain)			
6553 ± 803	2064 ± 439	60296 ± 9293	**2061 ± 15** (n = 33)
Migmatite CJ22 (melanosome, 4 grains)			
9525 ± 1523	3020 ± 2537	82491 ± 19035	**2167 ± 19** (n = 33)
Migmatite CJ22 (leucosome, 5 grains)			
9477± 1708	11402 ± 5947	49567 ± 22882	**2172 ± 4** (n = 43)
Petit Saut Monzogranite (5 grains)			
4783 ± 1145	1305 ± 1164	44871 ± 8180	**2059 ± 23** (n = 32)

Table 4.- Summary of electron microprobe analyses on monazites. The number of analyses taken into consideration for age calculation is given in brackets.

Tabl. 4.- Synthèse des analyses microsonde sur monazites. Le nombre d'analyses pris en considération pour le calcul de l'âge est donné entre parenthèses.

Isotopic results

Gabbro - 00CAY10-[13] (U-Pb on zircon) (N4° 56' 37.8"; W52° 19' 52.8"): The sample came from a foliated fine-grained Fe-gabbro of "Pointe des Amandiers (Saint Joseph)", which belongs to the "Île de Cayenne" trondhjemitic/gabbroic complex. Nine zircons were dated using the IMS 1270 (Table 3) and provided a U-Pb zircon age as old as 2208 ± 12 Ma, which is interpreted as the age of formation of the Fe-gabbro (Fig. 6A).

Granodiorite - 74-98OY-[66] (Pb-evaporation on zircon) (N2° 14' 43.1"; W52° 52'34.7"): Sample 74-98OY corresponds to a migmatitic gneiss with a granodioritic composition. It was collected along the Oyapok River, in the southeasternmost part of French Guiana. Twelve grains were selected for Pb isotopic analyses. $^{207}Pb/^{206}Pb$ measurements were obtained on two or three heating steps for each grain from the dated population of zircons (Table 2; Fig 7A). A set of six grains provided similar $^{207}Pb/^{206}Pb$ ages with a mean value of 2183 ± 3 Ma (USD = 2.93) calculated on 692 ratios. The other six grains yielded lower values, between 2.12 Ga and 2.17 Ga, probably reflecting Pb loss in the crystals after crystallization; these data were excluded from the mean calculation. The age of 2183 ± 3 Ma is interpreted as the emplacement age of the granodiorite.

Microdiorite - 40-98OY-[61] (Pb-evaporation on zircon) (N2° 31' 53.7"; W52° 33' 11.7"): This sample was collected along the Oyapok River, 45 km north from the previous sample. It comes from a weakly foliated fine-grained diorite with biotite and amphibole. Four grains were selected for Pb-Pb dating. In each grain, isotopic data were registered on at least two, and up to five, temperature steps (Table 2). The same value was obtained from the three steps of Zircon A, the second step of Zircon B and the four steps of Zircons C and D. The mean value calculated on the twelve steps furnished a well-defined age of 2161 ± 3 Ma (MSWD = 0.72), which corresponds to the crystallization age of the protolith of the microdiorite (Fig. 7B).

Tonalite - 50-98OY-[65] (Pb-evaporation on zircon) (N2° 26' 50.2"; W52° 36' 53.2"): The sample was collected along the Oyapok River, between the two previous ones, from a coarse-grained foliated migmatitic gneiss with abundant biotite. Only three grains provided isotopic results for dating by the Pb evaporation method (Table 2). Pb isotopic values were registered on two to four heating steps. Grain A furnished the same age on three steps, but only two of them were used for age calculation, as the third one provided too few ratios. Grains C and D displayed a similar age at the highest temperature step and, together with grain A, gave a mean value of 2161 ± 6 Ma (MSWD = 0.66), which corresponds to the emplacement age of the tonalite (Fig. 7C).

Granite - B107-[47] (Pb-evaporation on zircon) (N3° 19' 03.6"; W52° 11' 05.3"): Sample B107 comes from a coarse-grained amphibole-biotite tonalite collected along the Oyapok River, about 25 km downstream from the Camopi River. Twelve grains were selected for Pb-Pb analysis. At least two, and up to five, heating steps were obtained (Table 2). All the grains gave similar results, with the mean value for the 12 grains providing a $^{207}Pb/^{206}Pb$ age of 2163 ± 3 Ma (usd = 3.1) interpreted as the crystallization age of the zircon during magma emplacement (Fig. 7D).

Tonalite - Laussat-[4] (Pb-evaporation on zircon) (N5° 25' 24.7"; W53° 35' 06.12"): The Laussat tonalite corresponds to a migmatitic orthogneiss and came from a quarry along the Laussat River in northwestern French Guiana. Four grains were selected for age determination. Each grain furnished one to three steps of heating that gave increasing age with increasing temperature (Table 2). The four grains gave similar ages at the highest temperature step, with a mean $^{207}Pb/^{206}Pb$ age of 2172 ± 2 Ma (usd = 0.3), indicating the crystallization age of the tonalite (Fig. 7E).

Granite - 00CAY9f-[14b] (Pb-evaporation on zircon) (N4° 54' 38.4"; W52° 18' 54.1"): Sample 00CAY9f, from a folded pegmatite vein of granitic composition, was collected at the Madeleine quarry, close to the city of Cayenne. Apart from grain D, which displayed only one step of heating, the four other analysed grains gave isotopic results from at least three steps (Table 2). The intensity of the Pb signal was relatively low, and in some cases too few ratios were registered; the isotopic values obtained by only one block of analyses were included in the age calculation, even when similar to those of the other steps. The results obtained on three consecutive steps from zircon A are similar and furnished a mean value of 2165 Ma, which is identical to the value obtained on the highest temperature step on grains B and C, and on two steps of grain E. Zircon D furnished only one step of heating with a value that was significantly lower, and so was excluded from the mean calculation. The mean value determined on seven steps from grains A, B, C and E, provided an age of 2165 ± 6 Ma (MSWD = 1.06), which corresponds to the crystallization age of granite 00CAY9f (Fig. 7F).

Amphibole granodiorite – ARA 83A-[35b] (U-Pb on zircon) (N3° 13' 15.7"; W53° 44' 25.7"): The sample came from a granodiorite enclave within a gabbro of the Tampok basic-ultrabasic complex located in southwestern French Guiana. Nine zircons were dated using the IMS 1270 (Table 3), of which eight provided an upper intercept U-Pb zircon age of 2154.9 ± 2.8 Ma, which is interpreted as the crystallization age of the granodiorite (Fig. 6B).

Granite - GC60-[23] (Pb-evaporation on zircon) (N3° 45' 06.8"; W53° 39' 22.0"): Sample GC60 corresponds to a weakly foliated granite collected in the Inini region, in the western part of French Guiana. Three grains furnished isotopic results, two of them at only one step of heating and the third at three steps (Table 2). All the isotopic values are similar, close to 2140 Ma at all steps and between each grain. The weighted mean obtained on the five steps indicated an age of 2141 ± 8 Ma with MSWD = 0.042 (Fig. 7G). This age is interpreted as the crystallization age of the granite.

Metaandesite - GC269-[25] (Pb-evaporation on zircon) (N3° 55' 58.1"; W53° 21' 01.8"): Sample GC269, which corresponds to a foliated metaandesite from the Paramaca Formation, was collected upstream along the Mana River in the central part of French Guiana. Five grains provided isotopic results for age calculation (Table 2). One grain yielded three steps of heating, another yielded two steps and the last three yielded only one step. Excluding grain D, which gave only one block of results with a low $^{206}Pb/^{204}Pb$ ratio and a significantly lower age, all the isotopic values were homogeneous and provided a weighted average of 2137 ± 6 Ma (MSWD = 0.22), determined on four grains and 257 ratios (Fig. 7H). The mean age is considered as the age of metaandesite crystallization.

Granite - DAC147-[16] (Pb-evaporation on zircon) (N4° 22' 17.8"; W52° 35' 30.8"): Sample DAC147 is from a granite along the Comté River. Six grains of the sample were successfully analysed, providing isotopic results from at least three steps of heating (Table 2). The results are homogeneous at all heating steps and in all grains, which made it possible to determine a well-defined mean value of 2132 ± 3 Ma (MSWD = 0.42) for the age of emplacement of the granite (Fig. 7I).

Granite - MA29A-[6] (Pb-evaporation on zircon) (N5° 10' 27.4"; W53° 42' 05.9"): The sample is from a fine-grained foliated granite, with associated tourmaline-bearing pegmatite, along the Mana River. Four grains were selected for Pb-Pb dating, all of which furnished from two to five temperature steps and displayed homogeneous isotopic results (Table 2). Four steps from crystals C and D and the highest temperature step from crystals A and B indicate a weighted average of 2132 ± 3 Ma (MSWD = 0.62), which represents the crystallization age of the zircons in the granitic magma (Fig. 7J).

Granite ARA61-[36] (Pb-evaporation on zircon and U-Th-Pb on monazite) (N3° 06' 09.7"; W53° 41' 00.2": This sample, collected from the Tampok River, corresponds to a granite with basic enclaves. Eight grains of zircon were selected for dating. Except for grain #3, #5 and #6, which gave only one temperature step, the other grains yielded two temperature steps, most of them with the same value at both steps (Table 2). Six grains provided similar values; grain #3 gave significantly lower values and was discarded for the mean calculation, as was grain #7, which displayed a slightly older age, up to 2123 Ma at the highest temperature step. The mean $^{207}Pb/^{206}Pb$ value obtained on 730 isotopic ratios from the 6 grains is 2112 ± 2 Ma (USD = 1.9), which is considered to be the crystallization age of the granite (Fig. 7K).

Monazite grains extracted from the granite were also numerous, enabling them to be dated by the EPMA method. The 13 analysed grains show a rather constant U/Th ratio (Table 4). The summary of the electron microprobe analyses shows the constant amount of U and Th. This can also be observed on the Th/Pb vs. U/Pb plot (Fig. 8A). Consequently, despite the high number of analysis points, the uncertainty on the average age calculated at the centroid of the population is relatively high at 2127 ± 10 Ma. The age obtained on the monazite is slightly older than the 2112 ± 2 Ma age furnished by the zircon. The geochronological results may be interpreted into two different ways: either the age of 2112 Ma corresponds to the crystallization of the zircons in the granitic magma and the age on monazite represents an inherited age from the source of the granite, or the age of about 2.13 Ga indicated by the monazites corresponds to the age of granite emplacement and the lower age displayed by the zircons indicates a renewal of the U-Pb system a short time after the formation of the granite. The fact that inheritance is common in the U-Th-Pb system of monazite, together with the fact that the $^{207}Pb/^{206}Pb$ ages are similar at every step of heating and from one grain to another, favour the first hypothesis that considers the age of 2112 ± 2 Ma as the age of crystallization of the zircons in the granitic magma.

Granite - GC227b-[26] (Pb-evaporation on zircon) (N3° 34' 40.8"; W53° 10' 23.2"): Sample GC227b came from the central part of French Guiana, east of the Inini Massif, and represents an isotropic or weakly oriented K-feldspar granite from a large granitic complex. Four grains were selected for Pb dating, but only three provided isotopic results. Two to five steps of heating were obtained on the three grains (Table 2). Crystal A displayed five steps with the same age, identical to the two steps of zircon C and to the four steps of zircon D. Together, these eleven steps yielded a mean value of 2089 ± 4 Ma (MSWD = 0.27) which is interpreted as the age of granite crystallization (Fig. 7L).

Granite - DOC49-[27] (Pb-evaporation on zircon) (N 3°53' 45.5"; W 52°34' 57"): Sample DOC49 is similar to the previous sample, but came from along the Approuague River in the eastern part of the granitic complex. Four grains were dated by the Pb evaporation method (Table 2). Crystals B, C and E provided 4, 2 and 3 steps of heating, respectively. With zircon E, only the last heating step was retained for age calculation, while with grain B three of the four steps were retained, as were the two steps on grain C. The fourth grain, analysed previously, provided three homogeneous steps of heating. These nine steps yielded a mean value of 2089 ± 4 Ma (MSWD = 0.256) which corresponds to the emplacement age of the granite (Fig. 7M).

Gabbro - GUD32-[20] (Pb-evaporation on zircon) (N4° 11' 08.4"; W53° 19' 31.2"): Sample GUD32 was also collected along the Approuague River, downstream the previous sample. It comes from a small isotropic coarse-grained massif. Six grains were used for Pb dating (Table 2). Excluding zircon F, which furnished 6 steps of heating, the grains yielded results at one to three temperature steps. All the values obtained at each step are similar within the error. Only step #5 of zircon F was not included in the average calculation. The mean value determined on 15 steps and 851 isotopic ratios indicated an age of 2092 ± 18 Ma (MSWD = 0.15). This age is considered as the crystallization age of the gabbro (Fig. 7N).

Mg-K granite TH09-[64] (Pb-evaporation on zircon) (N2° 10' 34"; W 54° 11' 10"): Sample TH09 is from a foliated biotite-amphibole-bearing granitoid from southwesternmost French Guiana, at the border with Brazil. Four grains were dated, all of which provided 2 or 3 heating steps, displaying similar values at all steps (Table 2). The mean value for the 4 grains furnished a very precise 207Pb/206Pb age of 2100 ± 1 Ma (usd = 0.7) for the Mg-K granite formation (Fig. 7O).

Pegmatite - 89-98RC1 - [69] (U-Th-Pb on monazite) (N5° 06' 11.2"; W52° 46' 10.6"): Sample 89-98RCI is from a pegmatite from the Roche Corail area, in the northeastern part of French Guiana. A re-assessment of the analytical results indicated that two ages can be determined on the dated population, rather than the unique age of 2091 ± 8 Ma published in the legend of the geological map (Tables 1 and 4). Four grains of monazite yielded an age of 2095 ± 6 Ma, calculated on 104 analytical points (Fig. 8B). A fifth grain of monazite provided a younger age of 2061 ± 15 Ma, determined on 23 analytical points (Fig. 8C). These two values are statistically distinct. As the pegmatite crosscuts granitic rocks that have still not been dated, no geological geological argument is available to decide on the age. However, on the geological map, the granitic pluton hosting the pegmatite has been included in the youngest magmatic episode at about 2.06 Ga. If the age of 2095 Ma corresponds effectively to the crystallization age of the pegmatite, then the granitic pluton is older and probably belongs to the 2.11-2.09 Ga magmatic episode.

Granodiorite - 85-98OY-[67] (Pb-evaporation on zircon) (N2° 13' 10,4"; W52° 53' 12.4"): Sample 85-98OY corresponds to a well-foliated biotite-bearing leucocratic granodiorite from the Oyapok River. Four grains were analysed for the age determination (Table 2). As with the previous sample, all the grains gave similar values at all the temperature steps, as well as from one grain to another one. The mean value, calculated on 692 isotopic ratios, gave a $^{207}Pb/^{206}Pb$ age of 2104 ± 2 Ma (USD = 1.6) for the crystallization of the granodiorite (Fig. 7Q).

Tonalite - 89-98OY-[68] (Pb-evaporation on zircon) (N2° 17' 16.4"; W52° 50' 34.6"): This sample comes from a migmatitic orthogneiss of tonalitic composition. It

Sample No.	Sample	K (wt %)	Radiogenic ^{40}Ar (10^{-10} mol/g)	% Radiogenic ^{40}Ar	Calculated Age (± 1 s.d.)
ARA60	Dolerite (whole rock)	0.3179	5.823	84.76	811 ± 29 Ma
		0.3393	5.790	84.67	807 ± 29 Ma
		0.3749			
		0.3201			
		0.3443			
		0.3188			

Table 5.- K-Ar analysis of dolerite sample ARA60. Constants: $\lambda_{\varepsilon}+\varepsilon' = 0.581 \times 10^{-10}$/year; $\lambda_{\beta} = 4.962 \times 10^{-10}$/year; $^{40}K/K = 1.167 \times 10^{-4}$ mol/mol. Note: % Rad.$^{40}Ar = 100 \times {}^{40}Ar_{Rad.}/{}^{40}Ar_{Total}$

Tabl. 5.- Analyse K-Ar de la dolérite ARA60. Constantes : $\lambda_{\varepsilon}+\varepsilon' = 0.581 \times 10^{-10}$/an ; $\lambda_{\beta} = 4.962 \times 10^{-10}$/an ; $^{40}K/K = 1,167 \times 10^{-4}$ mol/mol. Note : % Rad.$^{40}Ar = 100 \times {}^{40}Ar_{Rad.}/{}^{40}Ar_{Total}$

corresponds to the southernmost sample from the Oyapok River and was been collected about 2 km south from the previous sample. Ten crystals of zircon were selected for the isotopic analyses (Table 2). The grains gave from one to four heating steps. The isotopic results were very different from one grain to another. Four grains provided a similar low age with a mean $^{207}Pb/^{206}Pb$ value of 2104 ± 2 Ma (USD = 2.2). The other grains displayed a large range of values between 2.14 Ga and 2.19 Ga (Fig. 7P). The 2104 ± 4 Ma age is interpreted as the formation age of the tonalite, and the $^{207}Pb/^{206}Pb$ ages between 2.14 Ga and 19 Ga as an inherited Pb component in crystals from the source of the tonalite. This interpretation is reinforced by the fact that tonalite 89-98OY underwent a partial melting event, which led to local migmatization. This melting event also produced magmatic rocks in the area represented by the previous sample (granodiorite - 85-98OY), which displayed the same age (2104 ± 2 Ma). The source rocks are represented in the area by the tonalitic-granodioritic-dioritic rocks dated at about 2.16 Ga and 2.18 Ga, i.e. in the same range as the ages of the inherited zircon from sample 89-98OY.

Migmatite - CJ22-[63] (U-Pb on zircon and U-Th-Pb on monazite) (N2° 16' 31.8"; W 54° 04' 36.8"): The sampled rock is a cordierite-sillimanite-garnet-bearing migmatitic gneiss. Two contrasting parts of the rock were sampled, and heavy minerals were separated from both melanocratic and leucocratic facies. The melanosome contained mainly zircons and some rare monazites whereas the leucosome contained only monazites. After a cathodoluminescence study it was possible to distinguish two zircon populations: one comprising clear elongate grains, in places surrounded by a U-enriched rim, and the other consisting of small, rounded, U-enriched grains (Table 3). After Shrimp analyses, the Concordia plot (Fig. 6C) shows contrasting ages related to the two zircon populations. Apart from three analyses resulting from mixing ages between the two populations, the analyses, mainly concordant, plot at two distinct ages. The core of elongate grains gave an old age at 2172.9 ± 9.4 Ma, whereas the rounded U-enriched grains and the border of the elongate grains gave a younger age at 2093.6 ± 7.3 Ma. Only four small monazite grains were extracted from the part of the rock from which zircon grains were separated. Despite the limited number of U-Th-Pb analyses (Table 4), obtained using the electron microprobe, an isochron age has been calculated at 2167 ± 19 Ma (Fig. 8D). Much larger monazite grains could be extracted from the leucosome. Due to the unusually high U/Th variation, a very precise isochron age at 2172 ± 4 Ma (Fig. 8E) was calculated after only 43 spot analyses; this is in complete agreement with the age of monazite grains extracted from the melanosome. In addition, this age fits particularly well with the zircon age calculated from the elongate zircon. By contrast, absolutely no young age (e.g. 2090 Ma) was obtained from the monazite analysis. The age of 2172-2173 Ma is interpreted as the age of the protolith, while the age at 2094 Ma would date the migmatization event. Consequently, monazite appears as very robust mineral.

Granite - Organabo-[1] (Pb-evaporation on zircon) (N5° 33' 06.6"; W53° 28' 04.8"): Sample Organabo is a weakly foliated granite from northern French Guiana. Five grains were selected for Pb dating. At least three temperature steps were obtained on each grain (Table 2). Zircon A displayed values increasing from 2086 Ma to 2154 Ma during the first three heating steps, while the following three steps provided similar values within the error with a mean value of 2159 ± 20 Ma. This result is significantly older than the value (between 2.06 Ga and 2.07 Ga) displayed by the other grains, and would probably correspond to the existence of an inherited core in a younger crystal. The isotopic results obtained on the other grains, especially on zircons E and F, are homogeneous, with the same value being obtained on several steps from the different crystals. Zircon C underwent a significant lead loss, as only the highest temperature step furnished a similar value as grains E and F. Zircon D displayed an uncommon behaviour as the two highest temperature steps gave lower values than a lower temperature step. Such behaviour has been observed elsewhere and is discussed in Rosa-Costa *et al*. (2003). Calculation of the weighted mean value on the five steps of zircon E, together with the three highest temperature steps of zircon C and the step at 1460 °C of zircon D, enabled us to define an age of 2069 ± 4 Ma (MSWD = 1.2), interpreted as the crystallization age of the Organabo granite (Fig. 7R).

Monzogranite - Petit Saut-[8] (U-Pb on zircon and U-Th-Pb on monazite) (N5° 04' 20.7"; W 53° 01' 57.6"): The Petit Saut granite is a small intrusive isotropic body about 3 km in diameter. The sample for geochronological

study was collected at the Petit Saut dam. Nine crystals were analysed using the IMS 1270 ion microprobe. In the Concordia diagram, the analytical points yielded a U-Pb age of 2060 ± 4.1 Ma (Fig. 6D), interpreted as the crystallization age of the granite. Grain 3 displayed a $^{207}Pb/^{206}Pb$ discordant age of 2.71 Ga (Table 3), which is interpreted as an inherited Archean Pb component from the source of the granite. Despite the limited number of available grains (i.e. 5) and the lack of U/Th variation (Table 4), the U-Th-Pb method using EPMA was successfully applied to monazite. An average age was calculated at 2059 ± 23 Ma (Fig. 8F).

Dolerite - ARA60 - [37] (K-Ar on whole rock) (N3° 05' 19.8"; W53° 41' 12.9"): Sample ARA60 came from the southern end of a NW-SE oriented dolerite dyke, N of Petit Saut on the Tampok River, western French Guiana. Potassium analysis of six fractions of the sample yielded potassium contents ranging from 0.3179 to 0.3749 wt.% (Table 5). This variation is unusual and indicates significant heterogeneity within the sample. An average value of 0.328 (± 3.44%) was used for the K-Ar calculations. Radiogenic argon yields at 84.8% and 84.7%, which is relatively high for whole-rock samples. In combination, the potassium and argon analyses give K-Ar ages of 811 ± 29 Ma and 807 ± 29 Ma, with a mean age of 809 ± 29 Ma, slightly different from the value of 808 ± 29 Ma displayed on the geological map (Delor *et al.*, 2001), after average value recalculation. The relatively large errors associated with these ages are due to the variation in potassium concentrations. The mean value of 809 ± 29 Ma is considered as the emplacement age of the dolerite dyke.